



NTNU – Trondheim
Norwegian University of
Science and Technology

Concrete Dams Constructed on Soil Materials

Dipen Bista

Hydropower Development

Submission date: June 2015

Supervisor: Leif Lia, IVM

Norwegian University of Science and Technology
Department of Hydraulic and Environmental Engineering

MASTERKONTRAKT

- uttak av masteroppgave

1. Studentens personalia

Etternavn, fornavn Bista, Dipen	Fødselsdato 04. nov 1988
E-post dipenb@stud.ntnu.no	Telefon 47162037

2. Studieopplysninger

Fakultet Fakultet for ingeniørvitenskap og teknologi
Institutt Institutt for vann- og miljøteknikk
Studieprogram Hydropower Development

3. Masteroppgave

Oppstartsdato 15. jan 2015	Innleveringsfrist 11. jun 2015
Oppgavens (foreløpige) tittel Concrete dams constructed on soil materials	
Oppgavetekst/Problembeskrivelse Concrete dams demand for good rock for foundation however dams cannot always be constructed on rock. There are number of dams whose foundation rest on soil materials. A lot of uncertainties for such types of dams are related to settlement and permeability. Different solutions and measures have frequently been tested but no general guidelines available so far is sufficient for all different conditions. In this thesis we will - Evaluate design principles for concrete dams founded on soil materials and typical challenges related to such dams. - Study typical foundation properties and behavior. - Evaluate specified requirements in international standards and guidelines and compared to conditions in Nepal. - Evaluation of design of different dams by use of FEM or similar software.	
Hovedveileder ved institutt Professor Leif Lia	Medveileder(e) ved institutt
Merknader 1 uke ekstra p.g.a påske.	

4. Underskrift

Student: Jeg erklærer herved at jeg har satt meg inn i gjeldende bestemmelser for mastergradsstudiet og at jeg oppfyller kravene for adgang til å påbegynne oppgaven, herunder eventuelle praksiskrav.

Partene er gjort kjent med avtalens vilkår, samt kapitlene i studiehåndboken om generelle regler og aktuell studieplan for masterstudiet.

.....
Sted og dato

.....
Student

.....
Hovedveileder

Originalen lagres i NTNUs elektroniske arkiv. Kopi av avtalen sendes til instituttet og studenten.

FOREWORDS

This report, which is entitled “Concrete dams constructed on soil materials”, is submitted to the Department of Hydraulic and Environmental Engineering at the Norwegian University of Science and Technology as a partial fulfillment of the requirements of the Master of Science in Hydropower Development.

This thesis was carried out from January 2015 to June 2015 at Norwegian University of Science and Technology, Trondheim under the supervision of Prof. Leif Lia.

The author hereby declares that the work presented in this report is his own and outside inputs are acknowledged appropriately.

Dipen Bista,
June 2015,
Trondheim Norway

ACKNOWLEDGEMENT

I would like to express my gratitude to my supervisor, Professor Leif Lia, Department of Hydraulic and Environmental Engineering, Norwegian University of Science and Technology (NTNU), for his continuous support and guidance. His advice, suggestion and field trips have been very helpful in developing this report. I am very delighted to have him as my supervisor for my thesis.

I would also like to thank Prof. Gudmund Reidar Eiksund and Prof. Steinar Nordal, Department of Civil and Transport Engineering, NTNU for their help and valuable suggestions.

I am grateful to Mr. Andrew Makdisi, Master student and graduate researcher at University of Washington for his help and useful information.

I would like to thank Mr. Santosh Budathoki and Mr. Nasib Maan Shrestha from Nepal Electricity Authority and Mr. Gopal Tamaku from Upper Tamakoshi Hydropower Company for their support in obtaining data for this study.

I am grateful to my wife, Ms. Sabina Basnet and my family for supporting and encouraging me during my studies.

Finally, I would like to thank and acknowledge all friends, seniors and juniors who have helped me directly or indirectly in developing this thesis.

ABSTRACT

Rock may not always be encountered at economical depth to have dam foundation onto the rock. It is a typical situation in Nepal where several meters deep alluvium is expected before reaching competent rock. Several dams have been constructed on soil materials and several other are in planning or construction. Uncertainties in foundation behavior of soil due to heterogeneous properties makes soil foundation unique. This study attempts to find the methods of estimating foundation response and applying it to Upper Tamakoshi hydroelectric project in Nepal.

A 2D model of dam was prepared in PLAXIS 2D. The model was built in a sequence similar to construction of dam at site to get reasonable response in FEM. Due to insufficient field studies all parameters required as input parameters in PLAXIS cannot be obtained. Hence, average values of soil parameters from literature were taken for soil of similar grain size distribution. Model was run for different loading (water level) scenarios at different sections of dam. In addition, liquefaction susceptibility study was carried out and possible consequences of liquefaction was studied.

Safety of dam against sliding and overturning were studied. In addition, settlement and differential settlement were studied and stress induced in dam body and on foundation soil due to differential settlement were evaluated at different stages of construction and operation. Furthermore, seepage analysis was carried out for different water level scenarios. Seepage analysis with different design of grout curtain was done and the results were evaluated and compared with current design. Bearing capacity in the soil was checked and stresses development in the dam body and foundation were checked with allowable stresses. As no penetration test were done, liquefaction susceptibility and their effects were presented in curves for different penetration resistance.

In conclusion, this study has been successful in identifying key issues related to concrete dams constructed on soil materials and estimating their magnitudes and effects. Foundation studies and input parameters play key role in estimation of response close to insitu situation. Improvements on this study can be made by applying this case to a monitored dam, and comparing the results of these analysis with monitored data.

Table of Contents

1	Introduction.....	1
1.1	Background	1
1.2	Objective of study	1
1.3	Scope of study	2
1.4	Structure of thesis.....	2
1.5	Limitations	2
2	Literature review.....	3
2.1	Soil types and related engineering challenge	3
2.1.1	Gravel.....	3
2.1.2	Sand.....	3
2.1.3	Silt.....	5
2.1.4	Clay.....	5
2.1.5	Non Uniform.....	5
2.2	Foundation requirement of different types of concrete dams	5
2.2.1	Concrete gravity dams	5
2.2.2	Arch dams	5
2.2.3	Buttress dams	6
2.3	Stability calculation.....	6
2.3.1	Overturning stability	7
2.3.2	Sliding stability	7
2.4	Settlement.....	8
2.4.1	Steps in settlement analysis	10
2.4.2	Theoretical or empirical models	10
2.4.3	Numerical models	20
2.5	Seepage.....	20
2.5.1	Permeability	20
2.5.2	Effect of seepage.....	21
2.5.3	Method of analysis of seepage.....	25
2.6	Bearing capacity.....	25
2.7	Liquefaction	27
2.7.1	Introduction.....	27

2.7.2	Liquefaction susceptibility	28
2.7.3	Preliminary screening of liquefaction hazard	29
2.7.4	Evaluation of liquefaction	29
2.7.5	Effects of Liquefaction	35
3	Upper Tamakoshi Hydroelectric project.....	43
3.1	Headworks.....	44
3.2	Geology of headworks	44
3.2.1	General.....	45
3.2.2	Grain size distribution.....	45
3.2.3	Permeability	45
3.2.4	Strength parameters	46
3.2.5	Abutments	46
4	Finite element model and input data preparation	47
4.1	Finite element modelling.....	47
4.1.1	Mesh.....	47
4.1.2	Model development	47
4.2	Data preparation	51
4.2.2	Input data	51
4.2.3	Cases of analysis	55
5	Result and Discussion	57
5.1	Settlement.....	57
5.1.1	Along a section in transverse axis.....	57
5.1.2	Along length axis of dam.....	63
5.2	Horizontal movement in the direction of river.....	66
5.2.1	At the end of construction.....	66
5.2.2	During filling of reservoir.....	66
5.2.3	Discussion	67
5.3	Seepage.....	68
5.3.1	Seepage discharge.....	68
5.3.2	Exit gradient.....	69
5.3.3	Discussion.....	69
5.4	Stability	69

5.5	Bearing capacity	69
5.6	Liquefaction	70
5.6.1	Liquefaction susceptibility	70
5.6.2	Reconsolidation settlement	70
5.6.3	Lateral spreading	71
5.6.4	Discussion	72
6	Conclusion	73
6.1	Settlement	73
6.2	Seepage	74
6.3	Downstream Erosion	75
6.4	Liquefaction	76
7	Recommendations	77
	Bibliography	79
	Appendix A – Drawings	
	Appendix B – Stability Calculation	
	Appendix C – Settlement Calculation	
	Appendix D – Bearing Capacity Calculation	

List of Figures

Figure 2-1: Schematic diagram for time-settlement history	9
Figure 2-2 : General parameters for improved equation for calculating elastic settlement. (Das, 2015)	14
Figure 2-3: Variation of I_G with β (Das, 2015)	14
Figure 2-4: An example of e-log (σ') curve for soft clay	16
Figure 2-5: Oedometer tests on soil with large variation in stiffness (Janbu, 1967)	18
Figure 2-6: Modulus numbers for sand (Janbu, 1967).....	19
Figure 2-7: Zone of susceptibility of different types of liquefaction.....	27
Figure 2-8: Schematic diagram of expected zone of liquefaction by comparing cyclic stress and cyclic resistance of soil. (Idriss and Boulanger, 2008)	30
Figure 2-9: Magnitude scaling factor after different researchers (Idriss and Boulanger, 2006)	31
Figure 2-10: Variation of stress reduction coefficient with depth and earthquake (Idriss and Boulanger, 2006).....	33
Figure 2-11: Variation of volumetric strain in saturated sand with SPT and CSR (After Tokimatsu and Seed, 1987) (Kramer, 1996).....	36
Figure 2-12: Variation of volumetric strain with factor of safety against liquefaction for clean sand, SPT and relative density after Ishihara and Yoshimine 1992 (Idriss and Boulanger, 2008)	36
Figure 2-13: Variation of volumetric strain with SPT resistance and CSR for clean sand (Idriss and Boulanger, 2008).....	37
Figure 2-14: Comparison of Volumetric strain by different models (Idriss and Boulanger, 2008)	37
Figure 2-15: Source distance (R) based on PGA and earthquake magnitude (M) after Bartlett and Youd 1992,1995. (Youd et al., 2002).....	40
Figure 3-1: Grain size distribution for headworks area (Norconsult, 2005).....	45
Figure 4-1: Stress strain relation between deviatoric stress and axial strain in standard drained triaxial test (Brinkgreve and Vermeer, 2002)	47
Figure 4-2: Mesh and nodes.....	48
Figure 4-3: Zoomed view of mesh and nodes around dam.....	48
Figure 4-4: Excavation and lowering of ground water table.	49
Figure 4-5: Construction of filter, sheet pile and stilling basin	49

Figure 4-6: Addition of u/s slab, and concrete layer.....	49
Figure 4-7: Phase 4, addition of concrete.	50
Figure 4-8: Completion of construction.....	50
Figure 4-9: Filling of reservoir	50
Figure 5-1: Vertical displacement at the end of excavation	58
Figure 5-2: Total vertical displacement at the end of construction	58
Figure 5-3: Vertical deformation after filling of reservoir at NWL.....	59
Figure 5-4: Deformed mesh geometry after filling of reservoir at NWL	59
Figure 5-5: Differential displacement at the end of construction	60
Figure 5-6: Differential vertical displacement after filling at NWL.....	60
Figure 5-7: Deviatoric stresses at the end of construction.....	62
Figure 5-8: Deviatoric stress after filling of reservoir	62
Figure 5-9: Areas for development of tensile stresses in concrete	63
Figure 5-10: Areas for development of tensile stresses in concrete (Different construction sequence).....	63
Figure 5-11: Expected vertical settlement of dam along its axis at the end of construction ...	64
Figure 5-12: Settlement profile along dam axis.....	64
Figure 5-13: Horizontal displacement at the end of construction.....	66
Figure 5-14: Horizontal displacement of central section of dam during filling	67
Figure 5-15: Horizontal displacement of dam during filling in the direction of flow	67
Figure 5-16: Groundwater flow pattern under the dam	68
Figure 5-17: Historical earthquake epicenters since 1934.....	70
Figure 5-18: Factor of safety against liquefaction for different (N1)60 values with Idriss and Boulanger and NCEER methods	71
Figure 5-19: Reconsolidation settlement according to different researchers and (N1)60	71
Figure 5-20: Settlement due to lateral spreading according to Kramer and Baska model	72
Figure 6-1: Downstream erosion during a big flood event of Lauvsnes dam Norway (Photo: Norsk Groønn Kraft).....	75

List of Tables

Table 2-1: USCS classification of soil (USB, 1998).....	4
Table 2-2: Factor of safety against sliding practiced in different countries (Ruggeri, 2004)....	8
Table 2-3: Relative importance of immediate, primary and secondary consolidation settlement for different types of soil (Holtz, 1991).....	10
Table 2-4: Variation of I_f with D_f/B , B/L , and θ_v (Das, 2015).....	12
Table 2-5: Typical modulus number (Fellenius, 2006).....	20
Table 2-6: Recommended factor of safety against critical gradient (USB, 2014).....	22
Table 2-7: Recommended factor of safety against heaving (USB, 2014).....	23
Table 2-8: Susceptibility of soil deposits to liquefaction during strong seismic shaking (Youd and Perkins, 1978).....	28
Table 2-9: Mean MSF of the range suggested at NCEER workshop, and MSF suggested by Idriss and Boulanger.....	32
Table 2-10: Stress reduction coefficient after different researchers.....	32
Table 2-11: SPT value calculation for clean sand.....	33
Table 2-12: Cyclic resistance ratio for effective vertical stress=1atm.....	34
Table 2-13: Calculation of overburden correction factor.....	34
Table 2-14: Conditions of applicability of (Youd et al., 2002) (Kramer, 2008).....	38
Table 2-15: Regression coefficients (Kramer, 2008).....	39
Table 2-16: Condition of applicability of Kramer and Baska model (Kramer, 2008).....	40
Table 3-1: Salient features of Upper Tamakoshi Hydropower Project (UTHL, 2015).....	43
Table 3-2: Average permeability at headworks (Norconsult, 2005).....	46
Table 4-1: Characteristics of meshing.....	47
Table 4-2: Permeability values used for PLAXIS model.....	52
Table 4-3: Input parameters for topmost layer (0-6 m depth).....	53
Table 4-4: Concrete properties input parameters.....	54
Table 4-5: Input parameters for rock.....	55
Table 5-1: Rotation angle and movement of top of dam due to unequal settlement of each section.....	65
Table 5-2: Different cases of seepage flow analysis.....	68
Table 5-3: Factor of safety.....	69

1 Introduction

1.1 Background

There are several types of concrete dams built around the world. The choice of type of concrete dam depends on physical factors such as topography, geology, foundation conditions, material availability etc. The strength, thickness and inclination of strata, permeability, faulting, etc. are important considerations when selecting the dam type (USBR, 1987).

In any dam type, provided that other conditions are similar, the foundation with rock is preferable over foundation with soil for a concrete dam. However, rock may not always be encountered at an economic depth.

Since it is not always possible to have rock in foundation, a number of concrete gravity dams have been constructed on soil around the world. In Nepal, due to deep layers of alluvium, several concrete gravity dams for hydropower and irrigation purpose have been constructed on soil and many more are either in construction or in planning phase.

Several uncertainties are involved in concrete dams constructed on soil materials. Hence, it is difficult to predict response of foundation such as settlement, seepage, etc. This leads to design and/or construction challenges, and probably instability of dam.

Thus, predicting foundation behavior of dam at early stage of project development is very useful in mitigating instabilities and time and cost overrun for a dam. However, lack of foundation properties are always a challenge for such a study. There are several theoretical, empirical and numerical models to predict the settlement and seepage in a foundation. In this study, several theoretical and empirical relations and PLAXIS 2D model are used to estimate settlement, seepage, bearing and liquefaction potential of soil at different stages of construction and operation. In addition, different aspects of stability of dam were studied.

1.2 Objective of study

Estimating foundation behavior should receive considerable attention in planning and design of concrete dams which are constructed on soil foundation. But there are a lot of uncertainties involved in doing so. On this background, the intention of this study will be to evaluate the design principles of concrete dams on soil foundation typical challenges related to them and evaluating the design of a dam in Nepal by using finite element model.

A true global and general method is however not going to be evaluated due to the limited time disposable. The theory will instead be applied on a dam in Nepal: Upper Tamakoshi

Hydroelectric project, which is considered to be a representative example. The prescribed methods, with some adjustments, can thus be assigned a semi global significance.

1.3 Scope of study

The following tasks will be carried out to meet the proposed objectives:

- Literature review on different types of soil and their engineering challenges.
- Literature review on methods of settlement, seepage, bearing capacity and liquefaction calculation.
- Analysis of stability of a concrete gravity dam constructed on soil materials and estimation of seepage, settlement and liquefaction potential.
- Modelling of a dam in PLAXIS 2D.

1.4 Structure of thesis

This report tries to cover all the necessary tasks which are required for estimating the foundation behavior of a concrete dam on soil material. Different chapters are assigned to describe the different sub tasks.

Chapter 1 gives a brief introduction to the need of foundation studies for dams, objectives and scopes of the study, and structure of the thesis.

Chapter 2 describes associated literature for studies of foundation characteristics.

Chapter 3 introduces about the structure and geology of dam for case study.

Chapter 4 presents the use of finite element model and input data preparation carried out for modelling.

Chapter 5 presents the results and discussion of analysis.

Chapter 6 gives main conclusion of studies.

Chapter 7 discusses recommendation for further research as an extension of current study.

1.5 Limitations

Very limited data on properties of soil are available because of insufficient field studies. In addition, no data are available on monitoring of dam on soil. Thus this study is carried out for the demonstration purpose. Therefore, there is sufficient room available for more work to improve this study and can be made as a useful operational tool after development.

2 Literature review

2.1 Soil types and related engineering challenge

Soil can be classified into different classes based on size, mineral composition, nature, etc. For the use of this thesis, Unified soil classification system (USCS) is used. This system classifies soil based on laboratory determination of particle-size characteristics, liquid limit, and plasticity index.

This classification system has divided soil into three main categories.

- i. Coarse grained soil
- ii. Fine grained soil
- iii. Highly organic soils

These three divisions are further subdivided into 15 basic soil groups, which is illustrated in [Table 2-1](#).

2.1.1 Gravel

- Structural characteristics of gravel mainly depends on the density, amount and shape of gravel particles and the amount and nature of matrix soils. (sand, silt and clay)
- High shear strength
- Low compressibility
- Challenge: Highly permeable

2.1.2 Sand

- Structural property of sand is dependent of amount and characteristics of matrix (silt and clay)
- The SW and SP soils are pervious; whereas, SM and SC soils are semi pervious to impervious depending upon the amount and character of the fines. Because of their low permeability, relatively high shear strength, and relatively low compressibility of SC soils, they are good for earthfill dams and other embankment materials if compacted properly (USBR, 1998).

Challenges:

- Non uniform settlement
- Potential for soil collapse upon saturation

- High uplift forces
- Excessive percolation losses and piping
- Protection of the foundation at the downstream toe from erosion (from piping)
- If there is considerable amount of silt and clay in saturated sand then the shear strength is dependent on water content. i.e. with higher water content shear strength decreases

Table 2-1: USCS classification of soil (USBR, 1998)

Criteria for Assigning Group Symbols and Group Names Using Laboratory Tests ^A				Soil Classification		
				Group Symbol	Group Name ^B	
COARSE-GRAINED SOILS	Gravels (More than 50 % of coarse fraction retained on No. 4 sieve)	Clean Gravels (Less than 5 % fines ^C)	$Cu \geq 4$ and $1 \leq Cc \leq 3^D$	GW	Well-graded gravel ^E	
			$Cu < 4$ and/or $[Cc < 1 \text{ or } Cc > 3]^D$	GP	Poorly graded gravel ^E	
		Gravels with Fines (More than 12 % fines ^C)	Fines classify as ML or MH	GM	Silty gravel ^{E,F,G}	
	More than 50 % retained on No. 200 sieve		Fines classify as CL or CH	GC	Clayey gravel ^{E,F,G}	
		Sands (50 % or more of coarse fraction passes No. 4 sieve)	Clean Sands (Less than 5 % fines ^H)	$Cu \geq 6$ and $1 \leq Cc \leq 3^D$	SW	Well-graded sand ^I
				$Cu < 6$ and/or $[Cc < 1 \text{ or } Cc > 3]^D$	SP	Poorly graded sand ^I
	Sands with Fines (More than 12 % fines ^H)	Fines classify as ML or MH	SM	Silty sand ^{F,G,I}		
		Fines classify as CL or CH	SC	Clayey sand ^{F,G,I}		
FINE-GRAINED SOILS	Silt and Clays	inorganic	$PI > 7$ and plots on or above "A" line ^J	CL	Lean clay ^{K,L,M}	
			$PI < 4$ or plots below "A" line ^J	ML	Silt ^{K,L,M}	
	50 % or more passes the No. 200 sieve	Silt and Clays	inorganic	$\frac{Liquid\ limit - over\ dried}{Liquid\ limit - not\ dried} < 0.75$	OL	Organic clay ^{K,L,M,N} Organic silt ^{K,L,M,O}
				PI plots on or above "A" line	CH	Fat clay ^{K,L,M}
		Silt and Clays	inorganic	PI plots below "A" line	MH	Elastic silt ^{K,L,M}
				$\frac{Liquid\ limit - over\ dried}{Liquid\ limit - not\ dried} < 0.75$	OH	Organic clay ^{K,L,M,P} Organic silt ^{K,L,M,O}
HIGHLY ORGANIC SOILS	Primarily organic matter, dark in color, and organic odor		PT	Peat		

^A Based on the material passing the 3-in. (75-mm) sieve.

^B If field sample contained cobbles or boulders, or both, add "with cobbles or boulders, or both" to group name.

^C Gravels with 5 to 12 % fines require dual symbols:

GW-GM well-graded gravel with silt
GW-GC well-graded gravel with clay
GP-GM poorly graded gravel with silt
GP-GC poorly graded gravel with clay

$$^D Cu = D_{60}/D_{10} \quad Cc = \frac{(D_{30})^2}{D_{10} \times D_{60}}$$

^E If soil contains ≥ 15 % sand, add "with sand" to group name.

^F If fines classify as CL-ML, use dual symbol GC-GM, or SC-SM.

^G If fines are organic, add "with organic fines" to group name.

^H Sands with 5 to 12 % fines require dual symbols:

SW-SM well-graded sand with silt
SW-SC well-graded sand with clay
SP-SM poorly graded sand with silt
SP-SC poorly graded sand with clay

^I If soil contains ≥ 15 % gravel, add "with gravel" to group name.

^J If Atterberg limits plot in hatched area, soil is a CL-ML, silty clay.

^K If soil contains 15 to < 30 % plus No. 200, add "with sand" or "with gravel," whichever is predominant.

^L If soil contains ≥ 30 % plus No. 200, predominantly sand, add "sand" to group name.

^M If soil contains ≥ 30 % plus No. 200, predominantly gravel, add "gravelly" to group name.

^N $PI \geq 4$ and plots on or above "A" line.

^O $PI < 4$ or plots below "A" line.

^P PI plots on or above "A" line.

^Q PI plots below "A" line.

2.1.3 Silt

- Silts are fairly impervious

Challenges:

- Have tendency to become quick when saturated
- Difficult to compact
- Highly susceptible to frost heaving.

2.1.4 Clay

- Low strength
- Virtually impervious

Challenges:

- High settlement and long term settlement
- Difficult to compact when wet
- Impossible to drain by ordinary means

2.1.5 Non Uniform

- Mix of above mentioned materials

In nature a single type of soil is very hard to find. Rather it will be a mix of different types of soils.

2.2 Foundation requirement of different types of concrete dams

A brief overview of foundation requirements for different types of concrete dams are presented below;

2.2.1 Concrete gravity dams

As these types of dams induce high stresses (stress levels in a concrete dam is generally 3-5 MPa) they are suitable for sites with reasonably sound rock foundation. However, low structures may also be founded on alluvial foundations provided that adequate cutoffs and sliding resistance ([Ref. 2.3.2](#)) are provided.

2.2.2 Arch dams

In this type of dam horizontal forces are transferred to the abutments while weight of the dam is transferred to the foundation. Generally, arch dams are thin in section so, the stress induced in foundation due to weight is high. Hence, such dams require strong solid rock abutment as

well as rock in the foundation. In principle, these types of dams can also be built even on soil foundation provided that abutments have strong rock. In such case, the weight of dam should be distributed evenly in the foundation over wide area to avoid bearing failure.

2.2.3 Buttress dams

These types of dam transfer load from deck to the foundation by buttresses. As load is transferred by thin buttress high stresses are developed on the foundation. Hence, this type of dam also requires rock foundation to transfer stresses. However, it can also be built on soil provided that the load from buttress are transferred to foundation in a much wider area by construction of horizontal plate.

2.3 Stability calculation

Concrete gravity dams are designed such that all the loads are resisted by the weight of dam itself. Concrete dams are assembly of similar sections where each section has its own separate failure mode (Berzell, 2014). The forces acting on a concrete gravity dam are;

- Weight of dam
- Headwater and Tailwater pressure
- Uplift forces
- Earth and silt pressure
- Ice pressure
- Wave pressure
- Reaction of foundation
- Temperature
- Earthquake forces

Determination of magnitude of these forces will not discussed in this report and can be referred to (USBR, 1976).

A concrete dam should satisfy the following stability conditions;

- Overturning stability
- Sliding stability
- Stress levels in concrete and in foundation soil.
- Water should not be allowed to pass through dam or its foundation.

2.3.1 Overturning stability

The prerequisite for an overturning failure is that the overturning moment about the toe of dam should not exceed the resisting moment about same point. According to Johansson, 2005, it is however a hypothetical failure mode and is unlikely to occur in reality as other failure modes would already have taken place before overturning.

Mathematically,

$$\text{Factor of safety} = \frac{M_{\text{overturning}}}{M_{\text{stabilizing}}} \quad \text{Eq. (2-1)}$$

Factor of safety

According to Swedish power companies guidelines for dam safety (RIDAS) the limits of factor of safety is given by

Normal load combinations	= 1.5
Exceptional load combinations	= 1.35
Accidental loads	= 1.1

In addition it is a general practice that, the resultant of all forces acting on the dam should fall within central third width of dam foundation (middle third of dam base). This requirement ensures that the dam base is in compression. However, for exceptional loads it is allowed to fall outside middle third provided that it stays within 3/5th area (Berzell, 2014).

2.3.2 Sliding stability

There are several definitions and factor of safety used in practice for sliding stability. The safety factor against sliding is given by the ratio of resisting force and the sum of horizontal forces causing instability. Mathematically,

$$FOS = \frac{c \cdot A + \sum V \cdot \tan \Phi}{\sum H} \quad \text{Eq. (2-2)}$$

Where,

C	= Cohesion of sliding surface considered
A	= Area of contact
Φ	= Friction angle
$\sum V$	= Sum of vertical forces
$\sum H$	= Sum of horizontal forces

Factor of safety

Several values of factor of safety are used around the world (Ref. Table 2-2). Comparison between these factors of safety is difficult as they are related to different criteria to define the exceptional or extreme loads, or to define the strength parameters. Hence, care has been taken in the selection of the comparisons. (Ruggeri, 2004)

Table 2-2: Factor of safety against sliding practiced in different countries (Ruggeri, 2004)

	Factor of Safety						
	France			Germany	Austria	Switzerland	Norway
	(1)	(2)	(3)				
Usual loads	4	1.33	1.5	1.2-1.5	1.5	1.5	1.5
Unusual loads	2.7	1.1	1.2	1.2-1.3	1.2-1.35	1.3	1.3
Extreme loads	-	1.05	1	1	1.1	1.1	1.1

(1); (2); (3): Barrages en aménagement rural; EDF; Coyne & Bellier

4): When cohesion is assumed = 0

	Factor of Safety			
	Canada- (5)	CDSA (6)	UK	USA-USBR
Usual loads	1.5	3	3	3
Unusual loads	1.3	2	2	2
Extreme loads	1	1.3	1	1

(5); (6): Residual strength; Peak strength (no tests)

2.4 Settlement

When stress is applied in a soil mass, it tends to reform and change its shape. The downward movement of ground due to application of vertical stress is known as settlement. Settlement is a time dependent process and depends on the characteristics of soil. Generally, permeable soils (sand and gravel) settle fast while low permeable (clay) and saturated soil experience gradual deformation called consolidation. Only a small portion of ground deformation are elastic in nature.

Soil settlement can be of two categories:

- i. Elastic settlement (immediate settlement).
- ii. Consolidation Settlement

- a. Primary consolidation settlement due to expulsion of pore water
- b. Secondary consolidation settlement due to plastic adjustment of soil skeletons.

Mathematically,

$$S_T = S_i + S_c + S_s$$

Where,

S_T = Total settlement

S_i = Immediate settlement

S_c = Primary consolidation settlement

S_s = Secondary consolidation settlement

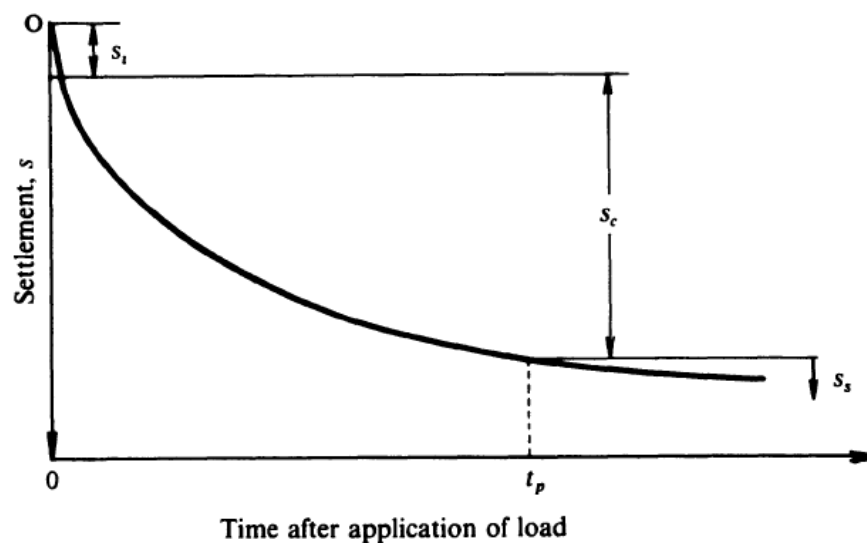


Figure 2-1: Schematic diagram for time-settlement history

The time–settlement relationship shown in Figure 2-1 is principally valid for all types of soil. However, large differences exist in the magnitude of the components and the rate at which they occur for different soils types. For granular soils, such as sand, the permeability is large enough to consolidate almost instantaneously when the load is applied. In addition, secondary compression is generally insignificant in granular soil though they exhibit some creep effects. For cohesive soils, such as clays, hydraulic conductivity is very small that the pore pressure dissipates slowly and the consolidation requires long time even years to complete. Secondary compression can be of considerable magnitude for these soil types. Unlike both sand and clay, peats and organic soils generally undergo rapid consolidation and high, long-term secondary compression. (Patrick, 2002)

Table 2-3: Relative importance of immediate, primary and secondary consolidation settlement for different types of soil (Holtz, 1991)

Soil Type	Immediate Settlement	Consolidation Settlement	Secondary consolidation
Sands	Yes	No	No
Clays	Possibly	Yes	Possibly
Organic soils	Possibly (Yes)	Possibly (No)	Yes

2.4.1 Steps in settlement analysis

- i. Establish the soil profile including that of groundwater table. Determine compressive layers in the soil and compute total and effective stresses.
- ii. Estimate the magnitude and rate of application of the loads, both during construction and during the service life of the structure.
- iii. Estimate change in stress levels with depth due to addition/removal of load.
- iv. Calculate the preconsolidation pressure and determine whether the soil is normally consolidated or overconsolidated by comparing with the effective stress profile computed in (i) above.
- v. Estimate the immediate settlement.
- vi. Calculate the consolidation settlements and time rate of settlement
- vii. Estimate the rate of secondary consolidation.

2.4.2 Theoretical or empirical models

Several theoretical and numerical approaches such as Boussinesq equation, Janbu's concept etc. have been proposed by different researchers to calculate settlement. These models are one dimensional and are used to calculate settlement at a point. Settlement can be predicted with reasonable accuracy at the center of foundation with these methods. However, due to influence of several factors in settlement and a lot of boundary conditions involved these methods can be troublesome for heterogeneous foundation. Also, these methods do not consider the unloading reloading stiffness. These methods can be used to estimate settlement at an early stage of project developments. Some of the methods are presented in this report. It is advisable to use two or more methods to calculate settlement.

2.4.2.1 Elastic Settlement

It occurs during or immediately after the construction of a structure. This type of settlement occurs in granular soil due to decrease in volume of voids. Theory of elasticity (Hooke's law) can be applied to estimate the settlement for these soil types. Several methods have been proposed to estimate the magnitude of elastic settlement. Static foundation settlements on granular materials are generally computed by one of two methods: (1) Using a formulation of the Boussinesq equation with an influence factor to account for depth and foundation shape; (2) Using a method proposed by Schmertmann (1970) based on an extensive studies of elastic settlements on sand (Bowles, 1987).

2.4.2.1.1 Using a formulation of the Boussinesq equation

The settlement of a perfectly flexible foundation is given by (Bowles, 1987)

$$S_e = q_0 \alpha B' \frac{1 - \vartheta^2}{E_s} I_s I_f$$

Eq. (2-3)

Where,

q_0 = Net applied pressure on the foundation

ϑ = Poisson's ratio of soil

E_s = Average modulus of elasticity of the soil under the foundation, measured from $z = 0$ to about $z = 5B$

B' = $B/2$ for center of foundation and $=B$ for corner of foundation

I_s = Shape factor (Steinbrenner, 1934)

$$= F_1 + \frac{1 - 2\vartheta}{1 - \vartheta} F_2$$

Eq. (2-4)

$$F_1 = \frac{1}{\pi} (A_0 + A_1)$$

Eq. (2-5)

$$F_2 = \frac{n'}{2\pi} \tan^{-1} A_2$$

Eq. (2-6)

$$A_0 = m' \ln \frac{(m' + \sqrt{m'^2 + 1}) \sqrt{m'^2 + n'^2}}{m'(1 + \sqrt{m'^2 + n'^2 + 1})}$$

Eq. (2-7)

$$A_1 = m' \ln \frac{(m' + \sqrt{m'^2 + 1}) \sqrt{1 + n'^2}}{m' + \sqrt{m'^2 + n'^2 + 1}}$$

Eq. (2-8)

$$A_2 = \frac{m'}{n' \sqrt{m'^2 + n'^2 + 1}}$$

Eq. (2-9)

$$I_f = \text{depth factor} = f\left(\frac{D_f}{B}, \vartheta, \frac{L}{B}\right) \text{ (Fox, 1948)}$$

α = a factor that depends on location of calculation of settlement

At center of foundation,

$$\alpha = 4$$

$$m' = L/B$$

$$n' = H/(B/2)$$

At corner of foundation,

$$\alpha = 1$$

$$m' = L/B$$

$$n' = H/B$$

Elastic settlement of rigid foundation is given by (Das, 2015)

$$S_{e(\text{rigid})} \approx 0.93 S_{e(\text{flexible, center})}$$

Eq. (2-10)

Table 2-4: Variation of I_f with D_f/B , B/L , and ϑ (Das, 2015)

ϑ	D_f/B	B/L		
		0.2	0.5	1
0.3	0.2	0.95	0.93	0.90
	0.4	0.90	0.86	0.81
	0.6	0.85	0.80	0.74
	1.0	0.78	0.71	0.65
0.4	0.2	0.97	0.96	0.93
	0.4	0.93	0.89	0.85
	0.6	0.89	0.84	0.78
	1.0	0.82	0.75	0.69
0.5	0.2	0.99	0.98	0.96
	0.4	0.95	0.93	0.89
	0.6	0.92	0.87	0.82
	1.0	0.85	0.79	0.72

2.4.2.1.2 Improved Equation for Elastic Settlement

Mayne and Poulos, 1999 presented a formula for calculating the elastic settlement of foundations which takes into account the rigidity of the foundation, the depth of embedment, increase in the modulus of elasticity of the soil with depth, and the location of rigid layers at a limited depth (Das, 2015). The equivalent diameter of a rectangular foundation used by Mayne and Poulos is given by

$$B_e = \sqrt{\frac{4BL}{\pi}}$$

Eq. (2-11)

Where,

B = width of foundation

L = length of foundation

In a foundation with thickness t at a depth D_f , the elastic settlement below the center of foundation is given by,

$$S_e = \frac{q_0 B_e I_G I_F I_E}{E_0} (1 - \nu^2)$$

Eq. (2-12)

Where,

I_G = influence factor for variation of E_s with depth (Ref. [Figure 2-3](#))

I_F = foundation rigidity correction factor

I_E = foundation embedment correction factor

$$I_F = \frac{\pi}{4} + \frac{1}{4.6 + 10 \left(\frac{E_f}{E_0 + B_e \cdot k/2} \right) \left(\frac{2t}{B_e} \right)^3}$$

Eq. (2-13)

$$I_E = 1 - \frac{1}{3.5 \exp(1.22\mu_s - 0.4) \left(\frac{B_e}{D_f} + 1.6 \right)}$$

Eq. (2-14)

(Das, 2015)

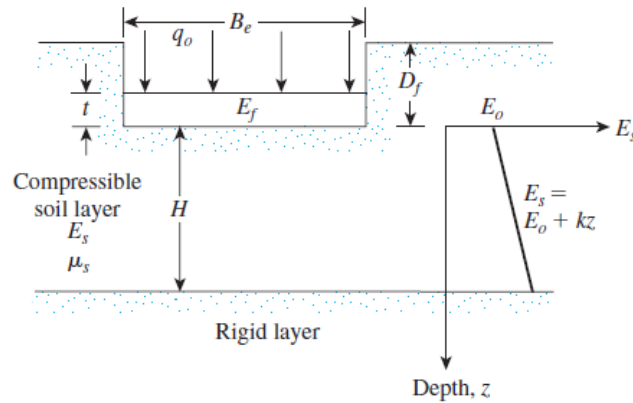


Figure 2-2 : General parameters for improved equation for calculating elastic settlement. (Das, 2015)

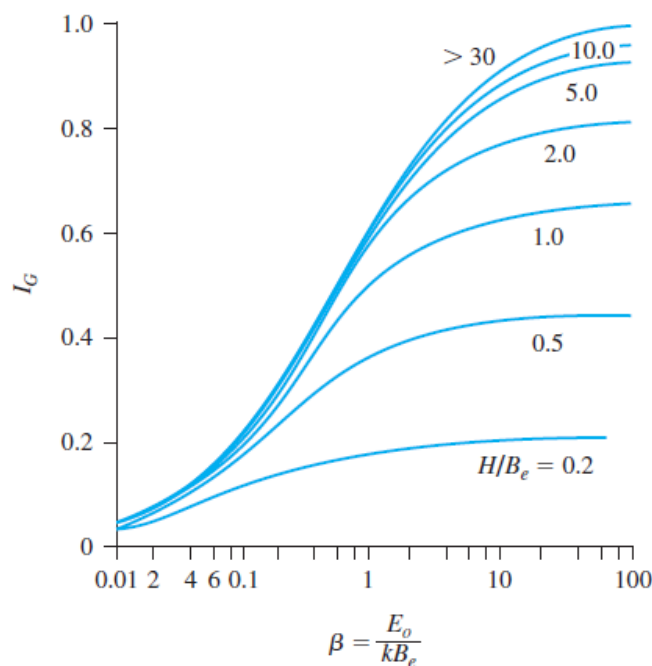


Figure 2-3: Variation of I_G with β (Das, 2015)

2.4.2.2 Consolidation Settlement

It is a process of gradual reduction in volume of saturated soil of low permeability due to drainage of pore water. This process continues until the excess pore water pressure in soil is completely dissipated. It is a two-step process:

1. Primary consolidation settlement – It occurs due to change in volume in saturated cohesive soils because of the expulsion of water from voids. However, high permeability of sandy, cohesion less soils result in almost immediate drainage due to the increase in pore water pressure and no primary consolidation settlement occurs
2. Secondary compression settlement – Occurs due to plastic adjustment of soil fabric in cohesive soils.

2.4.2.2.1 Primary consolidation settlement

The one dimensional consolidation settlement can be calculated by using the following equations:

For normally consolidated clays

$$S_{c(p)} = \frac{C_c H_c}{1 + e_0} \log \frac{\sigma'_0 + \Delta\sigma'_{av}}{\sigma'_0} \quad \text{Eq. (2-15)}$$

For overconsolidated clays with $\sigma'_0 + \sigma'_{av} < \sigma'_c$

$$S_{c(p)} = \frac{C_s H_c}{1 + e_0} \log \frac{\sigma'_0 + \Delta\sigma'_{av}}{\sigma'_0} \quad \text{Eq. (2-16)}$$

For overconsolidated clays with $\sigma'_0 < \sigma'_c < \sigma'_0 + \Delta\sigma'_{av}$

$$S_{c(p)} = \frac{C_s H_c}{1 + e_0} \log \frac{\sigma'_c}{\sigma'_0} + \frac{C_c H_c}{1 + e_0} \log \frac{\sigma'_0 + \Delta\sigma'_{av}}{\sigma'_c} \quad \text{Eq. (2-17)}$$

(Das, 2015) and (Gibbs, 1953)

Where,

σ'_0 = Average effective pressure on the clay prior to the construction of structure

$\Delta\sigma'_{av}$ = Average increase in effective stress on the clay due to construction of the structure

σ'_c = Preconsolidation pressure

e_0 = Initial void ratio of clay

C_c = Compression index

C_s = Swelling index

H_c = Thickness of the clay layer

The compression and swelling index are obtained by calculating the slope of loading and unloading zone of void ratio (e) vs log (σ') curve obtained from laboratory oedometer test. The test procedure can be referred to ASTM D 2435 - Standard Test Method for One-Dimensional Consolidation Properties of Soils.

2.4.2.2.2 Secondary consolidation settlement

After completion of dissipation of excess pore pressure some settlement may occur due to plastic adjustment of soil grains called as secondary consolidation. In this stage, the plot of

deformation vs. logarithm of time is linear. Hence secondary compression index can be defined as (Das, 2015)

$$C_{\alpha} = \frac{\Delta e}{\log t_2 - \log t_1} = \frac{\Delta e}{\log \left(\frac{t_2}{t_1} \right)}$$

Eq. (2-18)

Where,

Δe = change in void ratio

t_1, t_2 = time

The magnitude of settlement is calculated as (Das, 2015)

$$S_{c(s)} = C'_{\alpha} H_c \log(t_2/t_1)$$

Eq. (2-19)

Where,

$$C'_{\alpha} = C_{\alpha}/(1 + e_p)$$

e_p = void ratio at the end of primary consolidation

H_c = Thickness of clay layer

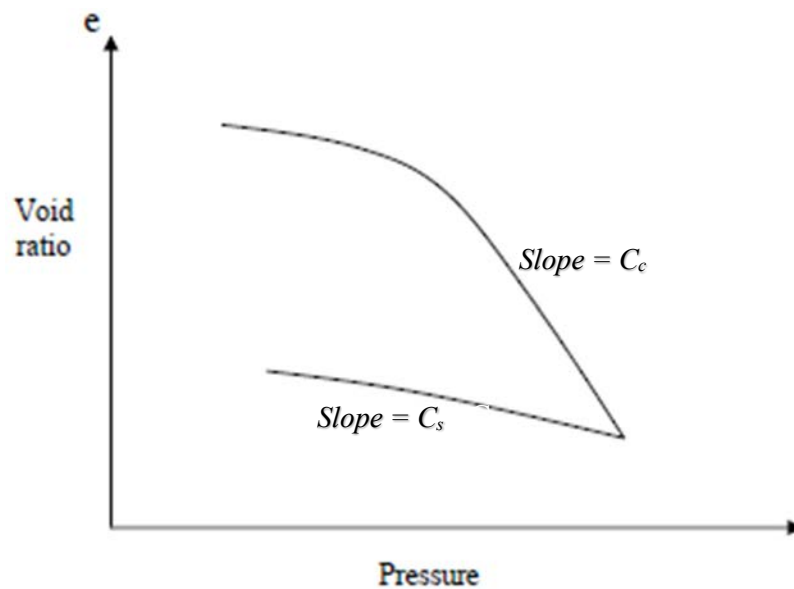


Figure 2-4: An example of e-log (σ') curve for soft clay

2.4.2.2.3 Time of Consolidation

According to Terzaghi, the time required for consolidation is given by

$$t = \frac{TH^2}{C_v}$$

Eq. (2-20)

Where,

- H = Longest drainage path length
 T = Time factor (dependent on the drainage conditions and the shape of the pressure distribution curve caused by the structure)
 C_v = Coefficient of consolidation obtained from consolidation test

2.4.2.3 Janbu concept

The Janbu tangent modulus method gives good approximation of settlement and applies to all soils, clays and sand. It combines basic principles of linear and nonlinear stress strain behavior. Oedometer test result of different types of soil is given in [Figure 2-5](#). The soil behavior may grossly be divided in three categories.

- 1) Constant stiffness with effective stress: Typical for overconsolidated clays.
- 2) Linearly increasing with effective stress: Typical for normally consolidated clays.
- 3) Parabolic increase with effective stress: Valid for sands and coarse silts, or any granular material.

Janbu's general equation for confined modulus is

$$M = m \cdot \sigma_a \left(\frac{\sigma'}{\sigma_a} \right)^{(1-i)} \quad \text{Eq. (2-21)}$$

Where,

M = One dimensional confined modulus, (found from oedometer test)

$$d\sigma' = M \cdot d\varepsilon \quad \text{Eq. (2-22)}$$

m = Modulus number

σ' = Actual effective stress level

σ_a = Stress equivalent to one atmosphere (100 MPa)

i = Stress exponent

$d\sigma'$ = Change in effective stress

$d\varepsilon$ = Strain due to change in stress

Combining equations 1-13 and 1-14 for change in soil stress from σ_0' to stress condition $\sigma' = \sigma_0' + \Delta\sigma'$

$$\varepsilon = \frac{1}{i \cdot m} \left[\left(\frac{\sigma'}{\sigma_a} \right)^i - \left(\frac{\sigma_0'}{\sigma_a} \right)^i \right] \quad \text{Eq. (2-23)}$$

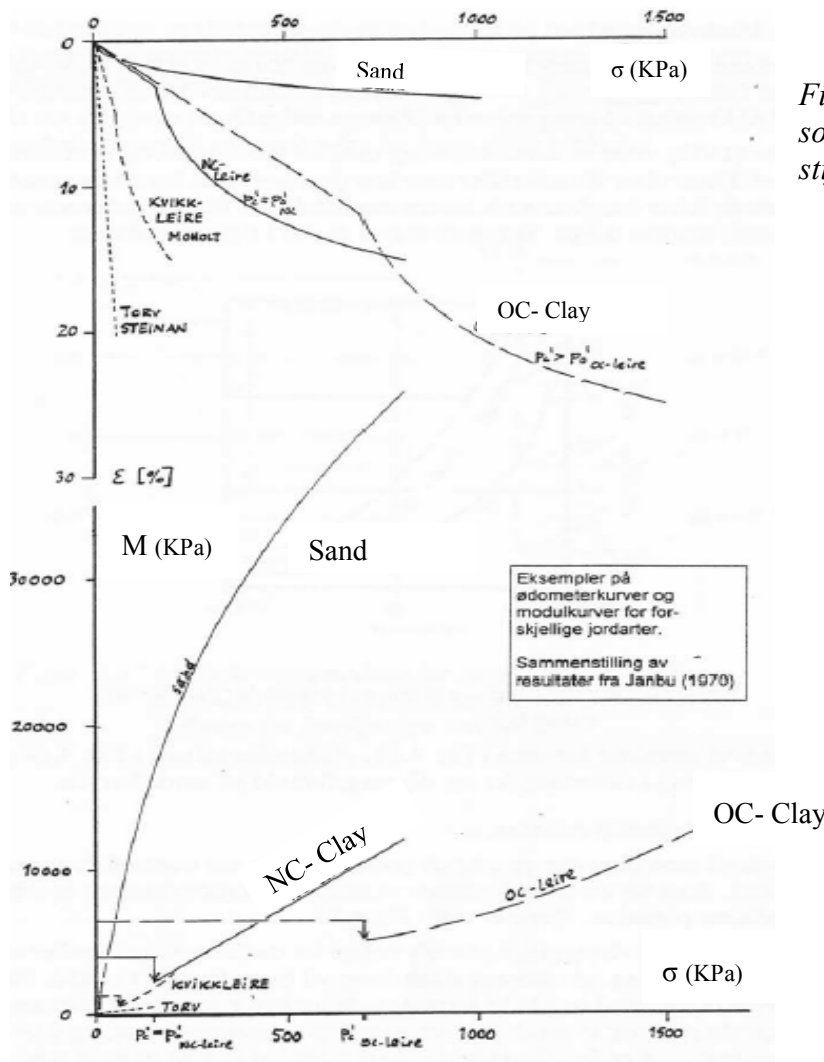


Figure 2-5: Oedometer tests on soil with large variation in stiffness (Janbu, 1967)

2.4.2.4 Settlement in Overconsolidated clays

The stress-strain behavior (settlement) in overconsolidated clays, can be assumed to be ‘elastic’, i.e. the stress exponent is equal to unity (i = 1). So,

$$M = m\sigma_a \tag{Eq. (2-24)}$$

And the strain is given by,

$$\epsilon = \frac{\Delta\sigma'}{m\sigma_a} \tag{Eq. (2-25)}$$

2.4.2.5 Settlement in Normally consolidated clays

The stress-strain behavior (settlement) in normally consolidated clays which is given when i=0. Hence,

$$M = m\sigma'$$

And, the strain equation is,

$$\varepsilon = \frac{1}{m} \ln \frac{\sigma'}{\sigma_0'}$$

Eq. (2-26)

2.4.2.6 Settlement in granular soils

For granular soils stress exponent close to 0.5 will represent the stress-strain-curve quite well.

The stiffness expression is given by,

$$M = m\sqrt{\sigma_a \cdot \sigma'} \quad \text{Eq. (2-27)}$$

And the strain equation is,

$$\varepsilon = \frac{2}{m} \left(\sqrt{\frac{\sigma'}{\sigma_a}} - \sqrt{\frac{\sigma_0'}{\sigma_a}} \right)$$

Eq. (2-28)

(Janbu, 1967)

According to Janbu, 1967, modulus numbers are related to relative porosity and K_0 . The relation for sands is shown in Figure 2-6.

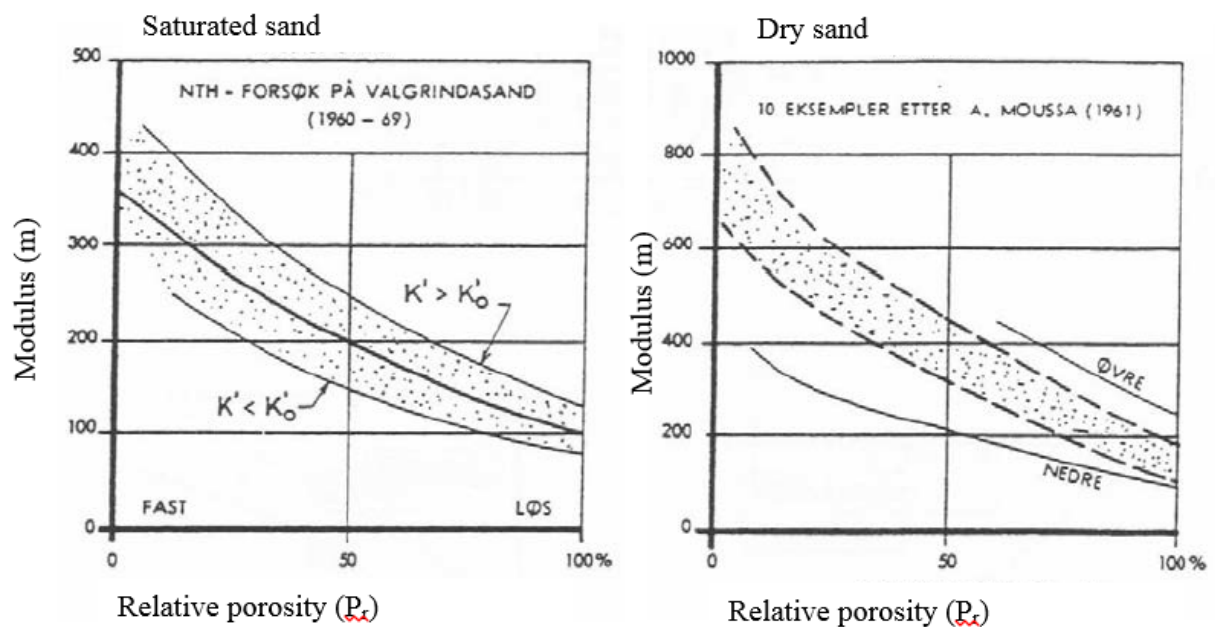


Figure 2-6: Modulus numbers for sand (Janbu, 1967)

Table 2-5: Typical modulus number (Fellenius, 2006)

SOIL TYPE	MODULUS NUMBER
Till, very dense to dense	1,000 — 300
Gravel	400 — 40
Sand dense	400 — 250
compact	250 — 150
loose	150 — 100
Silt dense	200 — 80
compact	80 — 60
loose	60 — 40
Clays	
Silty clay hard, stiff	60 — 20
and stiff, firm	20 — 10
Clayey silt soft	10 — 5 —
Soft marine clays and organic clays	20 — 5
Peat	5 — 1

2.4.3 Numerical models

Finite element models such as PLAXIS 2D/3D, Settle 2D, etc. can be used to calculate settlement. Different stages of development can be modelled in numerical models. However, they require a lot of soil parameters as an input for estimation of settlement.

2.5 Seepage

Seepage is the movement of water from reservoir through the dam, abutments or foundation. Water may flow through the pores of soil or through finite openings such as fractures or solution channels.

2.5.1 Permeability

The average rate of flow of water through porous medium under unit hydraulic gradient is termed as permeability. Permeability depends on the degree of saturation of the soil (USBR, 2014). Hydraulic conductivity is also used as a synonym for permeability.

USBR describes soils with permeability less than 1×10^{-6} cm/s as impervious, those with permeability between 1×10^{-6} cm/s and 1×10^{-4} cm/s as semipervious, and soils with permeability greater than 1×10^{-4} cm/s as pervious (USBR, 1998).

In stratified foundation the horizontal seepage is much higher than the vertical seepage. Hence the layers at depth may not transmit large amount of water as the layers upstream.

2.5.2 Effect of seepage

2.5.2.1 Exit gradient and uplift pressures

2.5.2.1.1 Exit gradient in cohesionless soil

Exit gradient is the hydraulic gradient at the free face or at the interface of more pervious material. In cohesionless soils with narrow distribution of fine sand and silt, if the exit gradient exceeds the critical gradient then it results in quick conditions making the soil mass boil. This results in loss of shear resistance at the toe of dam and may result in dam failure.

The fine particles present in a cohesionless soil with a high percentage of larger sized particles (medium to coarse sand and gravel), may be removed as “sand boil,” leaving the soil structure intact. This results in an increase in seepage flow without causing structural damage to soil (USBR, 2014).

The critical gradient occurs when the effective stress is zero. Critical gradient (i_c) can be expressed as

$$i_c = \gamma_b / \gamma_w \quad \text{Eq. (2-29)}$$

Where,

γ_b = Submerged unit weight of soil

γ_w = Unit weight of water

It is also expressed in the following way assuming the soil is saturated.

$$i_c = (G - 1) / (1 + e) \quad \text{Eq. (2-30)}$$

Where,

G = Specific gravity of soil

e = Void ratio of the soil

This phenomenon of boiling and heaving of soil grains only occur in cohesionless soils. Bonds between particles in most cohesive soils, make it less likely for these soils to loose strength due to seepage. Sands can typically move or become quick under an upward gradient of around 1.0, however tests have shown that clay particles may not move until threshold gradients reach higher values, even tens or hundreds. Hence, it is difficult to measure critical gradient in cohesive soils and it widely varies with percentage of fine particles, type of minerals, water content, density, etc. Hence critical gradient is only used for cohesionless soil (USBR, 2014).

Factor of safety

For cohesionless soil the factor of safety (FS) against quick condition is defined as

$$FS = i_c / i_e \quad \text{Eq. (2-31)}$$

Where,

i_c = Critical gradient

i_e = Predicted or measured exit gradient

Note: This safety factor is only a measure the possibility of boiling or heaving of cohesionless soil and do not provide the indication of safety against initiation of internal erosion.

Significant uncertainties are involved in determination of exit gradients due to lack of sufficient instruments, state of knowledge and inability to accurately model the natural foundation condition. For these reason conservative safety factor should be used when designing dams.

Table 2-6: Recommended factor of safety against critical gradient (USBR, 2014)

Recommended Factors of Safety Against Heave Type of Facility	Recommended Safety Factor
New dam	4.0
Existing dam	3.0

2.5.2.1.2 Uplift of confining soil

When a less permeable fine grained confining layer overlays a relatively pervious soil foundation, high pressure may exist in the pervious layer. If the seepage pressure in more permeable layer is higher than overburden pressure uplift (blowout) of confining layer may occur which may lead to quick condition of pervious layer below.

This situation is unlikely in a concrete gravity dam because the downstream of dam is protected by riprap to protect the downstream from erosion.

For a layer of cohesive soils, a critical exit gradient approach is not applicable to the evaluation of uplift evaluations (USBR, 2014). So, the concept of “total stress method” and “effective stress method” are used for evaluating uplift of confined layers.

The calculation of safety factor from both of these methods are similar. However, factor of safety from effective stress is more volatile in comparison to that from total stress method (USBR, 2014). Hence, USBR recommends the use of total stress method. Further discussion and illustration of calculation of safety factor by both the methods and their comparison can be found on USBR Design Standards No. 13 “Embankment Dams”. The factor of safety by total stress method is expressed as

$$F = \gamma_t \times t / \gamma_w \times h_p \quad \text{Eq. (2-32)}$$

Where:

- γ_t = Unit weight of the confining soil
 t = Vertical thickness of the confining layer
 γ_w = Unit weight of water
 h_p = Pressure head at the top of the pervious layer

Factor of safety

The factor of safety calculated from above formula do not account for the shear strength and cohesion of the confining layer however to cause uplift of clay layer, the uplift pressure should overcome cohesive strength of clay. Most evaluations discount the ability of clay layer to act against uplift failure because of lack of efficient ways of calculation it and lack information on piezometric levels (USBR, 2014).

Table 2-7: Recommended factor of safety against heaving (USBR, 2014)

Recommended Factors of Safety Against Uplift Type of Facility	Recommended Safety Factor
New dams	2.0
Existing dams	1.5

2.5.2.2 Unfiltered internal gradients

The internal gradients are different at different places along the seepage path due to heterogeneous nature of soil. In addition, the seepage path is never straight rather it is quite haphazard. So, different head loss occurs at different places along the seepage path. Hence there are a lot of uncertainties involved in determining the internal gradient through foundation soil and it is difficult to determine actual internal gradients. However, the use of numerical models helps in estimating important aspects of seepage behavior.

Lab experiments on clean fine sand and analysis of cases of dam failures from USBR have shown that internal erosion may be initiated by an internal gradient of as low as 0.02 to 0.08 which are much lower than the critical exit gradient of 1 as discussed in 2.5.2.1.

The potential for internal erosion is difficult to estimate therefore, all failure modes due to high internal gradient should carefully considered. According to USBR Design Standards No. 13 “Embankment Dams”, following are the areas that should be carefully to ensure no internal erosion within the foundation:

- Seepage through non-plastic, and highly erodible soils.
- Seepage along outlet works.
- Toe drains and appurtenant structure.
- Seepage along soil concrete interface.
- Horizontal seepage pathway with little obstruction
- Dams without fully penetrating foundation cutoffs

The following failure types may occur due to internal erosion.

2.5.2.2.1 Piping

Piping starts at the exit point and it erodes backward through the foundation. For piping to occur following conditions should be satisfied: (1) concentrated leakage water (2) an unprotected seepage exit point, (3) erodible material in the flow path, and (4) soil material being eroded should be capable of supporting a pipe or a roof (Von Thun, 1996) . If all of these conditions are met, piping will initiate which leads to uncontrolled erosion and eventually dam failure.

2.5.2.2.2 Internal migration

When the soil cannot sustain roof then the void created by erosion of soil materials in the pipe collapses. This mechanism has two important actions; it helps in healing of pipes and thus after collapse of void the piping action stops or void collapse occurs repeatedly until the void shortens and leads to uncontrolled erosion.

To evaluate the potential for initiation of erosion risk analysis of various failure modes of internal erosion can be done. A good reference for that is chapter on internal erosion in the *Best Practices in Dam and Levee Safety Risk Analysis* training manual by US Army Corps of Engineers. (Engineers) (Engineers) (Engineers) (Engineers) (Engineers) (Engineers) (Engineers) (Engineers)

2.5.2.3 Excessive seepage flow

Seepage flow through a dam foundation is acceptable if it does not affect the stability of dam. However high seepage flow may cause economic impact to the project. In addition, internal erosion is likely in a foundation with high seepage.

2.5.2.4 Differential settlement cracking

A number of factors influence the settlement of dam foundation and the presence of water affects the settlement behavior. Settlement is explained more in 2.4.

2.5.3 Method of analysis of seepage

Several graphical and numerical methods have been developed for analyzing seepage through permeable media based upon Darcy's Law and Laplace equation.

2.5.3.1 Graphical Method

The most widely used graphical method to analyze seepage is flow nets. It is a 2-D model. The flow discharge, pore pressure and hydraulic gradient can be estimated by using flow net.

A flow net consists of two sets of lines; flow lines and equipotential lines which must always be perpendicular to each other. Flow lines, indicates the flow direction, and equipotential lines show the distribution of water head. Flow nets are sketched through trial-and-error process.

Flow net method has some limitations as well. It requires experience to construct the flow net accurately, especially where foundations are stratified and where drains are installed. Experience has shown that piping failures are very much influenced by the grain size distribution of soil and that piping failures mostly occur after some time of operation. These failures are often a result of seepage through geological weakness in foundation soil. These types of failure cannot be analyzed by flow nets or other theoretical methods (USBR, 1987). Flow net method is best applied for simple and homogeneous systems.

2.5.3.2 Physical Model

When the foundation soil is downscaled, the soil grains often end up in cohesive range. Also, due to involvement of a lot of parameters and boundary conditions physical model cannot truly represent the field condition. Due to availability of powerful numerical models it has been possible to estimate seepage through soil with less cost and time. So, physical models are typically no longer used.

2.5.3.3 Numerical Model

Finite element models can simulate seepage flow with reasonable accuracy provided that all the input parameters and boundary conditions are defined accurately. Finite element models like PLAXIS can be used for seepage evaluation.

2.6 Bearing capacity

Concrete dams should be designed such that no stress developed should exceed the allowable stress both in concrete and in foundation. The compressive stresses developed in a gravity dam by primary loads are very low and seldom exceeds the strength of concrete. However, no tensile

stresses are permitted in a concrete gravity dam. Hence, the resultant force should lie within the middle one third of length of base of dam to avoid tensile stresses.

Designing a dam to account for induced settlements usually addresses all concerns except when the entire dam is underlain by a non rigid foundation such as soft clays or has vertical leachate sump risers in the design.

For foundation soil the stresses developed should not exceed the allowable bearing stress. Allowable bearing stress is obtained by dividing ultimate bearing stress by factor of safety.

$$\text{Allowable bearing capacity } (q_a) = q_u / FS \quad \text{Eq. (2-33)}$$

FS = factor of safety

q_u = ultimate bearing capacity

Factor of safety selected depends on the extent of information available on soil materials. Generally a factor of safety ≥ 2.5 is used but it should never be less than 2. (Engineers, 1992)

The ultimate bearing capacity is given by general bearing equation;

$$q_f = cN_c s_c d_c i_c + \gamma D N_q s_q d_q i_q + \frac{1}{2} \gamma B N_\gamma s_\gamma d_\gamma i_\gamma \quad \text{Eq. (2-34)}$$

Where,

c = cohesion of soil (c' for drained conditions, c_u for undrained conditions)

γ = unit weight of soil (value depends on position of Water table)

N_c, N_q, N_γ = bearing capacity factors, which depend on the value of friction angle, ϕ

s_c, s_q, s_γ = shape factors (to take account of the shape of the foundation)

d_c, d_q, d_γ = depth factors (to take account of the depth of embedment below GL)

i_c, i_q, i_γ = inclination factors (to take account of the inclination of the applied load from the vertical)

Terzaghi, Meyerhof, Hansen and Vesic have provided models to find the solution of general bearing capacity equation. Each of these models have different capabilities for considering foundation geometry and soil conditions. If practical it is recommended to use two or more models for each design case to increase confidence in the bearing capacity analyses. (Engineers, 1992). For different factors for calculation of ultimate bearing capacity Engineering Manual EM 1110-1-1905 can be referred.

2.7 Liquefaction

2.7.1 Introduction

Liquefaction is a phenomenon occurring during an earthquake where a saturated or partially saturated soil, tends to lose its strength to a point where it is unable to support structure or remain unstable due to generation of excess pore pressure. Liquefaction phenomenon can be divided into two main groups: Flow liquefaction and cyclic mobility.

Flow liquefaction:

This type of liquefaction occurs when the static shear stress of soil is greater than the shear strength of soil in liquefied state (Ref. Figure 2-7). The deformation produced during liquefaction are driven by static shear stress. Failure due to flow liquefaction sudden in nature, and liquefied materials can move to large distances.

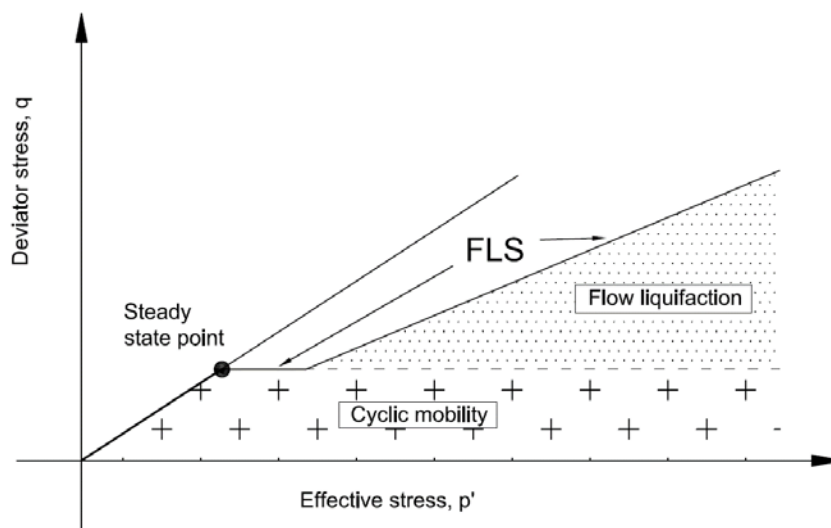


Figure 2-7: Zone of susceptibility of different types of liquefaction

Cyclic Mobility:

This type of liquefaction occurs when the static shear stress of soil is less than the shear strength of liquefied soil (Ref. Figure 2-7). This phenomenon can also produce large permanent deformations during earthquake. The deformation produced are driven by both cyclic and static stresses. Level-ground liquefaction is a special case of cyclic mobility which are caused by upward flow of water that occurs when excess pore pressure developed by cyclic loading dissipates. Level-ground liquefaction are characterized by excessive vertical and presence of sand boils.

There are enough evidences of damage to dams due to liquefaction during past earthquake events. Small concrete dams on river valley are often founded on sands and alluvial deposits

susceptible for liquefaction. So, an analysis of susceptibility and hazards needs to be addressed in the design of dams on soil foundation.

The assessment of potential liquefaction involves two questions:

1. Will liquefaction be triggered?
2. What are the possible consequences of liquefaction?

2.7.2 Liquefaction susceptibility

Not all soils are susceptible to liquefaction. Liquefaction susceptibility of a soil depends on historical, geological, compositional criteria and state of soil. The possibility of a soil to liquefy and magnitude of its effect depends on the distribution of cohesionless sediments and ground water table (Idriss and Boulanger, 2008). Generally, liquefaction has mostly been observed occurring within a few meters from ground surface. According to Idriss and Boulanger, 2008 Sst and sensitive cohesive sediments can also develop significant ground deformations during earthquake (Idriss and Boulanger, 2008).

Liquefaction susceptibility of different soils of different origin after (Youd and Perkins, 1978) is presented in [Table 2-8](#).

Table 2-8: Susceptibility of soil deposits to liquefaction during strong seismic shaking (Youd and Perkins, 1978)

Type of deposit	Distribution of cohesionless sediments in deposit	Likelihood that cohesionless sediments, when saturated, would be susceptible to liquefaction			
		< 500 years	Holocene	Pleistocene	Pre-Pleistocene
Continental					
River channel	Locally variable	Very high	High	Low	Very low
Floodplain	Locally variable	High	Moderate	Low	Very low
Alluvial fan	Widespread	Moderate	Low	Low	Very low
Marine	Widespread	—	Low	Very low	Very low
Delta and fan	Widespread	High	Moderate	Low	Very low
Lacustrine and	Variable	High	Moderate	Low	Very low
Colluvium	Variable	High	Moderate	Low	Very low
Talus	Widespread	Low	Low	Very low	Very low
Dunes	Widespread	High	Moderate	Low	Very low
Loess	Variable	High	High	High	Unknown
Glacial till	Variable	Low	Low	Very low	Very low
Tuff	Rare	Low	Low	Very low	Very low
Tephra	Widespread	High	High	?	?

Residual soils	Rare	Low	Low	Very low	Very low
Sebkha	Locally variable	High	Moderate	Low	Very low
Artificial fill					
Uncompacted	Variable	Very high	—	—	—
Compacted fill	Variable	Low	—	—	—

2.7.3 Preliminary screening of liquefaction hazard

According to (Martin and Lew, 1999) the following screening criteria may be applied to determine if further quantitative evaluation of liquefaction hazard potential is required or not:

- Liquefaction studies are not required if the estimated maximum ground water level is lower than 15 meters below the existing ground surface or proposed finished grade.
- Liquefaction assessments are not required if the corrected SPT blow count, $(N_1)_{60}$, is greater than or equal to 30 in all samples. For cone penetration test, the corrected CPT tip resistance, q_{cIN} , should not be less than 160 in all soundings.
- Clay materials are considered as non-liquefiable. However, clayey soils can be considered susceptible to liquefaction if it fulfills the following characteristics based on the “Chinese Criteria,” (Seed and Idriss, 1982):
 - Fraction finer than 0.005 mm $\leq 15\%$
 - Liquid limit, LL $\leq 35\%$
 - Natural water content ≥ 0.9 LL
 - Liquidity index ≤ 0.75

If a soil investigated shows that liquefaction hazard is not possible based on above parameters then no further analysis should be done. If not, detailed evaluation should be done to assess the liquefaction hazards.

2.7.4 Evaluation of liquefaction

Several approaches have been proposed for assessing the potential for liquefaction. Stress-based approach is the most widely used, which compares cyclic stresses with the cyclic resistance of the soil. Strain-based and energy-based approaches are also in practice but they are less common and greater uncertainties are involved in those approaches hence they are not advisable to use unless extensive field investigation of input parameters have been done. They are therefore not covered in here. These approaches can be referred to (Kramer, 1996).

2.7.4.1 Cyclic stress approach

In this approach the earthquake induced cyclic shear stress is compared with the liquefaction resistance of the soil. Liquefaction is expected where the induced stress exceeds the soil resistance. The earthquake induced cyclic stress is estimated using Seed-Idriss simplified procedure.

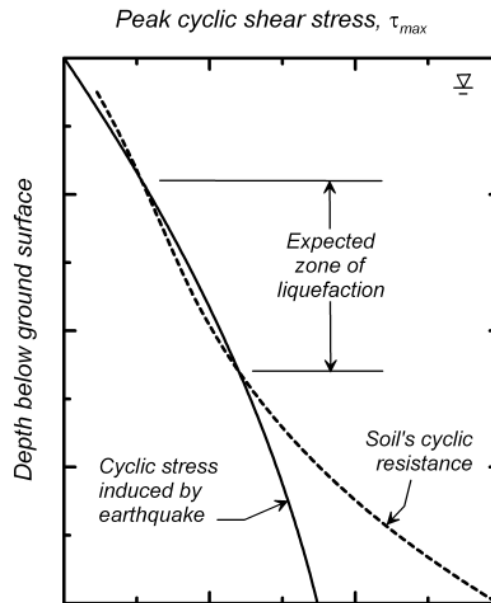


Figure 2-8: Schematic diagram of expected zone of liquefaction by comparing cyclic stress and cyclic resistance of soil. (Idriss and Boulanger, 2008)

2.7.4.2 Cyclic loading due to earthquake

According to Seed and Idriss (1971), the cyclic stress ratio (CSR) induced by earthquake is given as

$$CSR = 0.65 \frac{a_{max}}{g} \frac{\sigma_v}{\sigma'_v} \frac{r_d}{MSF}$$

Eq. (2-35)

Where,

a_{max} = Peak horizontal acceleration at ground

g = Acceleration due to gravity

σ_v = Total vertical stress

σ'_v = Effective vertical stress

r_d = Stress reduction coefficient

MSF = Magnitude scaling factor

Magnitude scaling factor

Magnitude scaling factor is a factor that accounts for the duration of ground motion by empirical correlations with magnitude. It is a factor used to adjust the cyclic stresses to a common value of earthquake of magnitude of 7.5. Mathematically, MSF is defined as (Idriss and Boulanger, 2008)

$$MSF = \frac{CRR_M}{CRR_{M=7.5}}$$

The magnitude scaling factors proposed by different researchers are shown in Figure 2-9. However, researchers in 1996 NCEER and 1998 NCEER/NSF workshops (Ref. (Youd et al., 2001)) recommended a range of values of MSF. For magnitudes <7.5, the average of range of MSF proposed in the workshop is given by Eq. (2-36).

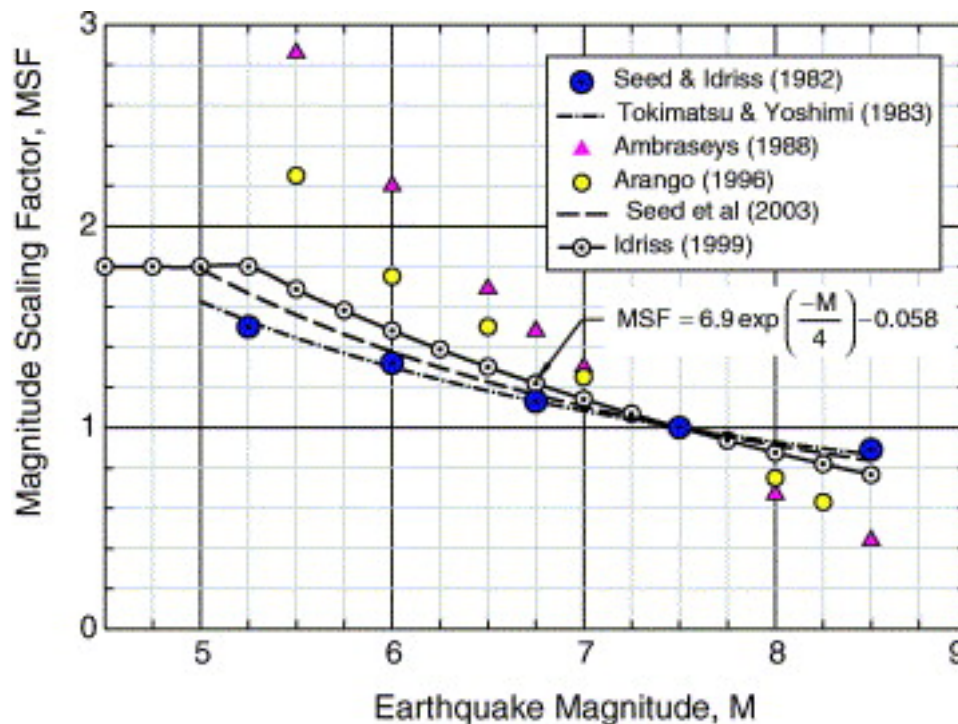


Figure 2-9: Magnitude scaling factor after different researchers (Idriss and Boulanger, 2006)

Table 2-9: Mean MSF of the range suggested at NCEER workshop, and MSF suggested by Idriss and Boulanger

NCEER (Youd et al., 2001)	(Idriss and Boulanger, 2006)
$MSF = \begin{cases} \left(\frac{7.5}{M_w}\right)^{-2.95} & M_w \leq 7.5 \\ \left(\frac{7.5}{M_w}\right)^{-2.56} & M_w > 7.5 \end{cases}$ <p style="text-align: center;">Eq. (2-36)</p>	$MSF = \begin{cases} 6.9 \exp(-M/4) - 0.058 \\ \leq 1.8 \end{cases}$ <p style="text-align: center;">Eq. (2-37)</p>

Stress reduction coefficient, r_d

This coefficient accounts for the reduction in shear stress with depth and magnitude of earthquake. This can be calculated by using the relation in Table 2-10.

Table 2-10: Stress reduction coefficient after different researchers

<p>NCEER (Youd et al., 2001)</p>	$r_d = \frac{(1 - 0.4113z^{0.5} + 0.04052z + 0.001753z^{1.5})}{(1 - 0.4177z^{0.5} + 0.05729z - 0.006205z^{1.5} + 0.00121z^2)}$ <p style="text-align: right;">Eq. (2-38)</p> <p>Where, z = depth below ground surface in meters</p>
<p>(Idriss and Boulanger, 2006)</p>	$r_d = \exp[\alpha_{(z)} + \beta_{(z)}M]$ <p style="text-align: right;">Eq. (2-39)</p> <p>Where, $\alpha_{(z)} = -1.012 - 1.126 \sin\left(\frac{z}{11.73} + 5.133\right)$ $\beta_{(z)} = 0.106 + 0.118 \sin\left(\frac{z}{11.28} + 5.142\right)$ z = depth below ground surface in meters, $\leq 20\text{m}$, if $z > 20\text{m}$, site specific response analysis should be done. M= magnitude of earthquake</p>

The variation of stress reduction factor with depth and earthquake magnitude after Idriss and Boulanger, 2006 is shown in Figure 2-10.

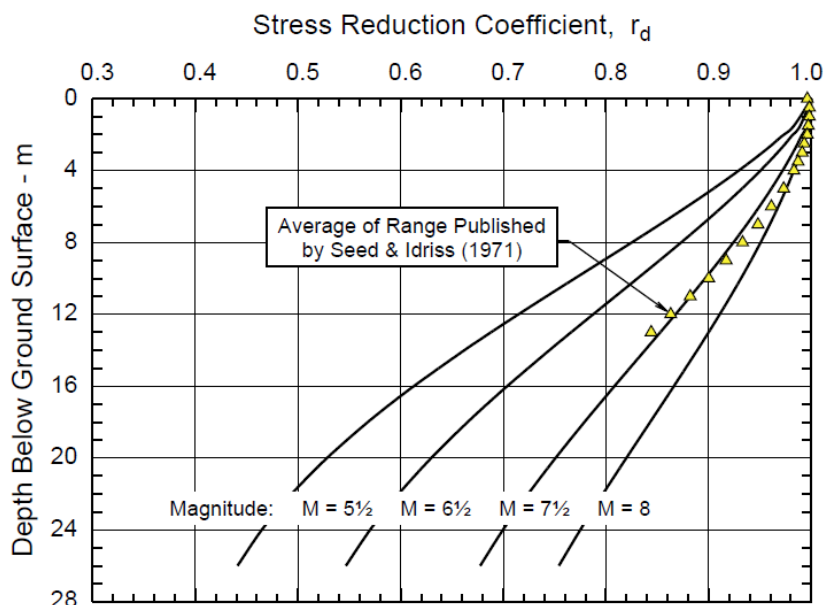


Figure 2-10: Variation of stress reduction coefficient with depth and earthquake (Idriss and Boulanger, 2006)

2.7.4.3 Resistance of soil to cyclic loading

Several researchers have correlated the resistance to liquefaction of soil with SPT and CPT tests with the former being more popular. Also, sample can be obtained in SPT for determining physical properties of soil. Hence, it is advisable to use SPT based procedure. For CPT based procedure standard geotechnical literatures can be referred.

Calculation of CRR based on SPT data

The process of finding resistance of soil based on SPT data is given below.

1. Study foundation soil and groundwater conditions in detail. SPT and CPT procedures are widely used for understanding soil properties. Correct the SPT value with corresponding correction coefficients to get normalized SPT blow count. Correction factors and procedures can be referred to (Idriss and Boulanger, 2008)
2. Calculate the clean sand corrected SPT resistance.

Table 2-11: SPT value calculation for clean sand

NCEER (Youd et al., 2001)	$(N_1)_{60,cs} = \alpha + \beta(N_1)_{60}$
	Where,
	$\alpha = \begin{cases} 0 & FC \leq 5\% \\ \exp(1.76 - 190/FC^2) & 5\% < FC < 35\% \\ 1 & FC \geq 35\% \end{cases}$
	$\beta = \begin{cases} 1 & FC \leq 5\% \\ 0.99 + FC^{1.5}/1000 & 5\% < FC < 35\% \\ 1.2 & FC \geq 35\% \end{cases}$
	FC = fine content in %

Idriss and Boulanger, 2006	$(N_1)_{60,cs} = (N_1)_{60} + \Delta(N_1)_{60}$ <p>Where,</p> $\Delta(N_1)_{60} = \exp \left[1.63 + \frac{9.7}{FC} - \left(\frac{15.7}{FC} \right)^2 \right]$
-----------------------------------	---

3. Calculate the cyclic resistance of soil at an effective vertical stress of 1 atm.

Table 2-12: Cyclic resistance ratio for effective vertical stress=1atm

NCEER (Youd et al., 2001)	$CRR_{M=7.5, \sigma'_v=1} = \frac{1}{34 - (N_1)_{60,cs}} + \frac{(N_1)_{60,cs}}{135} + \frac{50}{(10(N_1)_{60,cs} + 45)^2} - \frac{1}{200}$ <p>Note: This model is only applicable when $(N_1)_{60} < 30$. If $(N_1)_{60} \geq 30$ sand is too dense to liquefy. (Youd et al., 2001)</p>
Idriss and Boulanger, 2006	$CRR_{M=7.5, \sigma'_v=1} = \exp \left(\frac{(N_1)_{60,cs}}{14.1} + \left(\frac{(N_1)_{60,cs}}{126} \right)^2 - \left(\frac{(N_1)_{60,cs}}{23.6} \right)^3 + \left(\frac{(N_1)_{60,cs}}{25.4} \right)^4 - 2.8 \right)$

4. Calculate the cyclic resistance ratio for insitu vertical stresses.

Cyclic resistance ratio for insitu stresses is calculated by multiplying CRR at effective stress of 1 atmosphere with overburden correction factor K_σ .

$$CRR_{\sigma'_v} = CRR_{\sigma'_v=1} K_\sigma \quad \text{Eq. (2-40)}$$

Where, K_σ is calculated as presented in Table 2-13.

Table 2-13: Calculation of overburden correction factor

NCEER (Youd et al., 2001)	$K_\sigma = \min \left\{ \left(\frac{\sigma'_v}{p_a} \right)^{f-1}, 1.0 \right\}$ <p>Where,</p> $f = \begin{cases} 0.7 - 0.8 & \text{for } D_r = 40 - 60\% \\ 0.6 - 0.7 & \text{for } D_r = 60 - 80\% \end{cases}$ <p>p_a = atmospheric pressure</p>
----------------------------------	--

Idriss and Boulanger, 2006	$K_{\sigma} = \min \left\{ \begin{array}{l} 1 - C_{\sigma} \ln \left(\frac{\sigma'_{v}}{p_a} \right) \\ 1.0 \end{array} \right\}$ <p>Where,</p> $C_{\sigma} = \frac{1}{18.9 - 2.55\sqrt{(N_1)_{60,cs}}}, \quad (N_1)_{60,cs} \leq 37$
-----------------------------------	--

2.7.4.4 Evaluation of triggering of liquefaction

The factor of safety against triggering of liquefaction is calculated by taking the ratio of CRR to earthquake induced CSR;

$$FOS = \frac{CRR_{M,\sigma'_v}}{CSR_{M,\sigma'_v}}$$

Eq. (2-41)

2.7.5 Effects of Liquefaction

Liquefaction can have large range of effects depending on the soil type, earthquake loading and nature of structure. For concrete dams on soil foundation, the following consequences should be looked upon.

- Post liquefaction reconsolidation settlement.
- Lateral spreading of gently sloping ground
- Instability of slopes of side banks due to loss of shear strength. (*Note: This is not discussed in this thesis*)

2.7.5.1 Post liquefaction reconsolidation settlement

Several researchers have proposed relationships to estimate post liquefaction reconsolidation settlement based on laboratory studies and field studies. These relationships correlate penetration resistance and earthquake induced cyclic stress ratio with volumetric strains.

Calculation steps

1. Determine SPT resistance and fine content of all potentially liquefiable soils.
2. Correct the SPT resistance for deviations from standard equipment and procedures by applying appropriate coefficients.
3. Compute volumetric strain (ε_v) for each soil sublayer using the curves in [Figure 2-12](#), [Figure 2-11](#) and [Figure 2-13](#) and estimate settlement for each sublayer.
4. Compute expected settlement by summing settlement in all sublayers.

$$\Delta H = \sum_{i=1}^n t_i \varepsilon_v$$

Where, n is the number of sublayers.

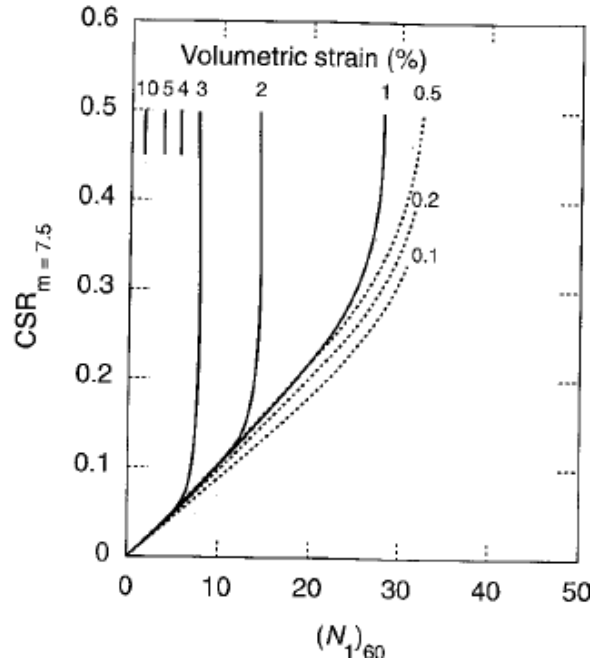


Figure 2-11: Variation of volumetric strain in saturated sand with SPT and CSR (After Tokimatsu and Seed, 1987) (Kramer, 1996)

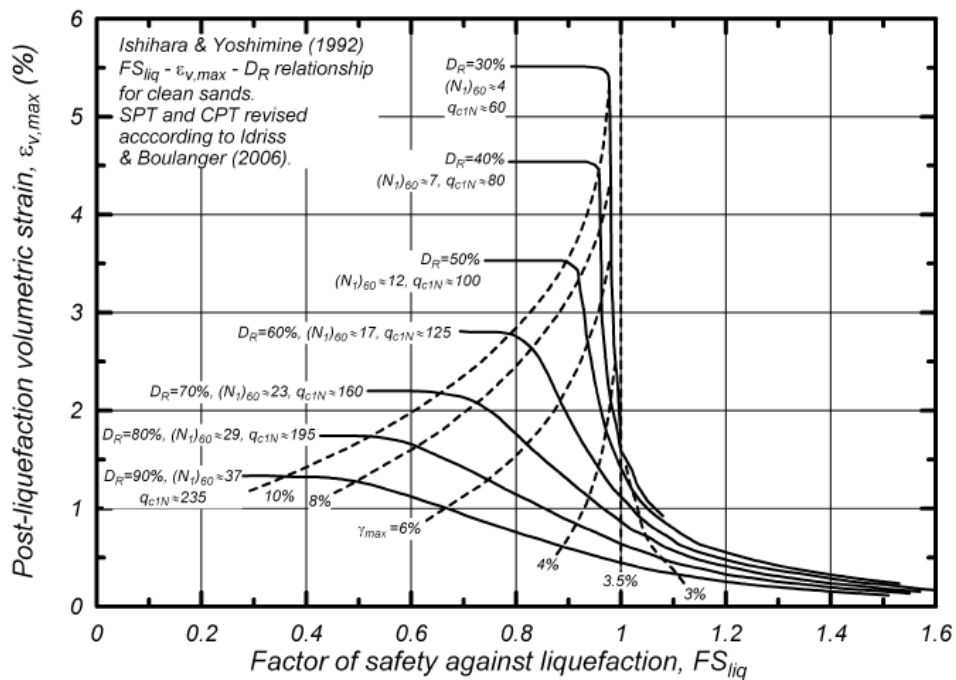


Figure 2-12: Variation of volumetric strain with factor of safety against liquefaction for clean sand, SPT and relative density after Ishihara and Yoshimine 1992 (Idriss and Boulanger, 2008)

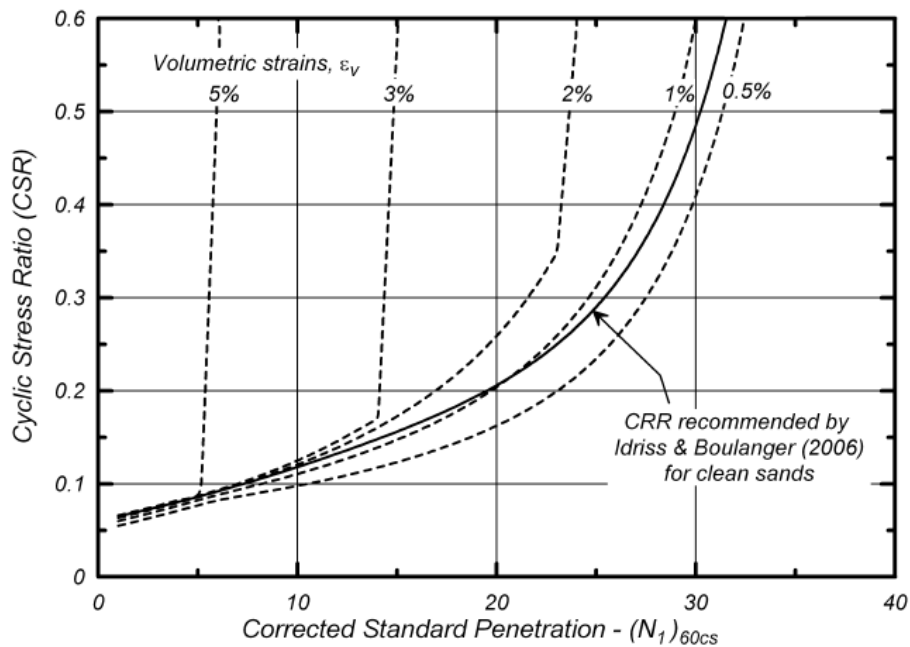


Figure 2-13: Variation of volumetric strain with SPT resistance and CSR for clean sand (Idriss and Boulanger, 2008)

Discussion

The post-liquefaction settlement estimation procedures discussed above predict average settlements of a group of case histories with about equal accuracy. However, they predict settlements of different case histories differently. Figure 2-14 illustrates the deviation of volumetric strains by calculated by different methods. Hence, using the average of all procedures, therefore, has the potential to improve prediction accuracy.

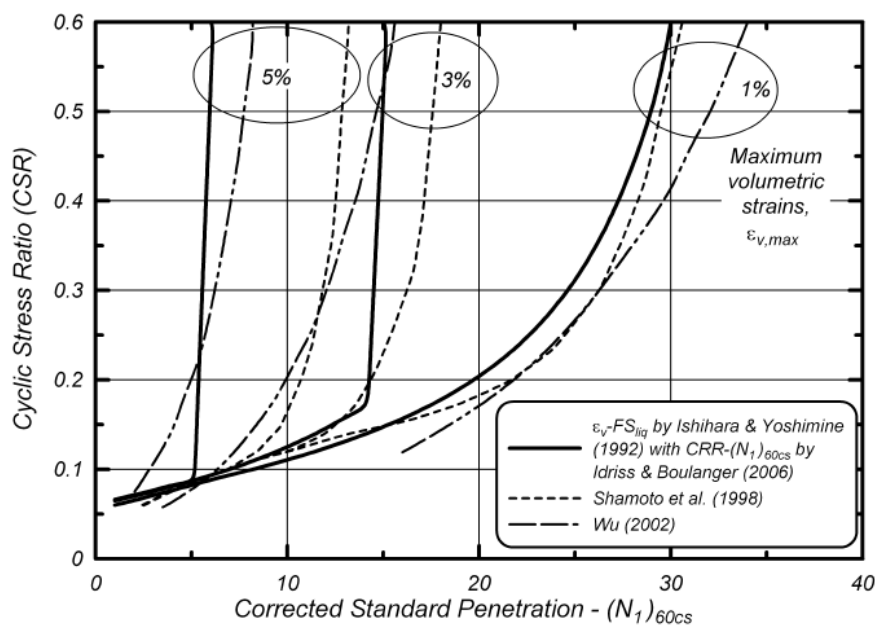


Figure 2-14: Comparison of Volumetric strain by different models (Idriss and Boulanger, 2008)

2.7.5.2 Lateral spreading

Liquefaction-induced lateral spreading occurs in gently sloping ground and in the vicinity of a free face. The driving stress for lateral spreading during an earthquake is cyclic mobility. The mechanisms of lateral spreading are very complex and are highly dependent on soil conditions and ground shaking.

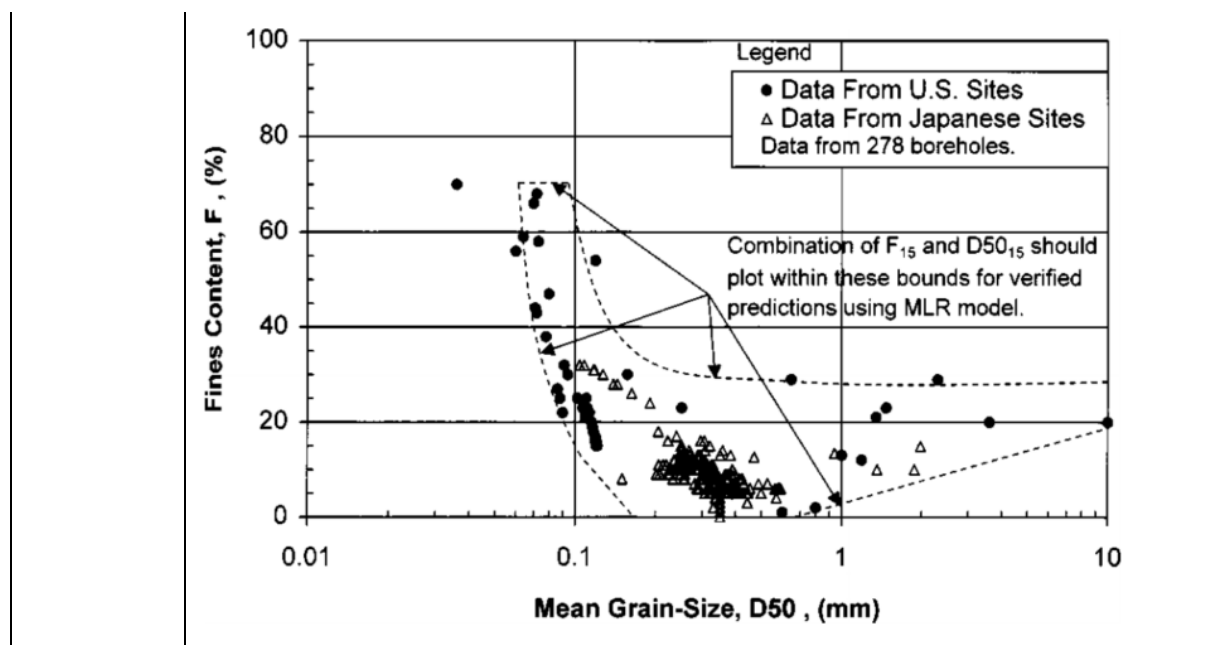
Several approaches for estimation of lateral spreading deformation have been developed based on empirical correlations, lab investigations and rigid block models. However, only empirical methods for predicting lateral displacements are presented in this chapter which are based on statistical regression to develop equations for predicting lateral displacements. Though there will be little deformation even if liquefaction do not occur, the models presented are only applicable when liquefaction occurs during an earthquake.

2.7.5.2.1 Youd et al. (2002)

According to (Youd et al., 2002) soils having SPT $(N_1)_{60}$ values greater than 15 are too dense for lateral spread to occur. The conditions of applicability of Youd et al. model is presented in [Table 2-14](#).

Table 2-14: Conditions of applicability of (Youd et al., 2002) (Kramer, 2008)

Parameter	Description	Range of applicability
T_{15}	Equivalent thickness of saturated cohesionless soils (clay content $\leq 15\%$) in m.	1 to 15 m
M	Moment magnitude of the earthquake.	6.0 to 8.0
Z_T	Depth to top of shallowest layer contributing to T_{15} .	1 to 15 m
W	Free face ratio.	1 to 20 %
S	Ground slope.	0.1 to 6 %
F_{15} , $D_{50_{15}}$	Fine content (F_{15}) % and mean grain size (D_{50}) should fall within the limit defined by dotted lines in the figure.	



The expected vertical displacement can be calculated by using the following equation:

$$\log D_H = b_0 + b_1 M + b_2 \log R^* + b_3 R + b_4 \log W + b_5 \log S + b_6 \log T_{15} + b_7 \log(100 - F_{15}) + b_8 \log(D50_{15} + 0.1)$$

Eq. (2-42)

Where,

- D_H = lateral displacement in meters
- b = regression coefficients

Table 2-15: Regression coefficients (Kramer, 2008)

Model	b_0	b_1	b_2	b_3	b_4	b_5	b_6	b_7	b_8
Ground Slope	-16.213	1.532	-1.406	-0.012	0.000	0.338	0.540	3.413	-0.795
Free face	-16.713	1.532	-1.406	-0.012	0.592	0.000	0.540	3.413	-0.795

- M = earthquake magnitude
- $R^* = R + 10^{-0.89M-5.64}$
- R = Earthquake source to site distance
- W = free face ratio, $W = H/L$
- H = Height of free face
- L = length from site to free face
- S = ground slope

T_{15} = Equivalent thickness of liquefiable material contributing to lateral deformations ($N < 15$)

F_{15} = Fines content

$D_{50_{15}}$ = mean grain size

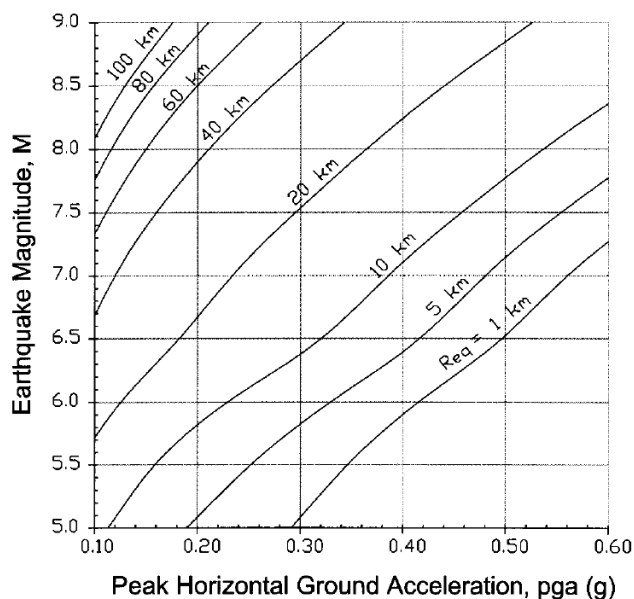


Figure 2-15: Source distance (R) based on PGA and earthquake magnitude (M) after Bartlett and Youd 1992,1995. (Youd et al., 2002)

2.7.5.2.2 Kramer and Baska model

This method is based on nonlinear regression analysis and was calibrated to field data for lateral spreading. Similar to Youd et al. model, this model is also applicable to certain range of input parameters which are given in Table 2-16. If the model is applicable following steps can be followed to estimate the vertical settlement due to lateral spreading.

Table 2-16: Condition of applicability of Kramer and Baska model (Kramer, 2008)

Variable	Description	Range
T^*	Equivalent thickness of saturated cohesionless soils in m	0.001 to 20m
M_w	Moment magnitude of the earthquake	6.0 to 8.0
R	Distance from the site to the hypocenter of the earthquake in km.	0 to 100km
W	Free face ratio (height of free face/distance to the free face from the point of displacement) in percentage.	$\leq 20\%$
S	Ground slope in percent.	0 to 6%

1. Find the ground parameters, slope inclination. S , for ground slope case or free-face ratio, W , for free face case.
2. Find the design earthquake magnitude and distance to earthquake source R .
3. Determine the average SPT resistance and fine content for each layer. It is advisable to use maxim 1m thickness for each layer.
4. Determine the clean sand corrected resistance by:

$$(N_1)_{60,cs} = \alpha + \beta(N_1)_{60} \quad \text{Eq. (2-43)}$$

Where,

$$\alpha = \begin{cases} 0 & FC \leq 5\% \\ \exp(1.76 - 190/FC^2) & 5\% < FC < 35\% \\ 1 & FC \geq 35\% \end{cases}$$

$$\beta = \begin{cases} 1 & FC \leq 5\% \\ 0.99 + FC^{1.5}/1000 & 5\% < FC < 35\% \\ 1.2 & FC \geq 35\% \end{cases}$$

FC = fine content in %

5. Compute thickness parameters for ground slope site (T_{gs}^*) or free face site (T_{ff}^*) for each sublayer using following equations

$$T_{gs}^* = 2.586 \sum_{i=1}^n t_i \exp(-0.05N_i - 0.04Z_i) \geq 0.001m$$

$$T_{ff}^* = 5.474 \sum_{i=1}^n t_i \exp(-0.08N_i - 0.10Z_i) \geq 0.001m$$

Eq. (2-44)

Where Z_i and t_i are the depth to and thickness of each sublayer.

6. Calculate mean lateral displacement $\overline{D_H}$ using the following equation

$$\overline{D_H} = \begin{cases} 0 & \text{for } \sqrt{D_H} \leq 0 \\ (\sqrt{D_H})^2 & \text{for } \sqrt{D_H} > 0 \end{cases}$$

Eq. (2-45)

Where,

$$\sqrt{\overline{D_H}} = \frac{\beta_1 + \beta_2 T_{gs}^* + \beta_3 T_{ff}^* + 1.231M - 1.151 \log R^* - 0.01R + \beta_4 \sqrt{S} + \beta_5 \log W}{1 + 0.0223(\beta_2/T_{gs}^*)^2 + 0.0135(\beta_3/T_{ff}^*)^2}$$

$$R^* = R + 10^{-0.89M-5.64}$$

R = Distance of hypocenter from site in km

M = Earthquake magnitude

W = Free face ratio (height of free face/distance to free face from site)

S = Ground slope in %

β = Regression coefficients

Coefficient	β_1	β_2	β_3	β_4	β_5
Ground Slope	-7.207	0.067	0	0.544	0
Free face	-7.518	0	0.086	0	1.007

3 Upper Tamakoshi Hydroelectric project

Upper Tamakoshi hydropower project is a peaking runoff the river power plant located in Dolakha district, 197 km east of Kathmandu. Under completion, this will be the largest power plant in Nepal with an installed capacity of 456 MW. A 22 m high and 60 m wide dam diverts Tamakoshi river through a 35 m long intake into the headrace. The dam creates a reservoir of 2 km long producing a live storage of 1.2 million m³.

Design discharge of the plant is 66 m³/s. The project comprises of an 8 km long headrace tunnel, two vertical shafts and six Pelton units. It produces an annual energy of 2281 GWh.

Table 3-1: Salient features of Upper Tamakoshi Hydropower Project (UTHL, 2015)

Salient Features	
Type of Development	Peaking Run-of-River (PRoR)
Location	Lamabagar VDC, Dolakha District, Nepal
Headworks Location	Lamabagar, Lamabagar VDC
Powerhouse Location	Gongar Gaon, Lamabagar VDC
Maximum Output	456 MW
Annual Energy	2,281 GWh
Gross Head	822 m
Design Discharge	66.0 m ³ /sec
Hydrology	
Catchment Area	1,745 km ²
Min. Mean Monthly Flow	14.1 m ³ /sec.
Mean Annual Flow	67.2 m ³ /sec.
Design flood Q _{1,000}	885.0 m ³ /sec
Diversion Dam	22 m x 60.0 m (H x L)
Live Storage	1.2 Million m ³
Settling Basins	2 Nos. L=225 m
Headrace Tunnel	8.4 km (Cross Sectional Area = 32.14 m ²)

Penstock (Vertical Shaft and Horizontal Tunnel)	1,134.0 m
Power House (Underground)	142.0m x 13.0m x 25.0 m
	(L x B x H)
Number of units	6
Tailrace Tunnel	2.9 km (Cross Sectional Area = 35.0 m ²)
Access Road from Charikot of Dolakha District	68.0 km
Transmission line	220 kVA Double Circuit, 47.0 km
Construction Cost	NRs.35.29 Billion equivalent to US\$ 441 Million (Excluding Interest During Construction)
Construction Time Period	6 Years

3.1 Headworks

The dam is a concrete gravity dam. It is a 60 m long 22m high gated structure (Ref. Appendix-I for drawings). It has four sections, each 15 m long with a radial gate of 5m x 5m. A 35 m long intake is also a part of dam. The intake consists of two sections. The dam consists of a 15 m long upstream apron and a 47.5m long stilling basin downstream of dam. Sheet piles are installed from the center line of dam extending 5m deep into the soil. Furthermore, a grout curtain extending 15m deep into the soil will also be built. Drainage filters will be constructed downstream of sheet pile and a horizontal drain to transfer the seepage water will also be built as shown in figures in Appendix-I.

3.2 Geology of headworks

The dam is placed on deep layers of alluvium extending upto 100m. The dam is sitting in an area which was a reservoir before. The reservoir was formed by damming of river by rock slide some thousands years ago. With time the reservoir was filled with sediments upon which the dam is being built. Rock with steep slope is exposed on both banks of river.

3.2.1 General

According to the feasibility report drilling was carried down to a depth of maximum 46.2 m which showed alluvial deposits of dense to very dense, non-cemented sand and gravel with content of cobble and boulder. Coarse-grained soil, with little sand content, and frequent appearance of boulders, up to 460 mm in size were found in upper 10-15 m. Sand content increases with depth, but cobble and boulder are found at all depths. Average dry unit weight of foundation soil is estimated as 16.86 kN/m^3 and saturated unit weight as 20.36 kN/m^3 .

DCPT results showed a very high penetration resistance in the upper 10 m and slightly lower below. The higher content of cobble and boulder in upper layers has influenced on the results.

3.2.2 Grain size distribution

The alluvium deposit on the river plain consists of granular soil ranging in size from fine sand to boulder. The grain size distribution curve showed high percentage of coarse grained materials while fines (below 0.075 mm) are just 2 %. Grain size distribution curve for foundation materials at headworks is presented in [Figure 3-1](#).

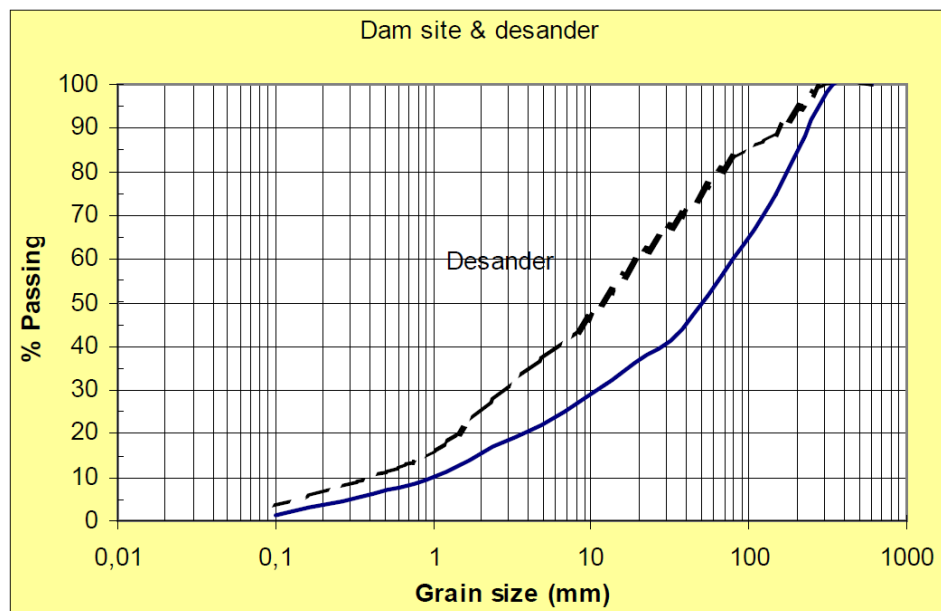


Figure 3-1: Grain size distribution for headworks area (Norconsult, 2005)

3.2.3 Permeability

Permeability in the alluvium was measured by constant head tests while in rocks it was tested by Lugeon test. Foundation material was found to have high permeability with an average of $1 \times 10^{-3} \text{ m/s}$. Generally, the vertical permeability was found to be lower than horizontal. The values of test result from constant head test in alluvium is shown in [Table 3-2](#).

Lugeon tests in rock at abutments show low permeability of rock ranging from 2-5 L.

Table 3-2: Average permeability at headworks (Norconsult, 2005)

Depth (m)	Average permeability
0-6	9.0E-04
6-12	1.6E-03
12-18	1.7E-03
18-25	6.0E-04
>25	4.0E-04
Overall Average	1.0E-03

3.2.4 Strength parameters

3.2.4.1 Friction angle

Direct strength test has been done to find the shear strength of soil. The results are shown as friction angle ϕ while the cohesion is 0 (i.e. the shear diagram curves run through origin). Average friction angle of 42-48 degrees were obtained at a normal stress of 88 to 354 kN/m². As the effective stress beneath the dam will be in the order of 150-250 kN/m² a design friction angle of 37° is considered being on conservative side of design.

3.2.5 Abutments

At right abutment fresh to moderately weathered gneiss was encountered at a depth of 1.5m. The compressive strength of the rock was found to be 16 to 50 MPa.

Left abutment comprises of moderately weathered schist to a depth of 30 m. Between 30 and 55 m partly highly weathered fragments of native rock with partly scree/colluvium and alluvial material were found. And from 50 m onwards moderately weathered schist was encountered during drilling. The questionable character of rock between 30 and 55 m depth in left bank may be due to

- The outermost 30 m is a block created by a slide in the left side of the valley, or
- The outermost 30 m is parent rock with a weakness zone below, containing scree and alluvial material.

4 Finite element model and input data preparation

4.1 Finite element modelling

PLAXIS 2D was used for modelling of foundation of the headworks. It is a two dimensional finite element model capable of analyzing deformation and seepage in geotechnical engineering. Hardening soil (HS) model was used for modelling of soil whereas Mohr-Coulomb model was used for modelling of concrete. This type of soil modelling function is based on the hyperbolic relation between deviatoric stress and axial strain as shown in Figure 4-1.

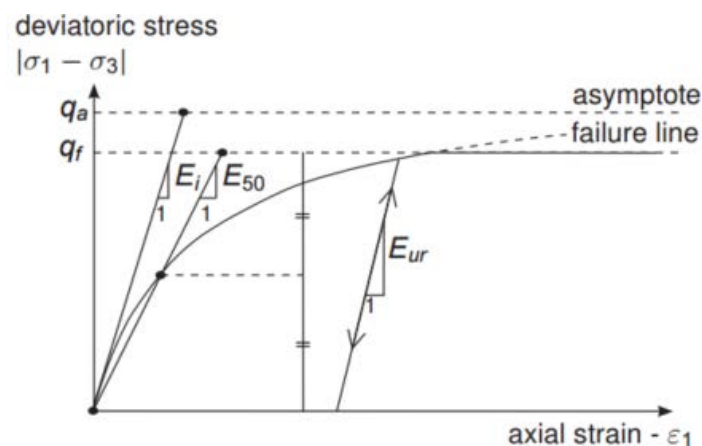


Figure 4-1: Stress strain relation between deviatoric stress and axial strain in standard drained triaxial test (Brinkgreve and Vermeer, 2002)

4.1.1 Mesh

For the mesh 15-noded triangular elements are used. The mesh as well as the nodes and the stress points are shown in the Figure 4-2 & Figure 4-3. Characteristic mesh data is given in Table 4-1.

Table 4-1: Characteristics of meshing

No. of Elements	No. of Nodes
1875	15418

4.1.2 Model development

The building of dam was simulated by a staged construction phase, where the corresponding cluster that was excavated was deactivated and concrete and other structure were added in steps with some time lag for each stage of construction. After finishing of dam construction, the dam

was filled with water at normal water level. Different stages of construction of dam as modelled in PLAXIS is shown in [Figure 4-4](#) to [Figure 4-9](#).

Each of the four dam sections was analyzed in PLAXIS 2D. Furthermore each section of dam was analyzed at three sections by modelling both edges and center of dam. Response of each dam section was taken as average at the three sections.

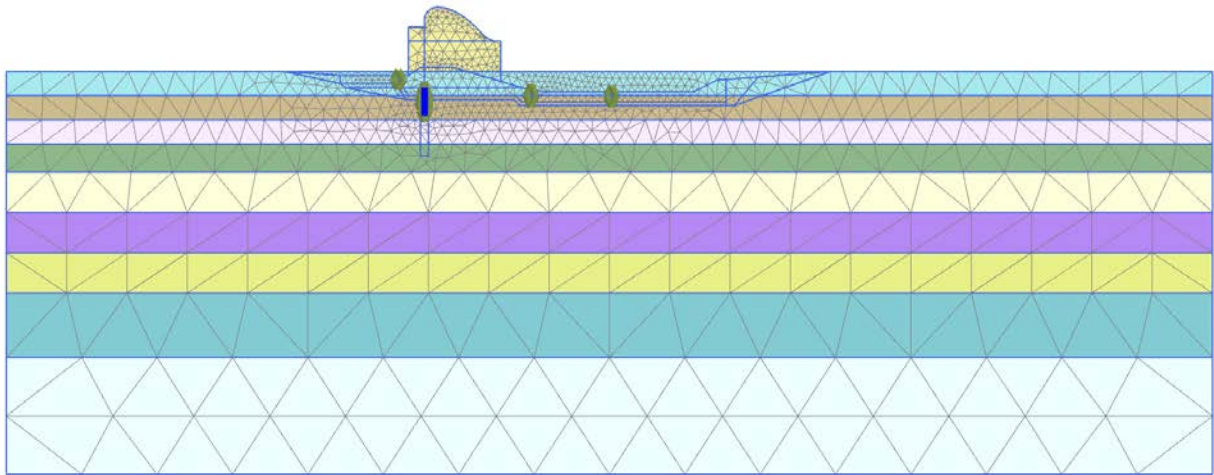


Figure 4-2: Mesh and nodes

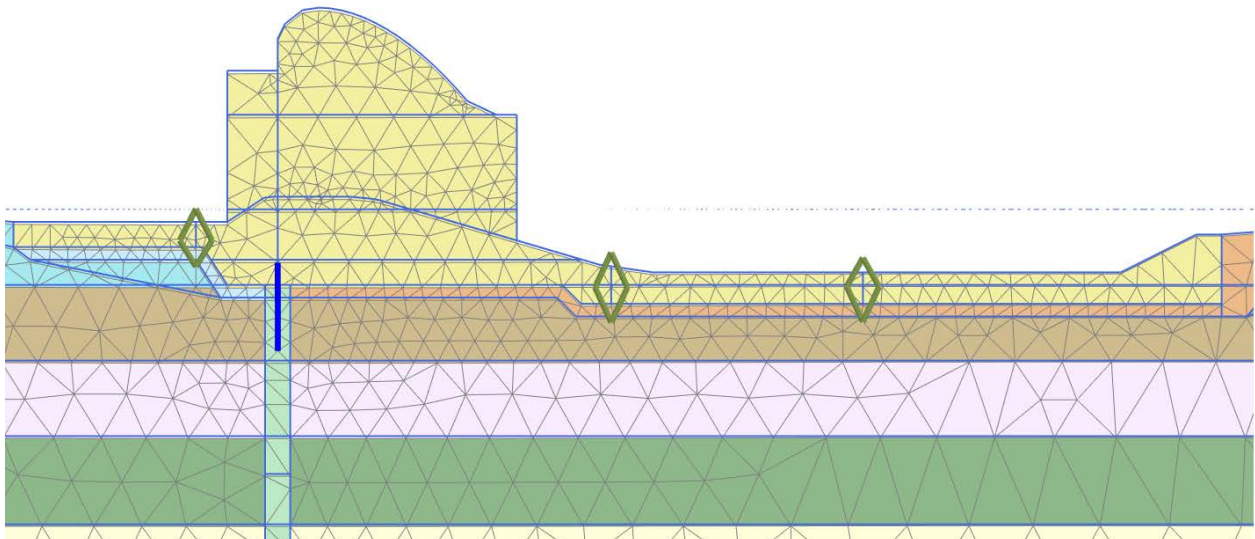


Figure 4-3: Zoomed view of mesh and nodes around dam

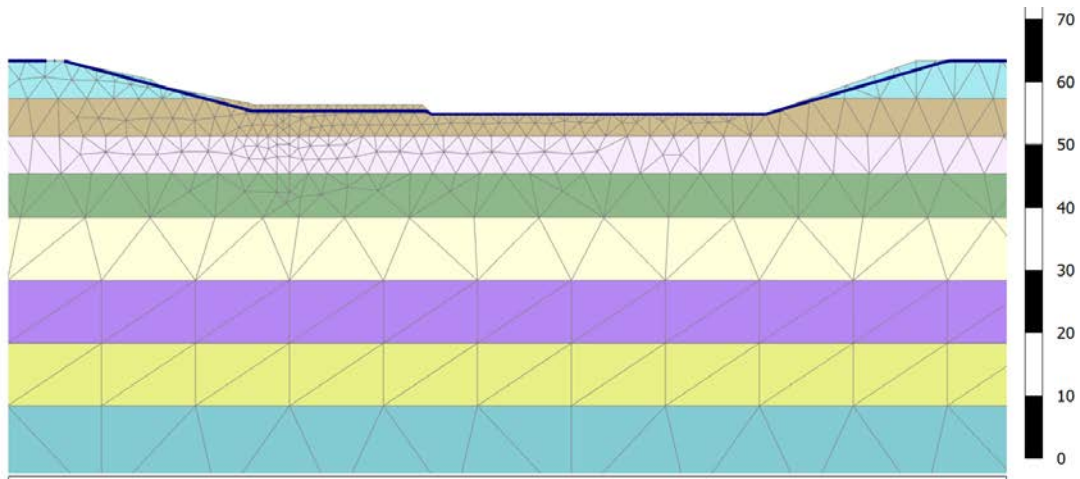


Figure 4-4: Excavation and lowering of ground water table.

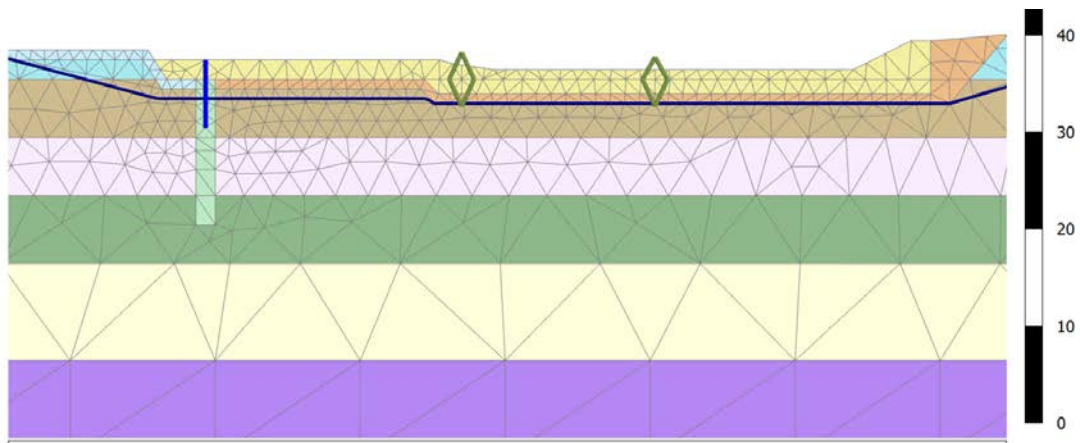


Figure 4-5: Construction of filter, sheet pile and stilling basin

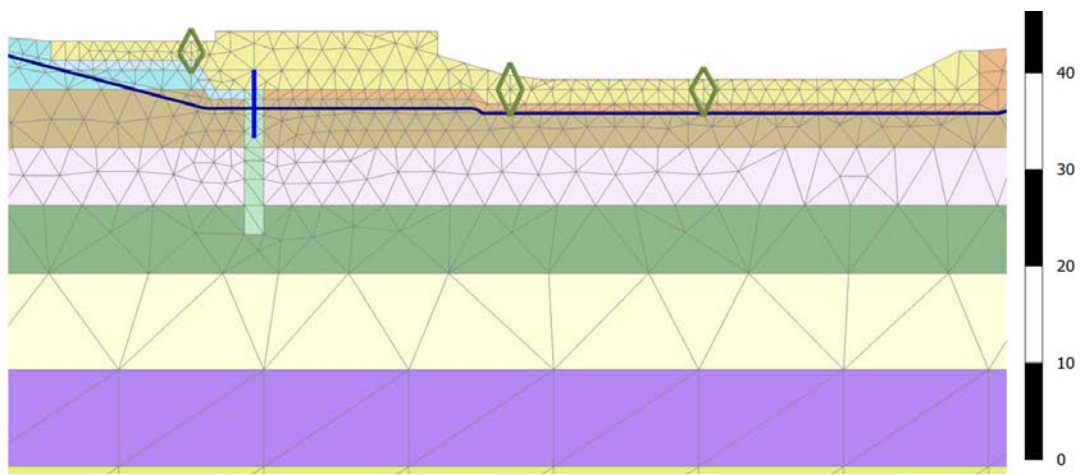


Figure 4-6: Addition of u/s slab, and concrete layer.

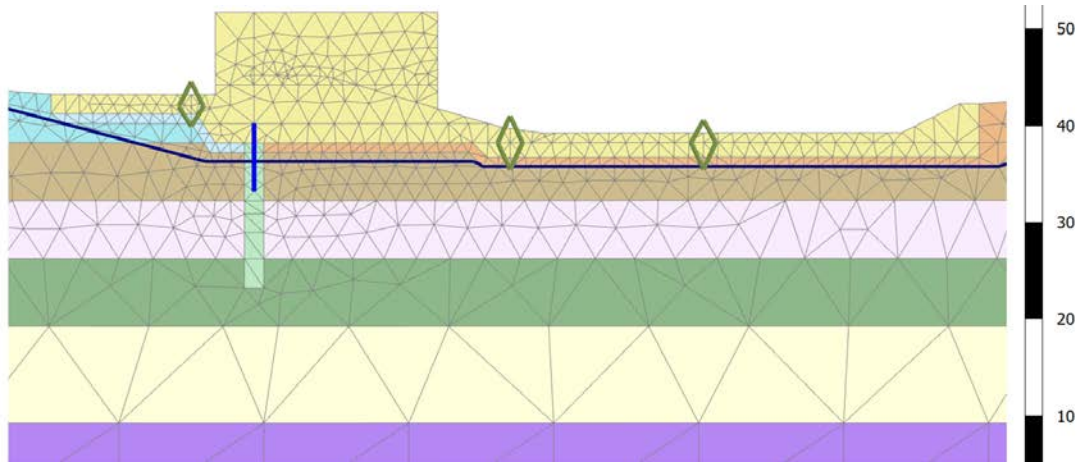


Figure 4-7: Phase 4, addition of concrete.

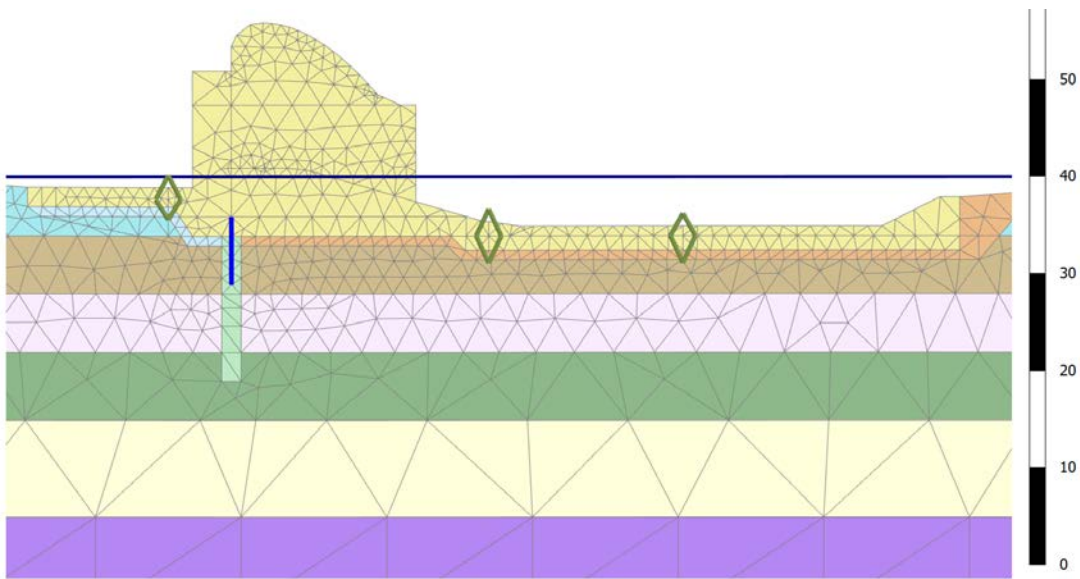


Figure 4-8: Completion of construction

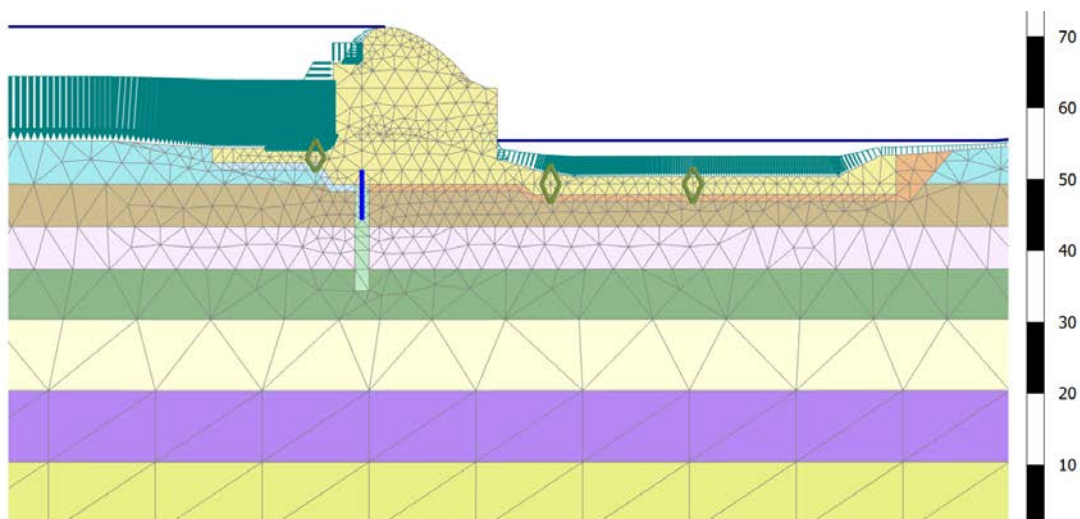


Figure 4-9: Filling of reservoir

4.2 Data preparation

4.2.1.1 Input parameters in PLAXIS 2D

Generally, in finite element model a lot of input soil parameters have to be defined. This is also true for PLAXIS 2D. The input parameters required in PLAXIS 2D for Hardening soil model are listed below;

General parameters:

γ_{unsat}	: Soil unit weight above phreatic level	[kN/m ³]
γ_{sat}	: Soil unit weight below phreatic level	[kN/m ³]
e_{init}	: initial void ratio	

Failure parameters:

c	: (Effective) cohesion	[kN/m ²]
φ	: (Effective) angle of internal friction	[°]
ψ	: Angle of dilatancy	[°]
t	: Tension cut-off and tensile strength	[kN/m ²]

Basic parameters for soil stiffness:

E_{50}^{ref}	: Secant stiffness in standard drained triaxial test	[kN/m ²]
$E_{\text{oed}}^{\text{ref}}$: Tangent stiffness for primary oedometer loading	[kN/m ²]
$E_{\text{ur}}^{\text{ref}}$: Unloading / reloading stiffness (default $E_{\text{ur}}^{\text{ref}} = 3E_{50}^{\text{ref}}$)	[kN/m ²]
m	: Power for stress-level dependency of stiffness	

Groundwater parameters:

k_x	: Horizontal permeability	[m/day]
k_y	: Vertical permeability	[m/day]
c_k	: Change in permeability	

4.2.2 Input data

It is typical that all the parameters needed for such FEM are not studied or not studied at early stages where most of the important decisions have to be made. Hence, some input parameters have to be estimated by correlation or taking typical range of values from literature based on available information of field data.

4.2.2.1 Permeability

Since, a single value of soil stiffness is used for analysis the soil layers are divided based on different permeability. In addition, no tests were performed below 25 m of alluvium and it is

stated in feasibility report that the permeability of layers decreases with depth. Hence, the permeability till 25 m depth is from field tests and below 25 m, it is assumed that the permeability from 25-100 m depth will decrease linearly with permeability at 100m depth being $1/10^{\text{th}}$ of the permeability at 25m. Table 4-2 shows the values of permeability used in the model for analysis.

Table 4-2: Permeability values used for PLAXIS model

Depth	Permeability
6	9.00E-04
12	1.60E-03
18	1.70E-03
25	6.00E-04
35	4.00E-04
45	3.30E-04
55	2.80E-04
71	2.10E-04
100	1.10E-04

4.2.2.2 Strength Parameters

Dynamic cone penetration test (DCPT) indicated a high shear strength of soil with friction angle between 42° and 48° and no cohesion. But some inconsistency was observed in one of the test result with lower friction angle. Hence, a friction angle of 37° was used for analysis to be on conservative side.

4.2.2.3 Stiffness of soil

Since, no triaxial or oedometer test were done the E modulus of soil was estimated from typical values of soil for similar grain size distribution. Though the E modulus changes with depth, the soil is assumed to be homogeneous due to lack of parameters for estimation of E modulus. For unloading reloading stiffness it is usually estimated that the reloading stiffness is three times the initial stiffness. The following are the values used for stiffness of soil;

Secant stiffness in standard drained triaxial test	$E_{ref, 50}$	$5 \cdot 10^4$	KN/m ²
Tangent stiffness for primary oedometer loading	$E_{ref, oed}$	$5 \cdot 10^4$	KN/m ²
Unloading / reloading stiffness	$E_{ref, ur}$	$15 \cdot 10^4$	KN/m ²

4.2.2.4 Grout curtain

It is always very hard to predict the efficiency of grouting and hence the permeability of grout curtain. For our analysis we have assumed that the grout curtain will be able to reduce the permeability to 1/50th of average permeability of soil which is equal to 2×10^{-5} (i.e. 1.7 m/day).

4.2.2.5 Sheet pile

A sheet pile is installed under the dam to limit the seepage. The properties of sheet pile used for the model are shown below;

Normal stiffness (EA_1)	= 2.74×10^9	kN/m
Stiffness in the out of plane direction (EA_2)	= 2.74×10^9	kN/m
Bending stiffness (EI)	= 23×10^6	kN/m ² /m

Table 4-3 shows typical input values for PLAXIS model for a layer extending from 0 to 6 m depth.

Table 4-3: Input parameters for topmost layer (0-6 m depth).

Parameter	Name	0-6m	Unit	Remarks
General parameters				
Material model	<i>Model</i>	Hardening soil	-	
Type of material behaviour	<i>Type</i>	Drained	-	
Soil unit weight above phreatic level	γ_{unsat}	16.86	KN/m ³	from feasibility report
Soil unit weight below phreatic level	γ_{sat}	20.36	KN/m ³	from feasibility report
Initial void ratio	e_{init}	0.35	-	Estimated
Parameters				
Secant stiffness in standard drained triaxial test	$E_{ref, 50}$	5 · 104	KN/m ²	Estimated
Tangent stiffness for primary oedometer loading	$E_{ref oed}$	5 · 104	KN/m ²	Estimated
Unloading / reloading stiffness	$E_{ref ur}$	15 · 104	KN/m ²	$E_{ref ur} = 3 \times (E_{ref, 50})$
Power for stress-level dependency of stiffness	m	0.5	-	

Modified compression index	λ^*		-	
Modified swelling index	κ^*		-	
Cohesion	c_{ref}'	0	kN/m ²	from feasibility report
Friction angle	ϕ'	37	°	from feasibility report
Dilatancy angle	ψ	0	°	estimated
Groundwater				
Horizontal permeability	k_x	77.76	m/day	from feasibility report
Vertical permeability	k_y	77.76	m/day	Taken equal to horizontal permeability

4.2.2.6 Properties of concrete

Concrete of compressive strength 25 MPa is used as the structural concrete and several other concrete of different compressive strength are used locally in the dam for different functions as erosion resistance and blinding concrete etc.

Concrete was modelled with Mohr-Coulomb model. Input parameters for concrete were obtained using the relations defined on Indian Standards (IS 456: 2000) for concrete which is used in Nepal where the dam is being constructed.

Table 4-4: Concrete properties input parameters

Parameter	Name	Concrete	Unit	Remarks
General				
Material model	<i>Model</i>	Mohr-Coulomb model (MC)	-	
Type of material behaviour	<i>Type</i>	Non Porous	-	
Soil unit weight above phreatic level	γ_{unsat}	24	kN/m ³	
Soil unit weight below phreatic level	γ_{sat}	-	kN/m ³	
Parameters				
Young's modulus	E	2.35E+07	kN/m ²	$E=5000 \sqrt{f_{ck}}$, $f_{ck} = 25\text{Mpa}$ from feasibility report
Poisson's ratio	ν	0.2		

Cohesion	c	500	kN/m ²	
Friction angle	ϕ'	35	°	
Dilatancy angle	ψ	-	°	
Tension cut-off and tensile strength	σ_t	3500	kN/m ²	$\sigma_t=0.7\sqrt{f_{ck}}$

4.2.2.7 Foundation rock

As per the site investigations two types of rock have been found in abutments. On right bank fresh to moderately weathered gneiss was encountered while on left bank fresh to moderately weathered schist was found. The input parameters for rock are given in Table 4-5.

Table 4-5: Input parameters for rock

Parameter	Name	Schist	Gneiss	Unit
General				
Material model	<i>Model</i>	Mohr-Coulomb model (MC)	Mohr-Coulomb model (MC)	-
Type of material behaviour	<i>Type</i>	Drained	Drained	-
Soil unit weight above phreatic level	γ_{unsat}	26.5	26.5	kN/m ³
Soil unit weight below phreatic level	γ_{sat}	27	27	kN/m ³
Parameters				
Young's modulus	<i>E</i>	1.50E+07	3.50E+07	kN/m ²
Poisson's ratio	ν	0.15	0.1	
Cohesion	c	1000	20000	kN/m ²
Friction angle	ϕ'	35	40	°
Dilatancy angle	ψ	-		°

4.2.3 Cases of analysis

The dam was checked for different loading conditions;

1. Usual loading condition
 - a. Normal operation level
 - Reservoir level at HRWL - El. 1987.00
 - All four gates are closed
 - Uplift based on tail water level (El. 1970.00) - drain in operation

2. Transient loading condition
 - a. Design flood level
 - Reservoir level at 1988.70
 - Two gates are closed
 - Uplift based on tail water level (el. 1974.00) - drain in operation
3. Extreme loading condition
 - a. Normal operation level + Earthquake
 - Reservoir level at HRWL - 1987.00
 - All four gates are closed
 - Uplift based on tail water level (el. 1970.00)- drain in operation
 - Earthquake with magnitude 0.34g
 - b. Extreme hydrological event (PMF)
 - Reservoir level at 1994.20
 - All gates are open
 - Uplift based on tail water level (el. 1976.00) - drain in operation
 - c. Extreme hydrological event (GLOF)
 - Reservoir level at 1997.0
 - All gates are closed
 - Uplift based on tail water level (el. 1983.00) - drain in operation

Each cases listed above was modelled in PLAXIS 2D for different water levels. However, due to limited data available on earthquake and lack of enough background knowledge on earthquake only liquefaction analysis is performed for dynamic loading.

5 Result and Discussion

5.1 Settlement

The expected settlement values calculated from Boussinesq equation, improved elastic equation and Janbu's theory as explained in 2.4.2 gave a value of 119.5 mm, 134.3 mm and 125.9 mm respectively. These methods give fairly similar values of settlement at the end of construction at the center of foundation. However, these methods give only 1D settlement value and do not account for differential settlement in the dam sections. In addition, as the dam is on soil some horizontal displacement is expected but these methods cannot give the horizontal displacement. So, the dam was modelled in finite element model and the results obtained from PLAXIS model are presented below.

5.1.1 Along a section in transverse axis

5.1.1.1 During construction

As the foundation material is granular soil most of the settlement was observed during construction. During excavation the soil was unloaded and groundwater table was lowered. Due to lowered groundwater table soil tend to settle but due to unloading of soil it expanded. As the expansion was higher than settlement the soil, upward displacement of 3.5cm was observed at the end of excavation as shown in [Figure 5-1](#).

After construction was completed groundwater table was raised to surface. At the end of construction, a maximum of 13.07 cm of vertical downward settlement was observed with maximum at upstream toe of dam. Settlement plot of dam at the end of construction is shown in [Figure 5-2](#).

5.1.1.2 During filling

When the reservoir is filled, due to increase in pore water pressure it tends to lift the dam. Hence, vertical movement of dam is observed as shown in [Figure 5-3](#). This vertical movement is almost negligible (4mm) for the main dam body. However, the stilling basin is raised by 1.5cm due to pore water pressure seeping under it.

The deformed mesh geometry at the end of filling of reservoir is shown in [Figure 5-4](#).

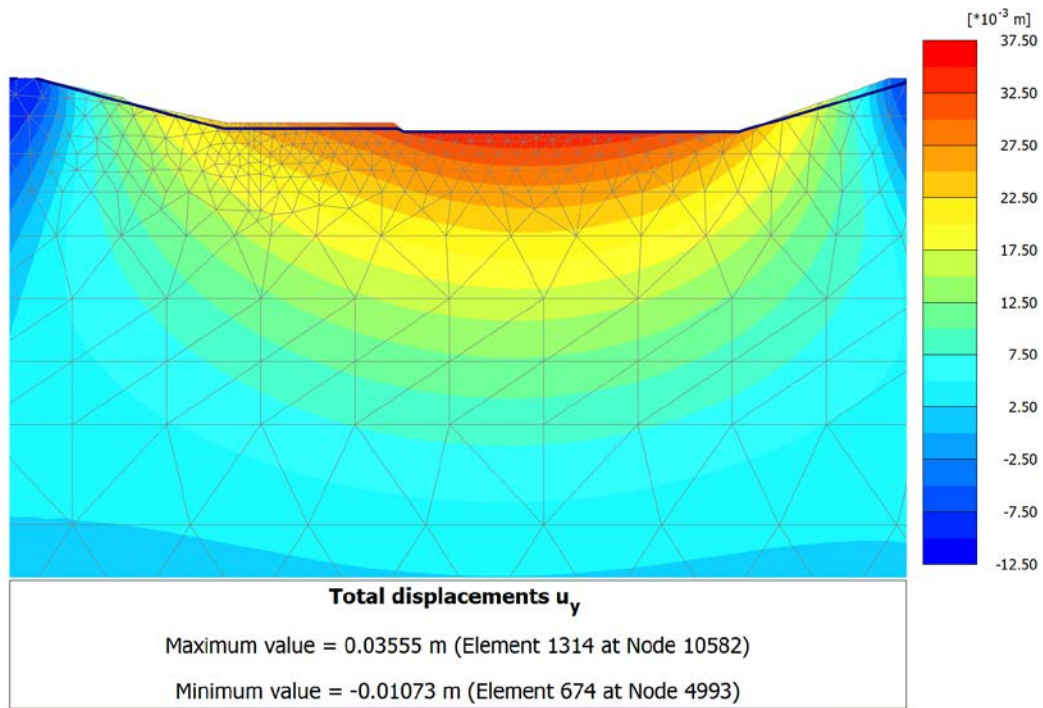


Figure 5-1: Vertical displacement at the end of excavation

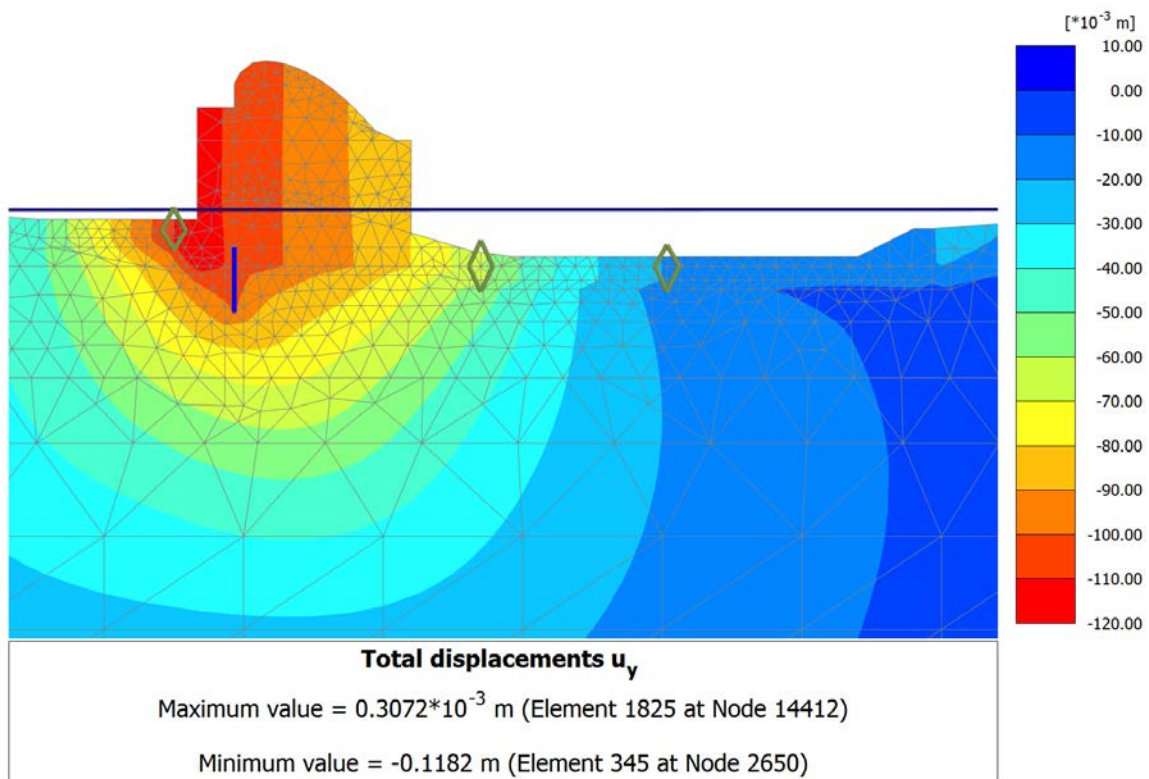


Figure 5-2: Total vertical displacement at the end of construction

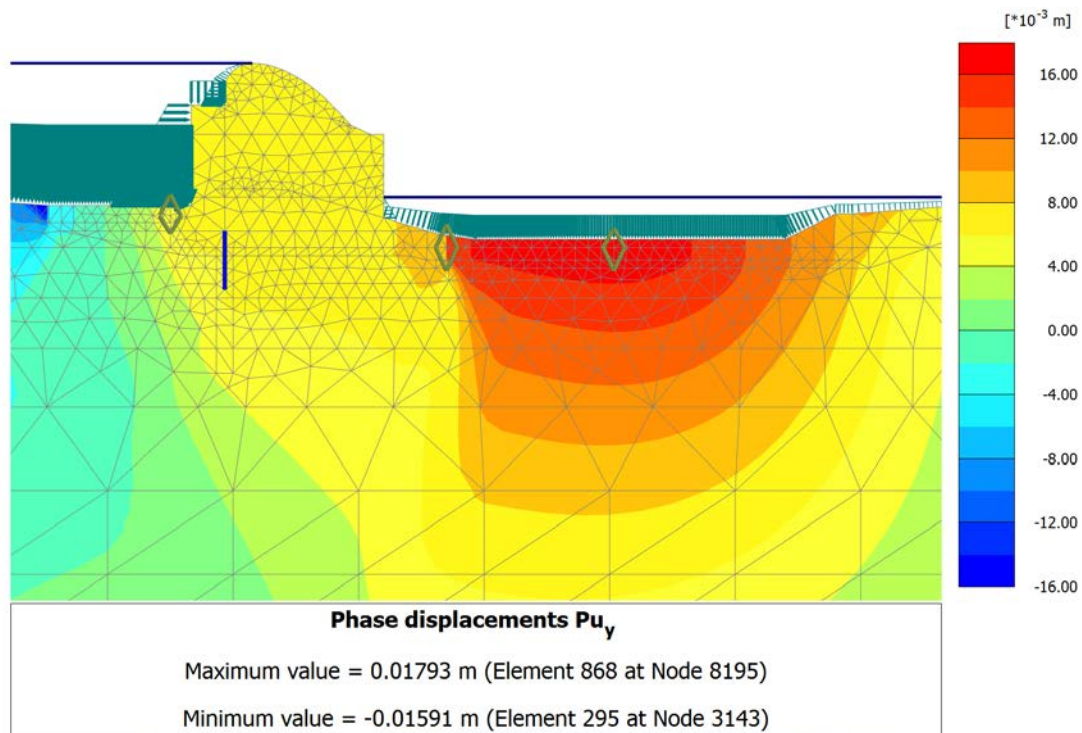


Figure 5-3: Vertical deformation after filling of reservoir at NWL.

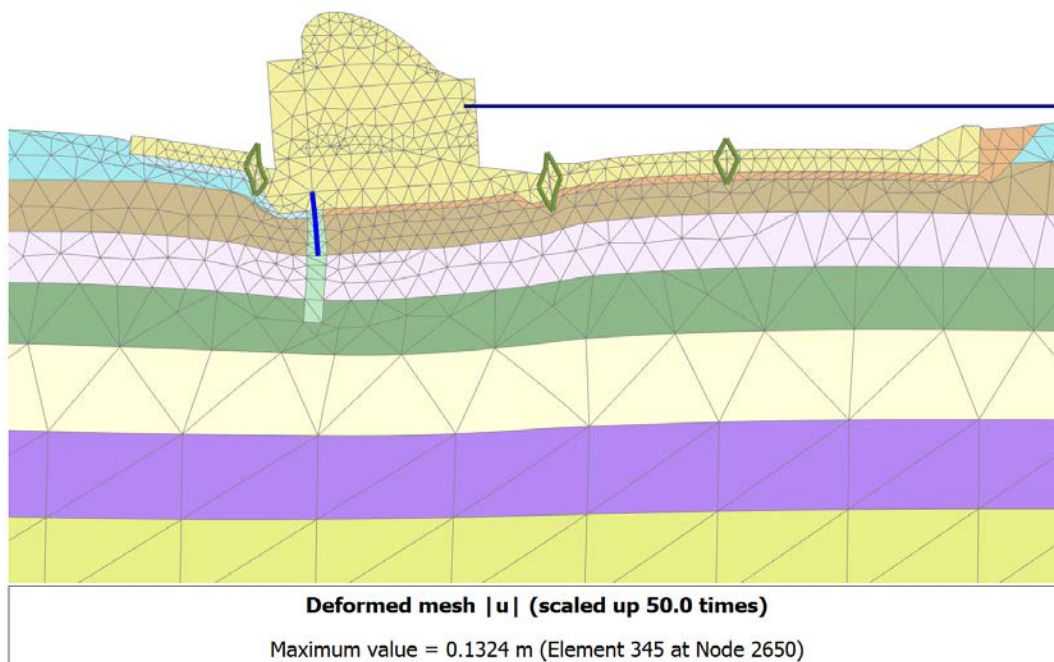


Figure 5-4: Deformed mesh geometry after filling of reservoir at NWL

5.1.1.3 Differential settlement along transverse axis

In the model concrete was added in steps so, different values of differential settlement was observed in each step. A differential settlement as high as 1 cm was observed in the joint between upstream apron and main dam body. Some millimeters of differential settlement were also observed in the dam body itself. As differential settlement induces stresses in dam, the

stresses were checked against allowable stresses in 5.1.1.4 to see if this value of differential settlement is acceptable to the dam or not. Differential settlement plots are presented in Figure 5-5 and Figure 5-6.

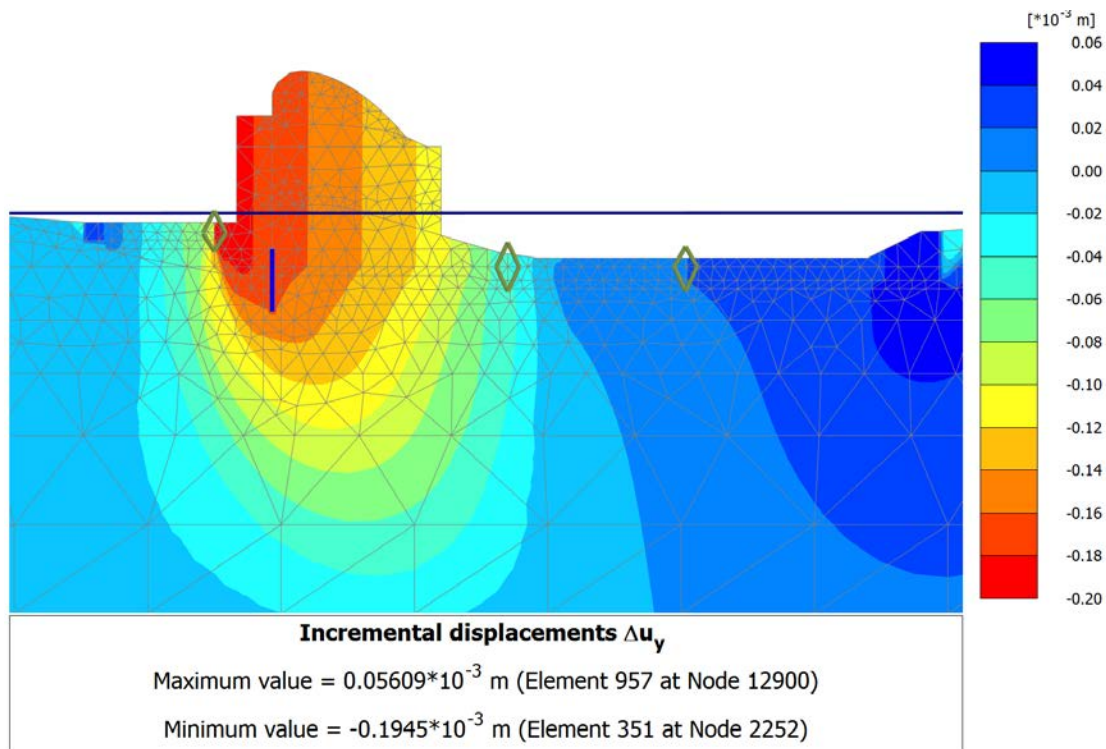


Figure 5-5: Differential displacement at the end of construction

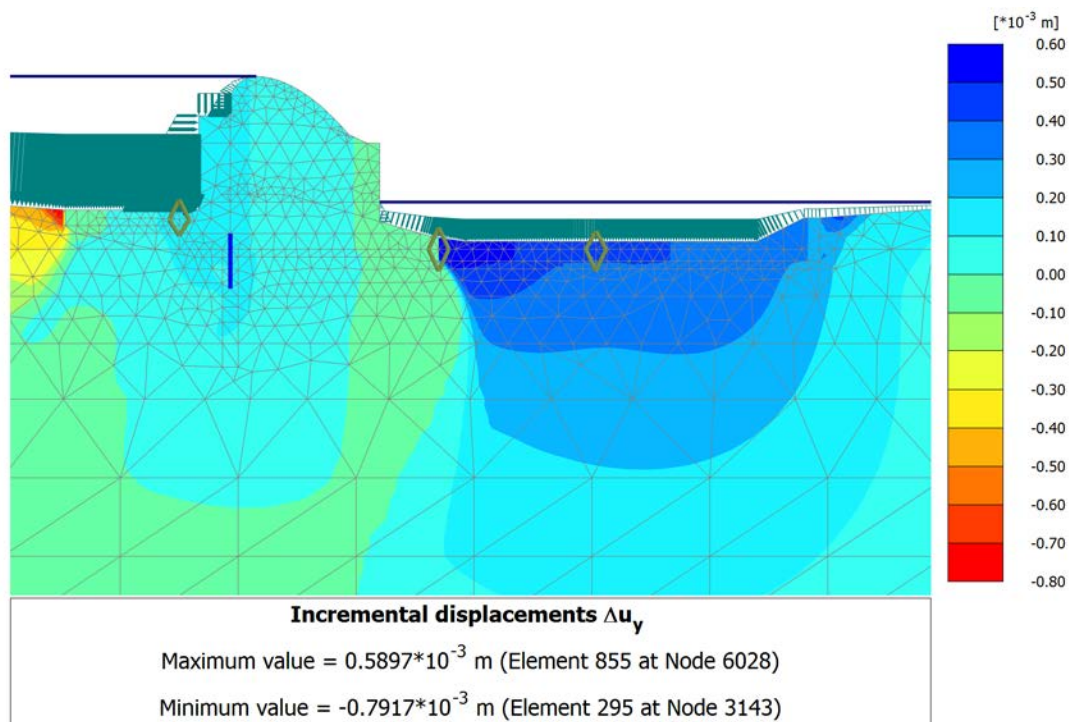


Figure 5-6: Differential vertical displacement after filling at NWL

5.1.1.4 Discussion

Differential settlement values may be accepted unless the stress induced due to differential settlement does not exceed allowable stress in concrete. This can be checked by observing the deviatoric stress and principal stress in the dam body. The plot of deviatoric stress is shown in [Figure 5-7](#) and [Figure 5-8](#). It can be seen that the deviatoric stresses are less than 4 MPa. Hence, it can be concluded that the compressive stresses do not exceed the concrete stress.

[Figure 5-9](#) shows that there are some areas in dam where tensile stress is developed (indicated by red circles) especially in the construction joints upstream and downstream of dam. Tensile stresses were also observed in the stilling basin as shown in [Figure 5-9](#).

It is obvious that these tensile stress areas are due to differential settlement of dam body. A maximum of 0.7 MPa tensile stress was developed in the dam. It is within the allowable limit for tensile stresses in concrete (according to Eurocode it is 1.7 MPa for M25 grade concrete). In addition, surface reinforcements are provided in dam for crack control which is also capable of resisting tensile stresses. Hence, the magnitude of tensile stress developed for this dam is acceptable. However, concrete gravity dams are assumed to have no tensile stress developed in it.

To see the effect of construction sequence in the dam, the dam was also modelled with a sequence of construction where main dam body was constructed first and upstream apron and downstream stilling basin were added later.

In such an analysis, no tensile stress in the stilling basin was observed ([Ref. Figure 5-10](#)). In addition, the tensile stresses in the joint between dam body and upstream apron was very much reduced and it was occurring locally.

Hence, it can be clearly seen that, stress induced due to differential settlement can very much be handled by following specific construction sequence in a dam on granular material.

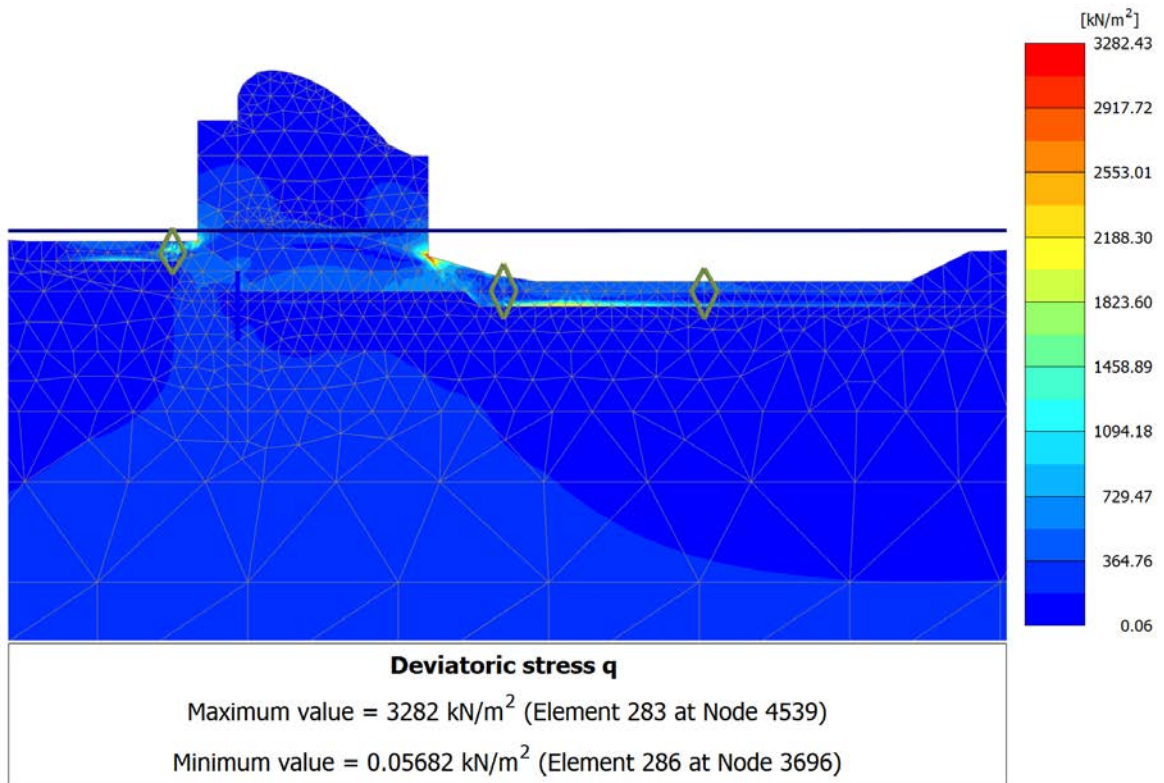


Figure 5-7: Deviatoric stresses at the end of construction

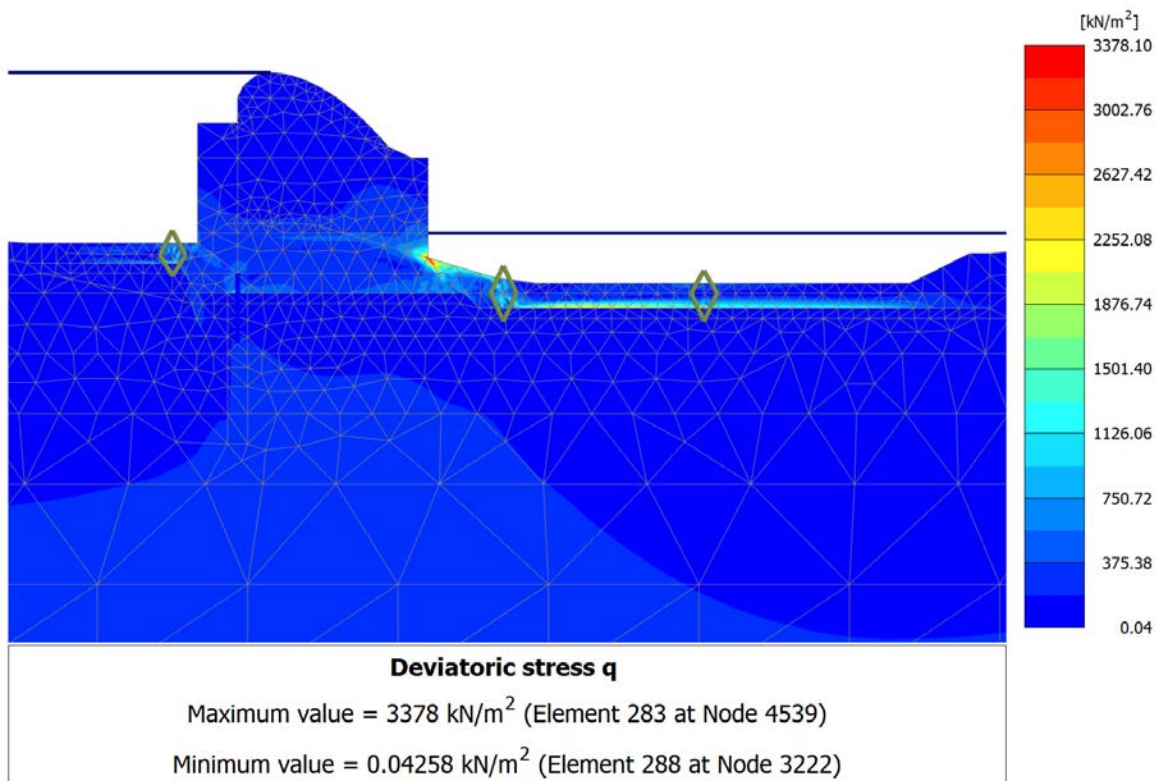


Figure 5-8: Deviatoric stress after filling of reservoir

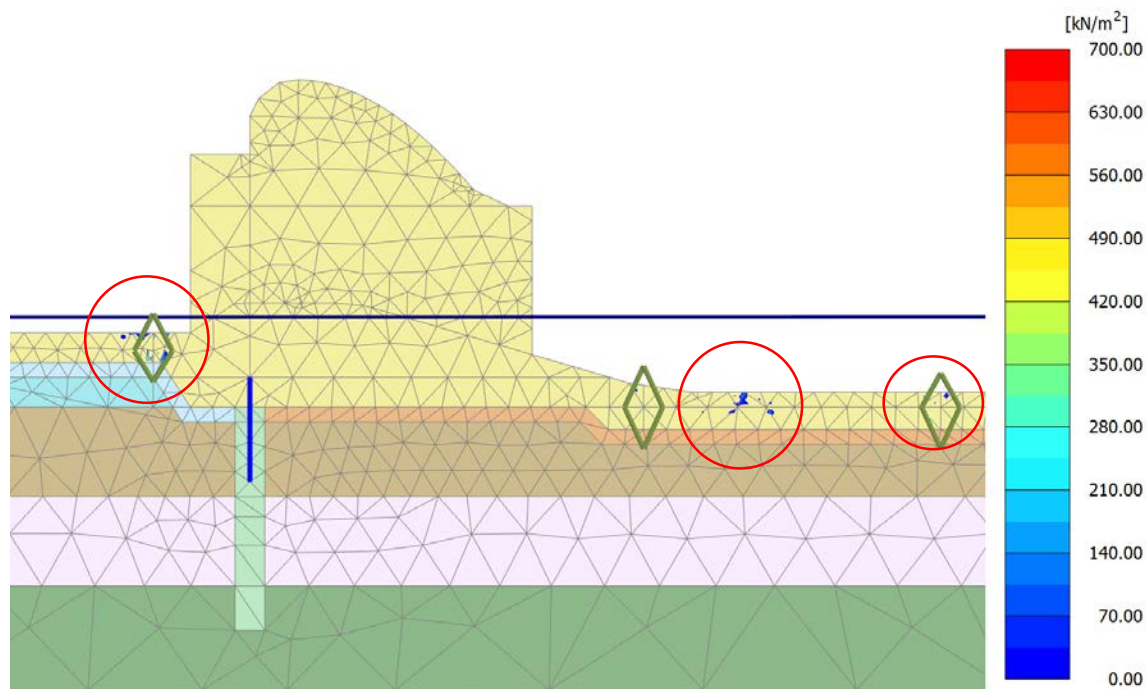


Figure 5-9: Areas for development of tensile stresses in concrete

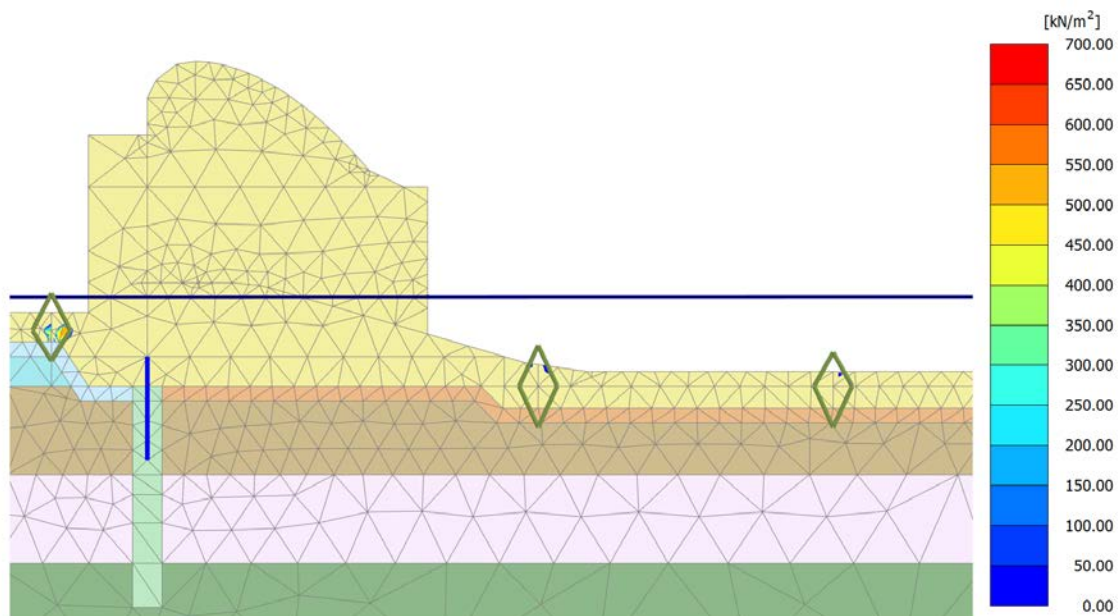


Figure 5-10: Areas for development of tensile stresses in concrete (Different construction sequence)

5.1.2 Along length axis of dam

5.1.2.1 Settlement of dam sections

As dam foundation is rigid we expect it to settle uniformly. The expected average settlement of dam sections along the length axis at the end of construction is presented in Figure 5-11. The sections at the middle founded on deepest layer of alluvium is expected to settle the most, by 12cm while the abutments will settle by slightly over 5 cm. So, the maximum differential

settlement between two sections is maximum between the abutments and its neighboring section which is about 5 cm.

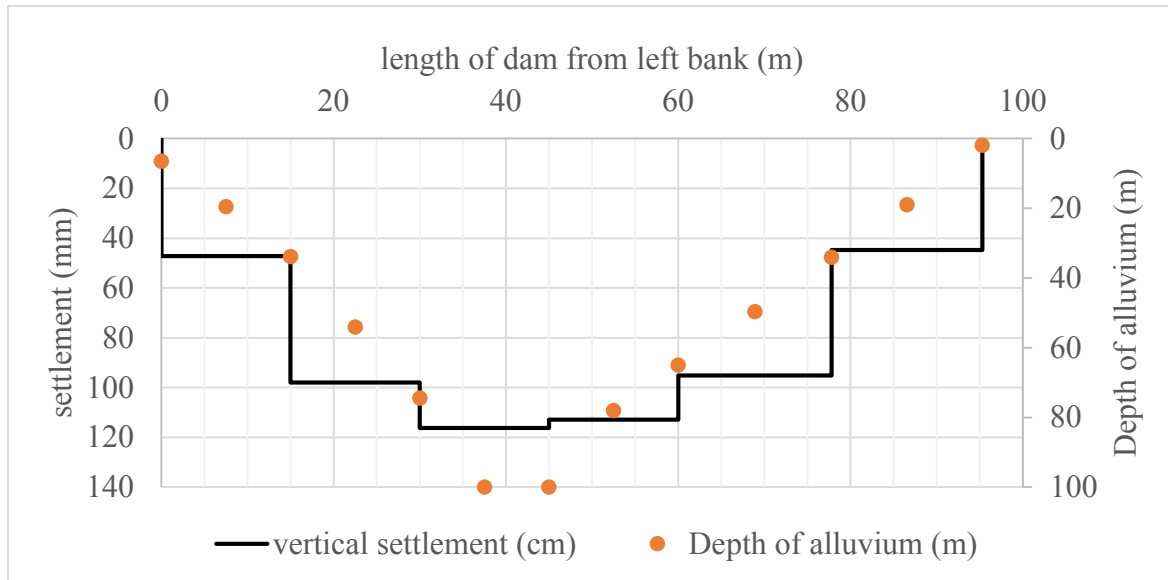


Figure 5-11: Expected vertical settlement of dam along its axis at the end of construction

5.1.2.2 Rotation

In practice no foundation is perfectly rigid so, they do not settle uniformly. Within each section of the dam there will be differential settlement hence, it tends to rotate. Figure 5-11 shows the expected settlement of each section of dam however the true settlement of dam will be similar to Figure 5-12. Table 5-1 presents the summary of rotation and sidewise movement of dam sections due to unequal settlement. The values of horizontal movement presented are at the top of the dam.

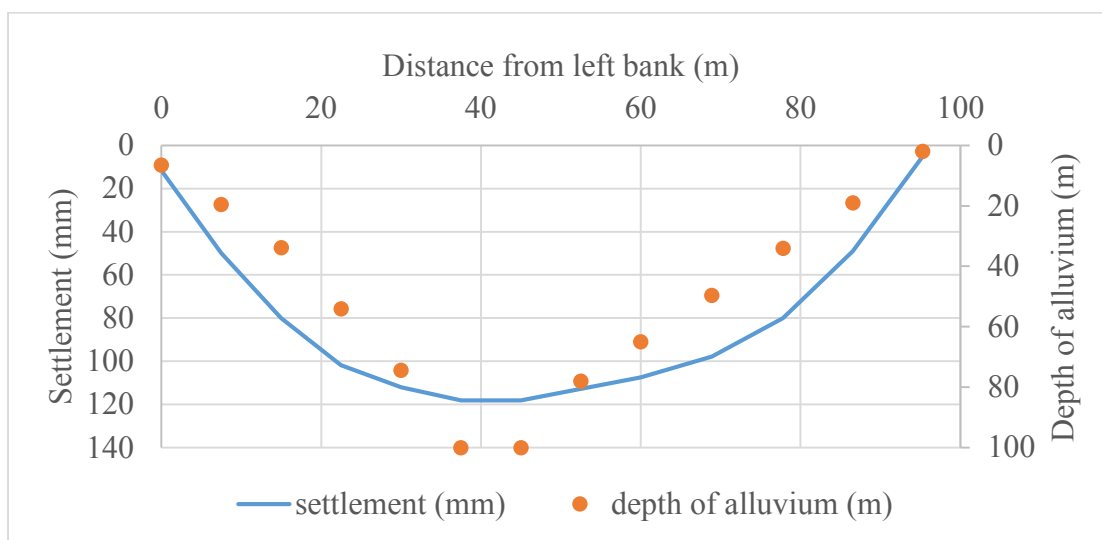














Figure 5-12: Settlement profile along dam axis

Table 5-1: Rotation angle and movement of top of dam due to unequal settlement of each section

		Settlement (mm)	Angle of rotation	Direction	Horizontal movement of top of dam (mm)	direction
Section 1 (Abutment)	left	11.70	0.26		107	
	right	80.00				
Section 2	left	80.00	0.12		50	
	right	112.10				
Section 3	left	112.10	0.02		10	
	right	118.20				
Section 4	left	118.20	0.04		17	
	right	107.50				
Section 5	left	107.50	0.11		43	
	right	80.00				
Section 6 (Abutment)	left	80.00	0.29		118	
	right	5.00				

5.1.2.3 Discussion

Differential settlement along the length axis of dam cause each dam section to rotate. This rotation bring dam sections closer and this resulted the dam sections hit each other. Crushing of concrete is likely to occur at the point of contact. Though it is not studied here but it is also possible that rotation of dam section may lift the other half of dam which results in reduction in contact area of dam with foundation and reduces the shear strength.

The values presented in the tables and figures are maximum values of settlement for each section. Analysis are done taking higher values to be on conservative side during design. Due to lack of sufficient field studies E modulus of soil was taken from typical values which may have resulted in higher values of settlement and lateral movement.

Small values of lateral movement of dam can be accommodated by construction joint. However higher values seek special design considerations and construction method such as inclined section, foundation preparation, etc.

5.2 Horizontal movement in the direction of river

5.2.1 At the end of construction

Some horizontal movements were observed in dam along the direction of river flow. During construction, the dam tend to settle more towards the upstream side (Ref. [Figure 5-4](#)). This made the dam tilt upstream by a maximum of 3cm at the top of dam as shown in [Figure 5-13](#). The stresses induced in the dam due to this movement was found within acceptable limit.

5.2.2 During filling of reservoir

During filling of reservoir due to horizontal force of water, unlike movement during construction, the whole dam body slides as a block as shown in [Figure 5-14](#). In addition, different sections of dam have different horizontal movement due to different foundation condition. Maximum horizontal displacement of 40 mm was observed at the center sections while sections at abutment displace by about 10 mm. The expected profile of horizontal displacement is presented in [Figure 5-15](#).

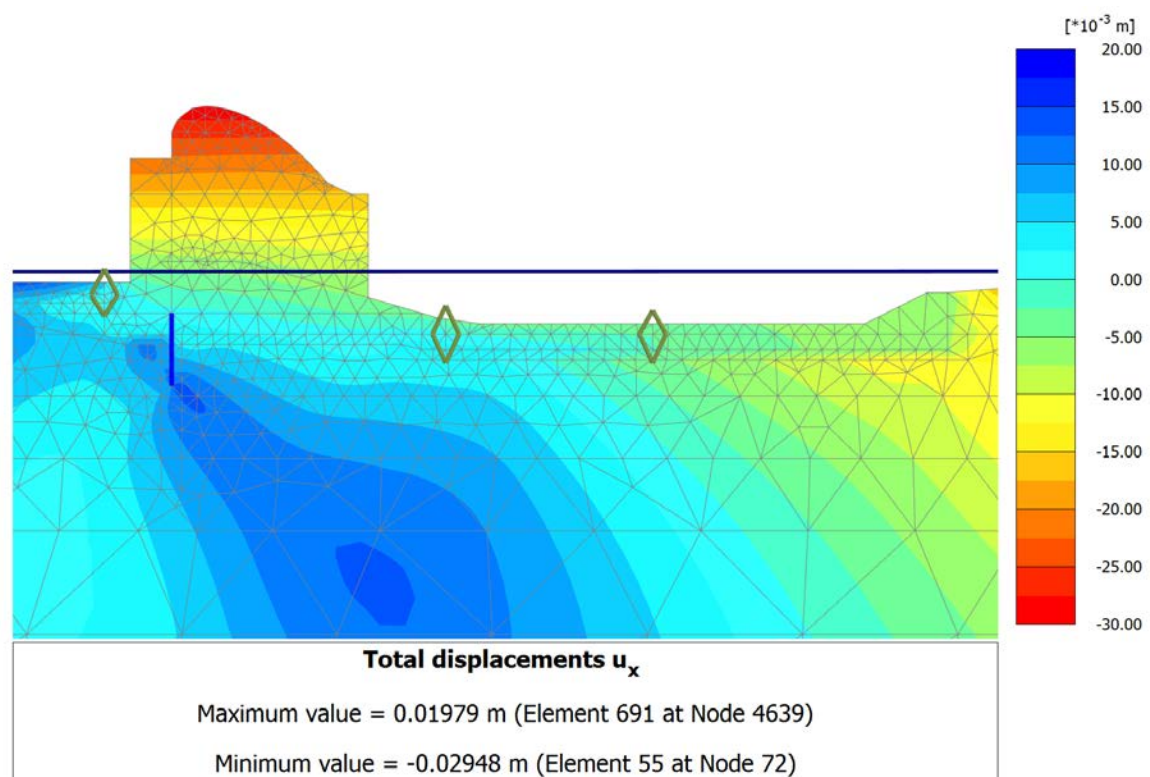


Figure 5-13: Horizontal displacement at the end of construction

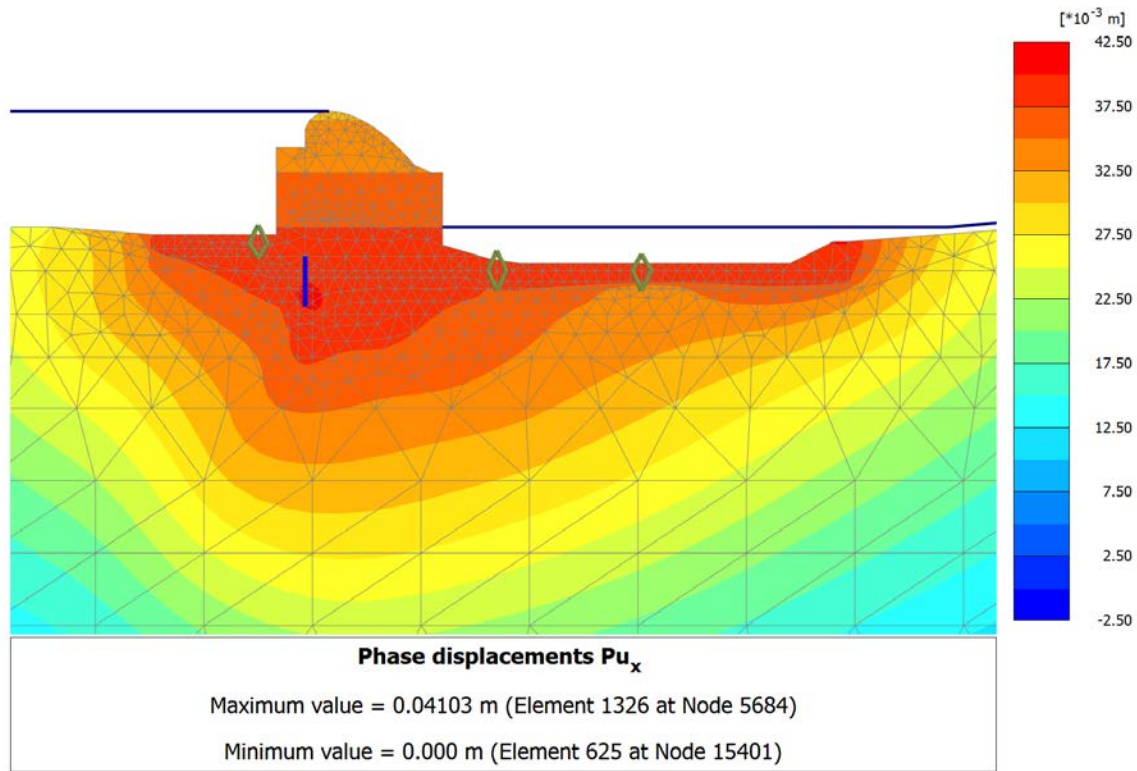


Figure 5-14: Horizontal displacement of central section of dam during filling

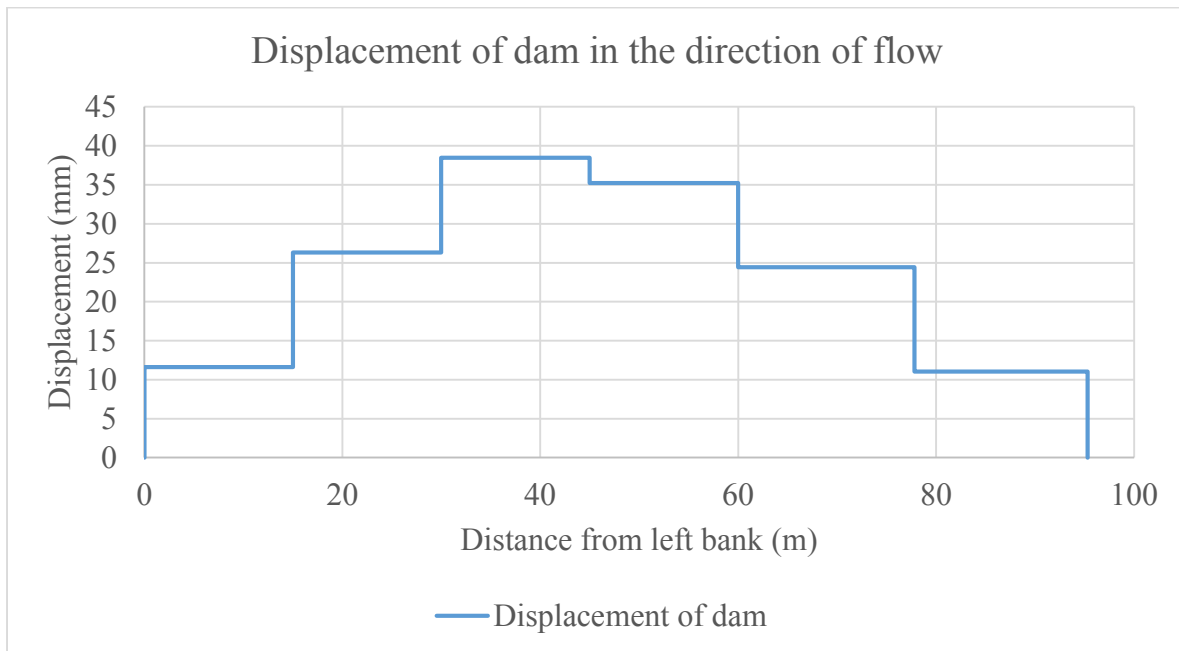


Figure 5-15: Horizontal displacement of dam during filling in the direction of flow

5.2.3 Discussion

Maximum differential horizontal movement of 20 mm was observed between dam section at abutment and its neighboring dam section whereas differential movement was least at sections

at the center. To avoid stress due to differential movements these sections should be allowed to move freely.

5.3 Seepage

5.3.1 Seepage discharge

A seepage quantity of $0.26 \text{ m}^3/\text{s}$ was observed in PLAXIS 2D seepage analysis which equals 2.7 l/s per m of dam. The seepage quantity obtained is relatively higher. It may be because of existence of high permeable layers below the grout curtain and presence of coarse materials and boulders throughout the foundation soil.

Alternative analysis was run with; (a) extended grout curtain to El. 1940 masl with same permeability of grout curtain (b) grout curtain at El. 1950 masl with a reduced permeability of grout curtain to $1/100^{\text{th}}$ of initial permeability (c) extended grout curtain to El. 1940 masl and permeability of $1/100^{\text{th}}$ of initial permeability. The summary of result of all three cases are presented in

Table 5-2.

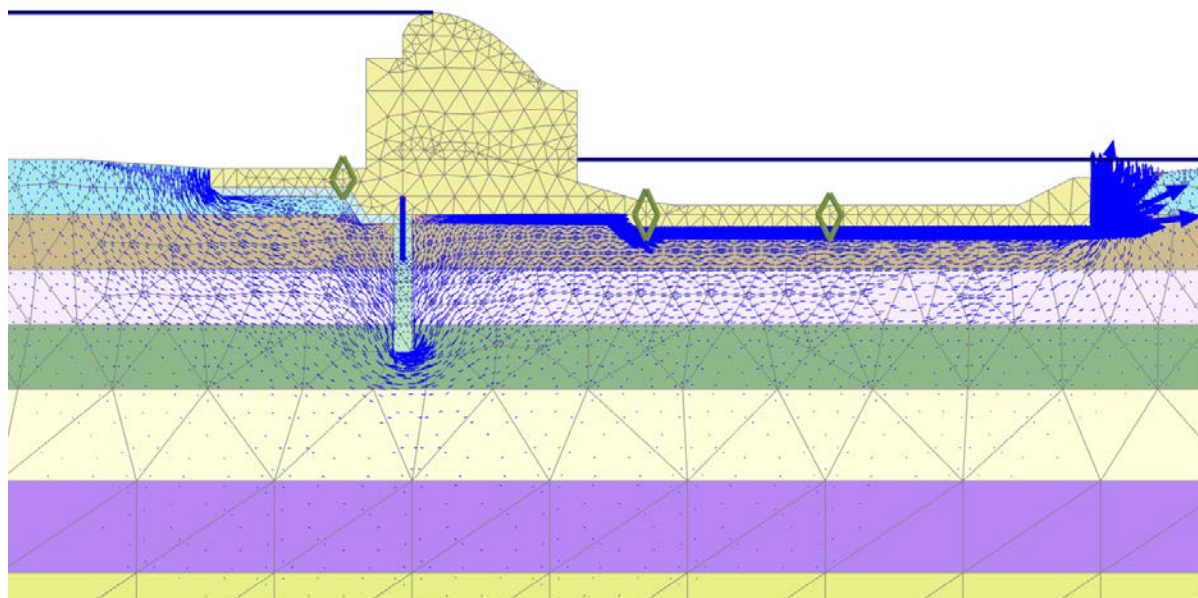


Figure 5-16: Groundwater flow pattern under the dam

Table 5-2: Different cases of seepage flow analysis

	Current design	Extended grout curtain by 10 m	Reduced permeability of grout curtain	Extended grout curtain + Reduced permeability of grout curtain
Seepage discharge (m^3/s)	0.26	0.22	0.25	0.19

5.3.2 Exit gradient

A seepage gradient of 0.3 is measured at the outlet. This gives a factor of safety of 6.6 against boiling as explained in 2.5.2.1.1. Hence no blowout of sand layer occurs.

5.3.3 Discussion

The seepage through the dam is not reducing significantly with extended grout curtain or more efficient grout curtain or both. It is because of highly permeable layers below the grout curtain and presence of boulders and other coarse materials throughout the foundation soil. Furthermore, the exit of drainage was found safe against boiling. So, the seepage is acceptable if it does not hamper the economy of project. The water loss through seepage is equivalent to 9 GWh of annual energy produced through the dam.

A necessary condition for piping to start is unprotected exit point as explained in 2.5.2.2.1. As piping starts at downstream and as this dam is provided with filter at the drainage exit and no blowing of sediment occurring at exit. Hence, it is assumed that the foundation is safe against piping.

5.4 Stability

The factor of safety for different load cases obtained by spreadsheet calculation is presented in Table 5-3. The factor of safety for all loading cases are in accordance with the factor of safety defined in 2.2 hence, the dam is safe for all cases of analysis.

Table 5-3: Factor of safety

Load Cases	Factor of safety		Bearing stress (KN/m ²)	
	Slide	Overturning	Toe	Heel
Normal operation	3.4	2.4	436.6	71.1
Design flood	3.6	2.3	428.0	88.7
Before filling	410.6	1868.9	636.6	98.2
Normal operation + Earthquake	1.3	1.6	9.1	498.6
PMF	2.9	2.2	385.7	147.9
GLOF	2.3	2.0	326.8	233.5

5.5 Bearing capacity

Allowable bearing capacity of foundation soil calculated by Meyerhof's method considering a factor of safety of 3 is 667 kN/m². The bearing stress developed for different loading conditions as presented in Table 5-3 do not exceed the allowable bearing capacity of soil or concrete. In

addition, as the bearing stress is always positive, no tension is developed. Hence, the dam is safe against bearing.

5.6 Liquefaction

Historical record of earthquake shows a number of earthquake epicenters in the vicinity of the area (Ref Figure 5-17) hence the area is susceptible to liquefaction. However, no cyclic stress test or standard penetration has been done. Hence, for the analysis of liquefaction susceptibility, a range of SPT values were assumed and analysis was done.

5.6.1 Liquefaction susceptibility

Factor of safety against liquefaction was calculated from Idriss and Boulanger method and NCEER methods. It was found that, the soil with a SPT blow count of less than 25 is susceptible to liquefaction (Ref Figure 5-18).

5.6.2 Reconsolidation settlement

Reconsolidation settlement was calculated by different methods as explained in 2.7.5.1 and the expected settlement for different $(N1)_{60}$ values are presented in Figure 5-19. A maximum of 32 cm settlement is expected if liquefaction to happen for $(N1)_{60}=15$. Of course, further studies on penetration resistance of soil is to be done by SPT test.

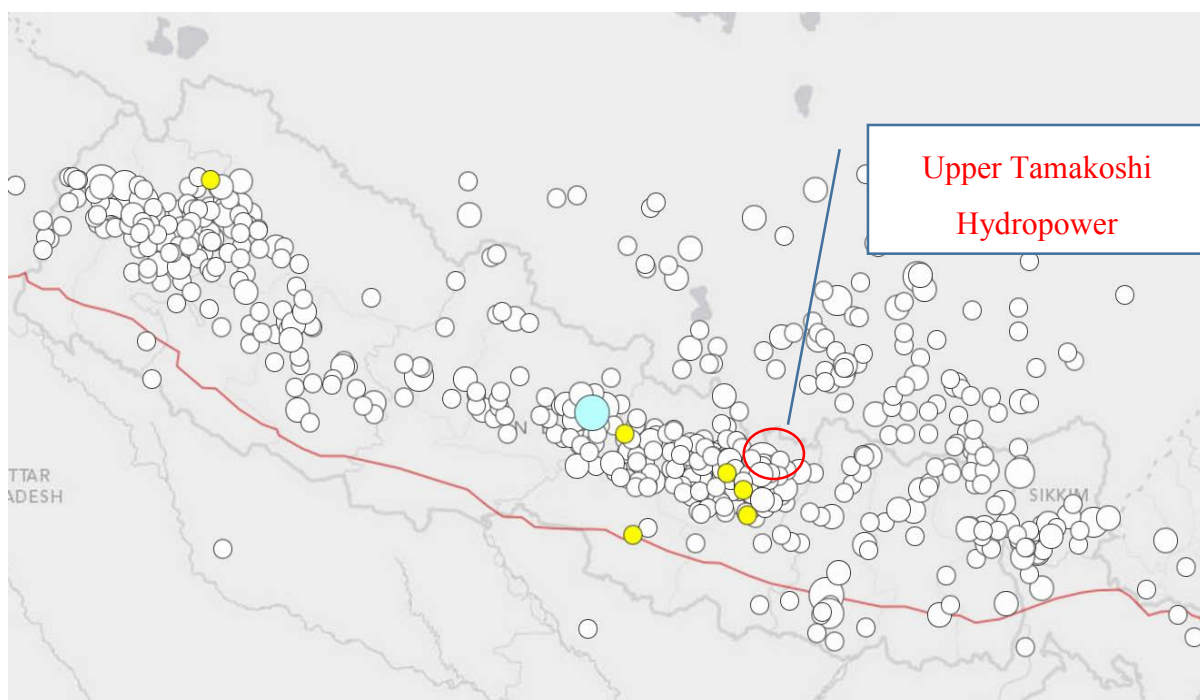


Figure 5-17: Historical earthquake epicenters since 1934.

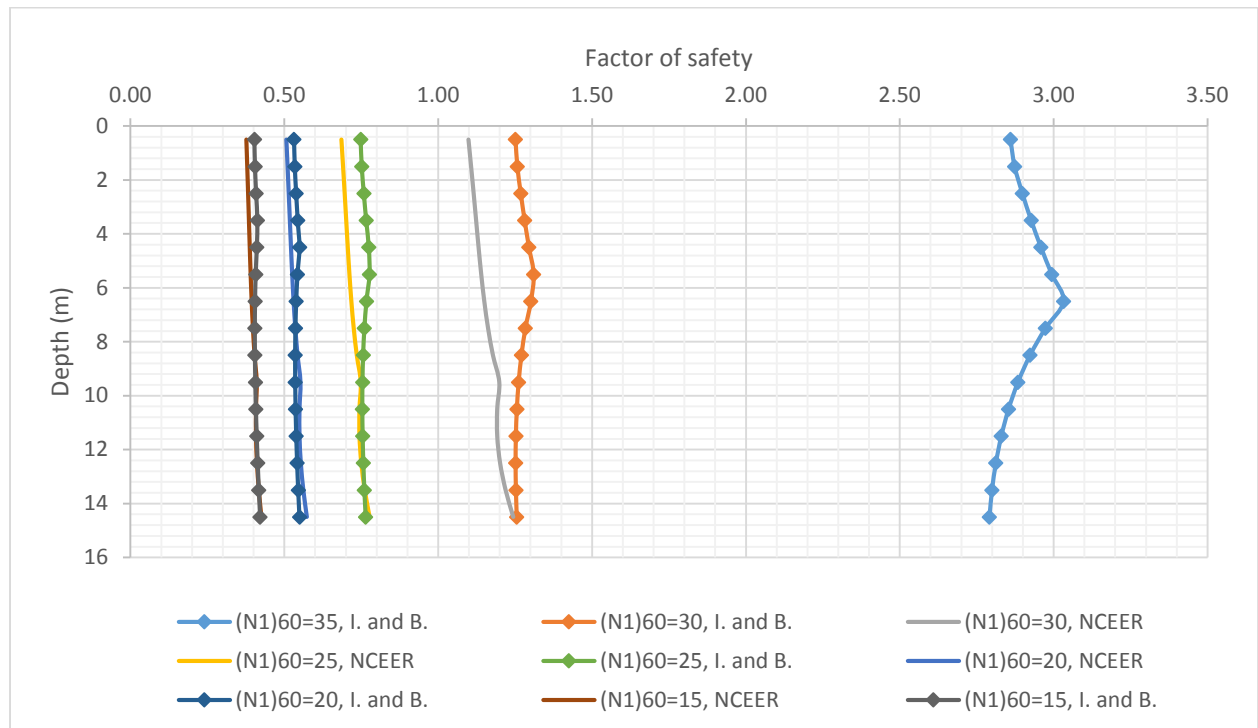


Figure 5-18: Factor of safety against liquefaction for different $(N1)_{60}$ values with Idriss and Boulanger and NCEER methods

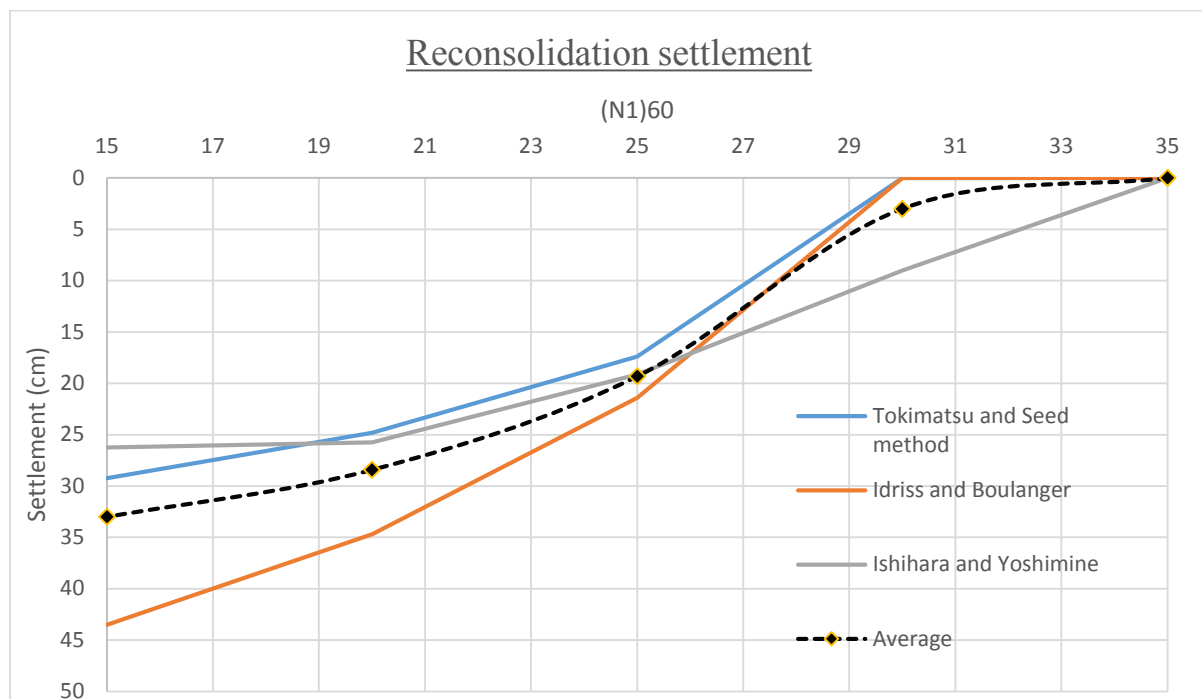


Figure 5-19: Reconsolidation settlement according to different researchers and $(N1)_{60}$

5.6.3 Lateral spreading

Settlement due to lateral spreading is calculated for different $(N1)_{60}$ values have been done for different distance of epicenter of earthquake as explained in 2.7.5.2. The estimated values of lateral spreading if it is going to occur are presented in Figure 5-20.

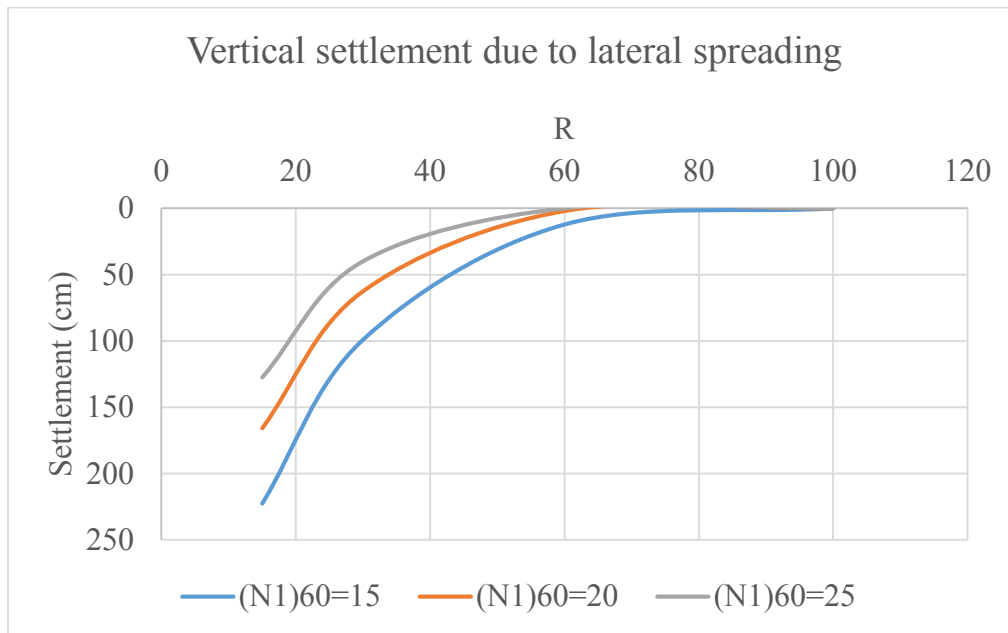


Figure 5-20: Settlement due to lateral spreading according to Kramer and Baska model

5.6.4 Discussion

As there has not been any studies on penetration resistance the values proposed above shows the possible effects for different SPT values likely on site. Further field studies should be done to check the liquefaction susceptibility and its effects.

The conditions of occurrence of liquefaction and different types of settlements should be checked according to 2.7. If both reconsolidation settlement and settlement is likely to occur, then the total settlement by liquefaction during an earthquake event will be the sum of both types of settlements.

Reports from the recent earthquake on 25th April, 2015, in Nepal says that this dam settled by 17 cm. This also highlights the importance of liquefaction studies in such areas.

6 Conclusion

The design principles of dam are the same whether it is on rock or on a soil foundation. A dam should be safe against overturning, sliding, the stresses should not exceed the allowable limit for dam and foundation materials and water should not pass through the dam or its foundation. However, there are a lot of uncertainties involved in foundation response in soil than in rock. So, proper foundation investigation is very important for predicting foundation behavior with ease and accuracy.

In addition to stability analysis of dam, settlements, differential settlement, seepage, bearing capacity, downstream erosion and liquefaction should be studied for concrete dams constructed on soil materials.

Theoretical and empirical methods as discussed in [Chapter 2](#) gives reliable estimation of foundation response. However, these methods have limited applications. Hence, modelling of dam and foundation in finite element model should be done for dam foundation on soil. Numerical models gives reliable estimate of foundation response both in magnitude and in temporal scale and can also handle heterogeneous foundation properties.

The estimated values of foundation response should be verified at site at early stage of construction and necessary steps should be taken to accommodate the differences.

Concrete dams on soils should always be constructed in sections. In addition these sections should not be rigidly connected. This allows free movement of each section and prevents from developing high stresses due to differential settlement and movement of dam. The length of each dam section depends on foundation properties, settlements, differential settlements, horizontal movement expected and construction technology available.

6.1 Settlement

In a concrete dam on soil materials the magnitude and rate of settlement of dam can have a wide range of values depending on the type and properties of soil. Uniform settlement of dam might not be an issue for stability of dam itself. In such case, the allowable settlement of dam or dam sections is dependent on the stability and functionality of appurtenance structures such as gates, penstock, intake etc.

Differential settlement within a dam or dam section is responsible for inducing stresses. The allowable value of settlement and differential settlement should be such that it should not cause failure of material. This value of allowable settlement depends on the soil materials, strength

of dam concrete, construction method and tolerable limits of movement for appurtenance structures.

In granular soil most of the settlements are expected to occur in construction stage while in fine particles where settlement is due to expulsion of pore water, it lasts for a longer period. It may even continue for years after construction.

Settlements in dam on granular soil can be handled during construction with appropriate construction sequence, foundation preparation or by allowing joints to move freely. In cohesive foundation soil, it is important to install drains to accelerate settlement. Furthermore, special design of structures and joints to accommodate long term settlement is necessary in fine soils.

Differential settlement can also induce rotation of dam causing the dam to move horizontally along dam axis (perpendicular to flow of river). The rotation of dam should not cause any tension in soil materials in the foundation. Situation as such decreases the area of contact between dam and foundation and can affect the stability of dam. In addition, if the dam sections collide due to rotation crushing of concrete may occur at the point of contact. Though this will not cause global failure of dam, but will have local failure issues. Such cases of differential settlement and rotation is typical for heterogeneous foundation material.

Rotation of dam section can be minimized by foundation preparation (making foundation of each section homogeneous). Furthermore, special construction techniques such as inclined sections can be constructed such that at the end of expected settlement the sections are vertical, do not collide with other sections and are in line with other sections.

Also, fracturing and arching can be caused because of interaction of dam and foundation where abrupt differences in the stiffness of the foundation materials along the dam axis occurs and/or sharp irregularities in the foundation base is existing (ICOLD, 2005). Foundation preparation by removing soil layer/s up to a certain depth and replacing it by more homogeneous materials can be done to avoid such conditions.

6.2 Seepage

The quantity and amount of seepage through the foundation depends on the type and properties of soil. It can have a wide range of values depending on the type of soil. High seepage gradient can cause quick condition or heaving of exit layer as explained in [2.5.2.1](#). Also, high quantity of seepage may not affect the stability of structure but may affect economy of the project.

It is almost impossible to limit seepage to zero so some seepage is expected. However, high concentrated leakage that can cause erosion of particles should not be accepted.

The allowable seepage through a dam should be such that it does not create;

- High exit gradient that can cause washout or heaving of soil layer at exit point.
- Concentrated leakage of high quantity that can cause erosion of materials

6.3 Downstream Erosion

The stability of a concrete dam is not only dependent on stability of dam itself but it is also very much dependent on the stability of soil in the foundation. Erosion to downstream of dam has been observed in a number of dams during large floods. These floods though may not risk the structural integrity of dam body itself but can cause serious downstream erosion. Downstream erosion of riprap leads into progressive backward erosion which can eventually compromise the safety of dam. It also shortens the seepage path and increase hydraulic gradient which may result in piping.

Figure 6-1 shows the downstream erosion in Lauvsnes dam in Norway during a large flood event in 2006. Severe downstream erosion almost led the dam to failure though there was no damage in dam structure itself.



Figure 6-1: Downstream erosion during a big flood event of Lauvsnes dam Norway (Photo: Norsk Groønn Kraft)

Hence, the energy dissipating structures should be designed such that energy is dissipated within the stilling basin in all cases of hydrological events. The materials for energy dissipating structures should be sized and placed such that no transporting of such materials occur. In

addition, the river banks downstream should be designed to withstand extreme hydrological events. Furthermore, it should be confirmed that the river section downstream has enough capacity during an extreme hydrological event to prevent increase in uplift pressure in dam and washing out of banks due to increased tail water level.

6.4 Liquefaction

In an area susceptible to earthquake liquefaction is likely to occur provided that the condition discussed in [chapter 2.7](#) are met. Since liquefaction can have serious effects on dam, it should be studied for a concrete dam constructed on soil foundation.

In conclusion, concrete dams constructed on soil materials are much more demanding in terms of field studies and design considerations. However, it is always not possible to find rock where a dam should be built so, a soil foundation for a concrete dam is inevitable. Determination of response of foundation and its effects on dam stability is quite a challenge in concrete dams constructed on soil materials. Hence, the methods presented in this report along with other considerations should be followed for design and analysis of such dams.

7 Recommendations

Since the dam used for case study is now under construction, no verification of estimated values could be done. It is recommended to verify the estimated values with field measurements on dams constructed on soil materials preferably both on granular materials and cohesive soils.

Stress fields onto the dam by foundation has 3D effects however PLAXIS 2D could only simulate two dimensional section of dam. Analysis without considering confining stresses could affect the results. Hence, it is recommended to use 3D finite element model and compare the results with values from 2D analysis and field studies.

It is also recommended to analyze the dam in a separate finite element model meant for modelling for structural analysis. The results (settlements and rotations) from PLAXIS should be applied as loads in the FEM.

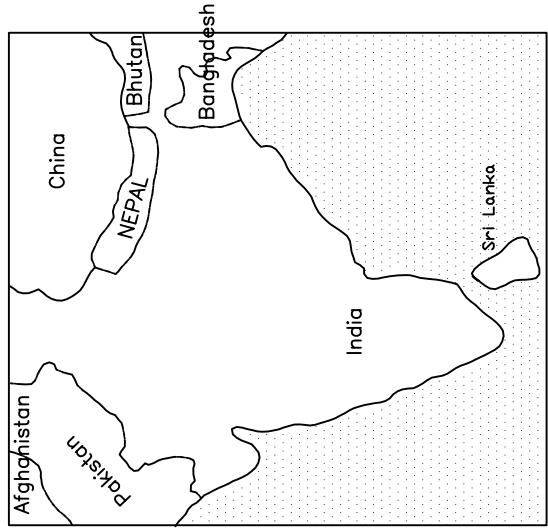
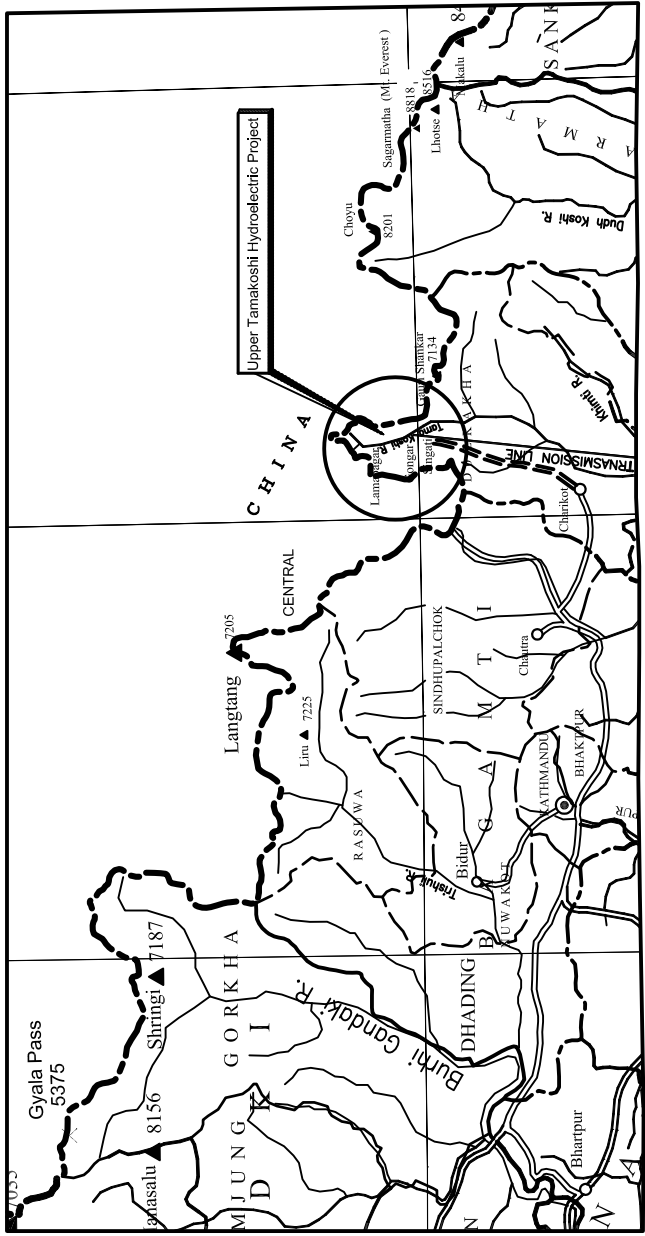
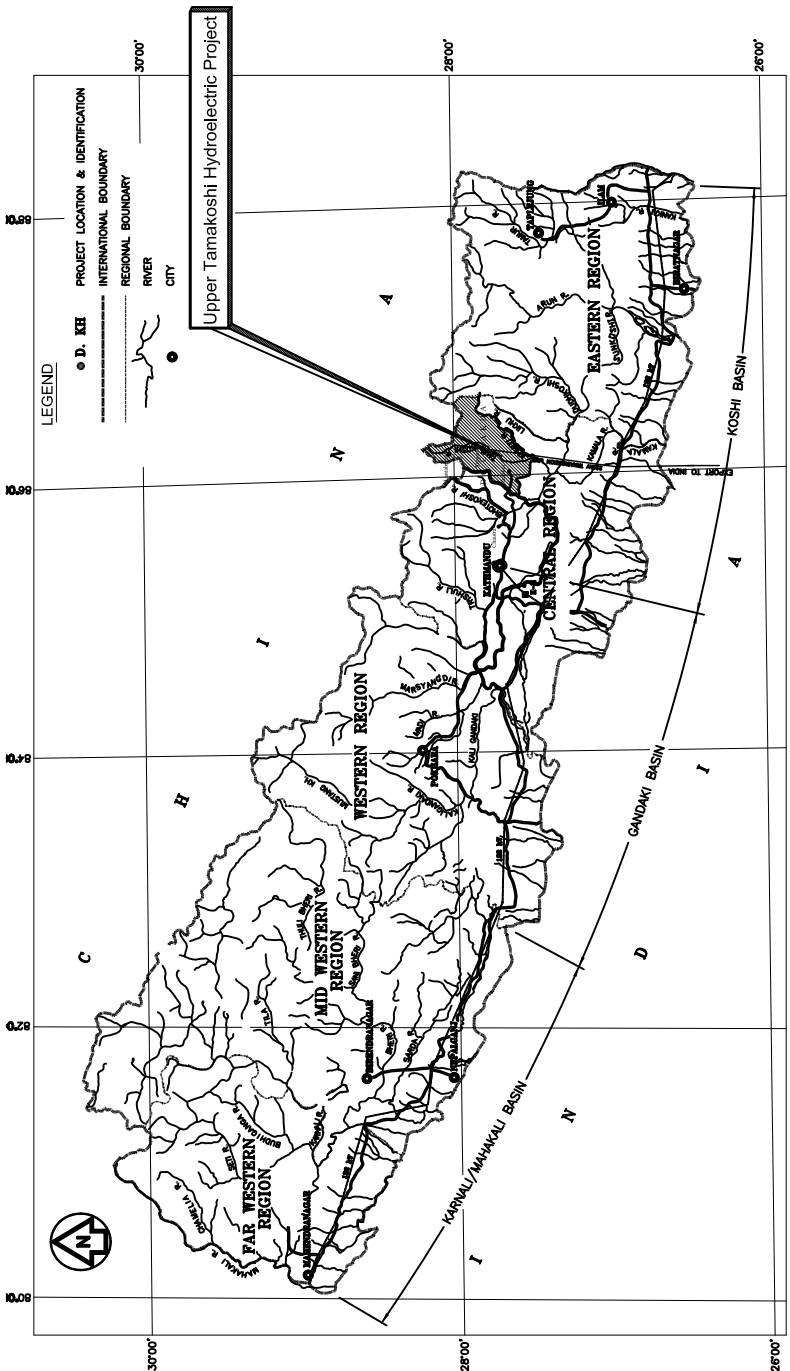
Also, a detailed field investigation requirements for such dams should be prepared.

Bibliography

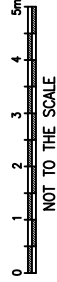
- BERZELL, C. 2014. *Load capacity of grouted rock bolts in concrete dams*. Royal Institute of Technology (KTH).
- BOWLES, J. 1987. Elastic Foundation Settlements on Sand Deposits. *Journal of Geotechnical Engineering*, 113, 846-860.
- BRINKGREVE, R. & VERMEER, P. 2002. Plaxis users manual. *Balkema, Rotterdam (The Neetherlands)*.
- DAS, B. 2015. *Principles of foundation engineering*, Cengage learning.
- ENGINEERS, U. A. C. O. *Best Practices in Dam and Levee Safety Risk Analysis training manual*, Denver, Colorado, Bureau of Reclamation and U.S. Army Corps of Engineers.
- ENGINEERS, U. A. C. O. 1992. Bearing Capacity of Soils. 30 October 1992 ed. Washington, DC: US Army corps of Engineers.
- FELLENIUS, B. 2006. Basics of foundation design. Electronic ed.
- FOX, E. The mean elastic settlement of a uniformly loaded area at a depth below the ground surface. Proc. 2nd Int. Conf. Soil Mechanics and Foundation Engng, 1948. 129.
- GIBBS, H. J. 1953. *Estimating Foundation Settlement By One-Dimensional Consolidation Tests*, Technical Information Office.
- HOLTZ, R. 1991. Stress Distribution and Settlement of Shallow Foundations. In: FANG, H.-Y. (ed.) *Foundation Engineering Handbook*. Springer US.
- ICOLD 2005. Dam Foundations, Geologic Considerations, Investigation Methods, Treatment, Monitoring. *ICOLD Bulletin*.
- IDRISS, I. & BOULANGER, R. 2006. Semi-empirical procedures for evaluating liquefaction potential during earthquakes. *Soil Dynamics and Earthquake Engineering*, 26, 115-130.
- IDRISS, I. & BOULANGER, R. W. 2008. *Soil liquefaction during earthquakes*, Earthquake engineering research institute.
- JANBU, N. 1967. *Settlement calculations based on the tangent modulus concept: three lectures comprising*, Trondheim, Instituttet.
- KRAMER, S. L. 1996. *Geotechnical earthquake engineering*, Upper Saddle River, N.J., Prentice Hall.
- KRAMER, S. L. 2008. Evaluation of liquefaction hazards in Washington State. Washington State Department of Transportation, Office of Research and Library Services.
- MARTIN, G. R. & LEW, M. 1999. *Recommended procedures for implementation of DMG special publication 117, guidelines for analyzing and mitigating liquefaction hazards in California*, Southern California Earthquake Center, University of Southern California.
- NORCONSULT 2005. Feasibility Study of Upper Tamakoshi Hydroelectric Project. Nepal: Nepal Electricity Authority.
- PATRICK, J. F. 2002. Consolidation and Settlement Analysis. *The Civil Engineering Handbook, Second Edition*. CRC Press.
- RUGGERI, G. 2004. Sliding Safety of Existing Gravity Dams - Final Report. *ICOLD, European Working Group*.
- SEED, H. B. & IDRIS, I. 1982. *Ground motions and soil liquefaction during earthquakes*, Earthquake Engineering Research Institute.
- USBR 1976. Design of gravity dams. Denver, Colorado: United States Department of Interior, Bureau of Reclamation.
- USBR 1987. *Design of Small Dams*, Washington, United States Department of Interior, Bureau of Reclamation.
- USBR, U. 1998. Bureau of Reclamation 1998 Earth Manual. *Denver CO*.

- USBR, U. 2014. *Design Standard No. 13: Embankment Dams*, Washington, U.S. Department of Interior, Bureau of Reclamation.
- UTHL. 2015. *Salient Features of Upper Tamakoshi Hydropower* [Online]. Nepal: Upper Tamakoshi Hydropower Limited. Available: <http://www.tamakoshihydro.org.np/information/8> [Accessed 21-June 2015].
- VON THUN, J. L. Understanding Seepage and Piping Failures – the No. 1 Dam Safety Problem in the West. Association of Dam Safety Officials Western Regional Conference, 1996 Lake Tahoe, Nevada.
- YOUD, T., IDRIS, I., ANDRUS, R. D., ARANGO, I., CASTRO, G., CHRISTIAN, J. T., DOBRY, R., FINN, W. L., HARDER JR, L. F. & HYNES, M. E. 2001. Liquefaction resistance of soils: summary report from the 1996 NCEER and 1998 NCEER/NSF workshops on evaluation of liquefaction resistance of soils. *Journal of geotechnical and geoenvironmental engineering*, 127, 817-833.
- YOUD, T. L., HANSEN, C. M. & BARTLETT, S. F. 2002. Revised multilinear regression equations for prediction of lateral spread displacement. *Journal of Geotechnical and Geoenvironmental Engineering*, 128, 1007-1017.
- YOUD, T. L. & PERKINS, D. M. 1978. Mapping liquefaction-induced ground failure potential. *Journal of the Geotechnical Engineering Division*, 104, 433-446.

Appendix A - Drawings



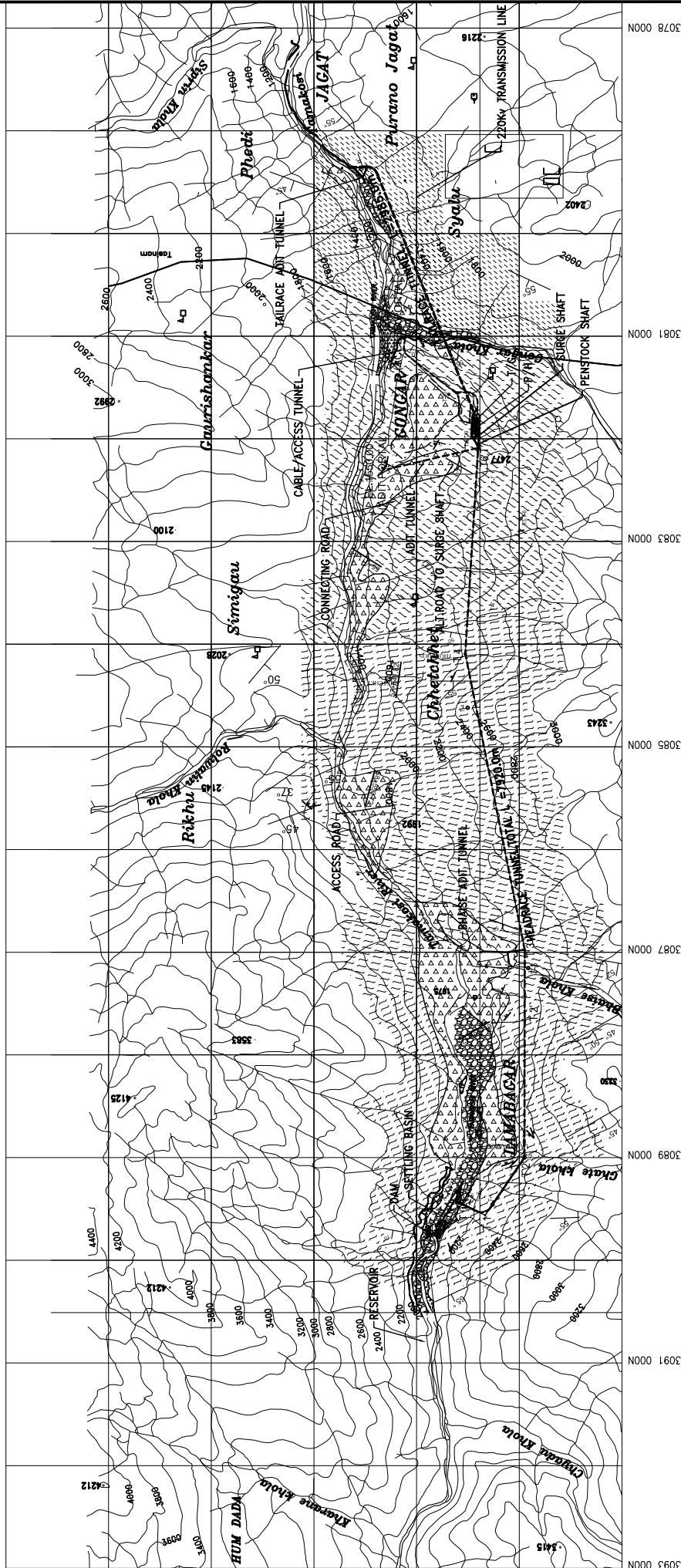
Key Plan



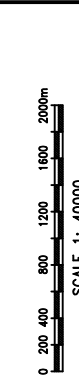
TENDER DRAWING (NOT FOR CONSTRUCTION PURPOSES)	
Rev.	Description
Drawn/ Appr.	Date
Scale: Not to the scale	
Drawn: S JOSHI	Checked: G Solovng
Approved: G Solovng	
Date : Dec 08, 2008	
Project No:	
UPPER TAMAKOSHI HYDROPOWER LIMITED Kathmandu, Nepal	
UPPER TAMAKOSHI HYDROELECTRIC PROJECT LOCATION MAP	
LAHMEYER INTERNATIONAL Engineering and Management consultant	
Norconsult Engineering and Management consultant	
Dwg No.:	3101
Rev.	



427 000E
425 000E
423 000E
421 000E



3093 000N
3091 000N
3089 000N
3087 000N
3085 000N
3083 000N
3081 000N
3078 000N

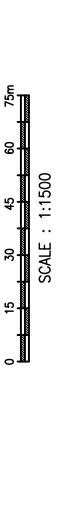
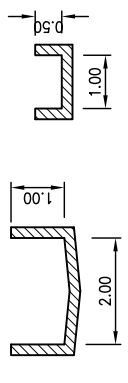
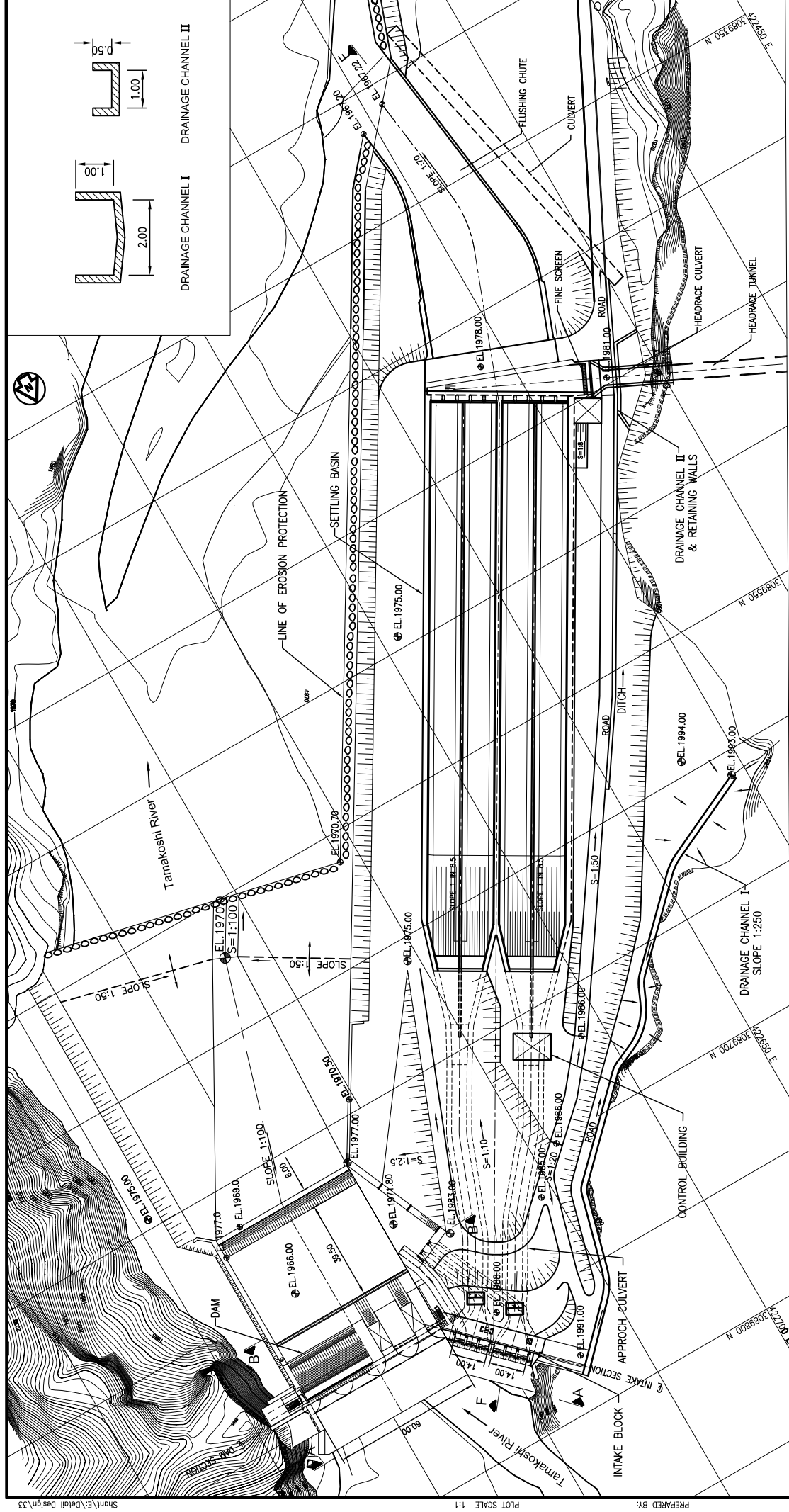


LEGEND

	ALLUVIAL DEPOSIT		LANDSLIDE BOUNDARY
	COLLUVIUM DEPOSIT		GEOLOGICAL BOUNDARY
	GNISS ROCK		DIP AND STRIKE OF FOLIATION (FIGURE INDICATE DIP AMOUNT)
	SCHIST ROCK		DIP AND STRIKE OF JOINT (FIGURE INDICATE DIP AMOUNT)

Rev.	Description	Drawn/Appr.	Date
03	CORRECTIONS		03.09.08
02	REFINING		Aug.05.08
01	UPDATED		June.2008

Scale:	
Drawn:	UPPER TAMAKOSHI HYDROPOWER LIMITED Kathmandu, Nepal
Checked:	
Approved:	
Date :	
Project No:	



TENDER DRAWING
(NOT FOR CONSTRUCTION PURPOSES)

Rev.	Description	Drawn by	Date

Scale: 1:1500
Drawn: S JOSHI
Checked: G Solwang
Approved: G Solwang
Date: Dec 08, 2008
Project No:

UPPER TAMAKOSHI HYDROPOWER LIMITED
Kathmandu, Nepal

UPPER TAMAKOSHI HYDROELECTRIC PROJECT
HEADWORKS
GENERAL LAYOUT PLAN

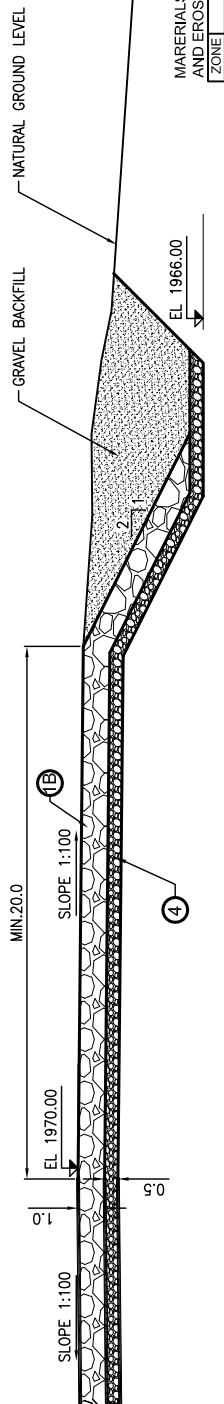
Lahmeyer International
Engineering and Management Consultant

Norconsult
Engineering and Management Consultant

Dwg No.: 3301
Rev.

MATERIALS FOR BACKFILL AND EROSION PROTECTION

ZONE	MATERIAL
1B	BLOCKS, 400-600mm
4	PROCESSED GRAVEL > 60mm



SECTION END OF CANAL
SLOPE 1:200



3090 000N

3090 500N

3091 000N

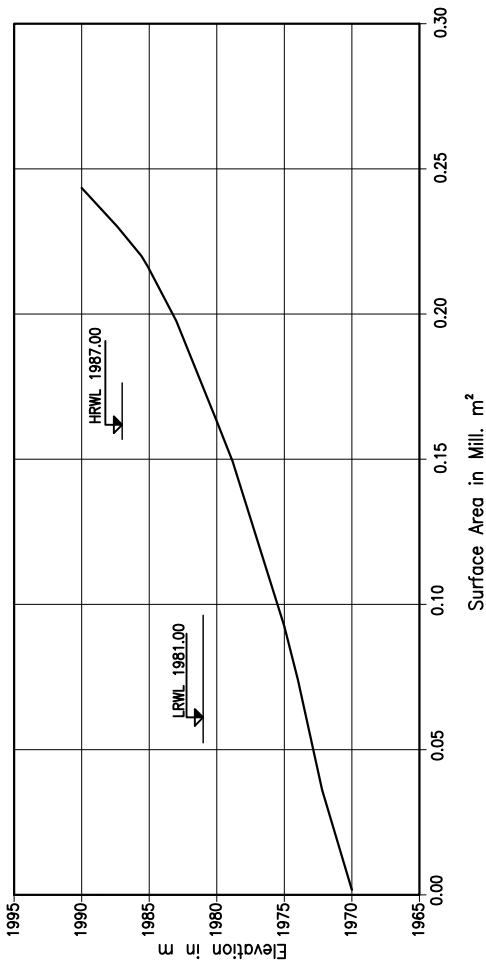
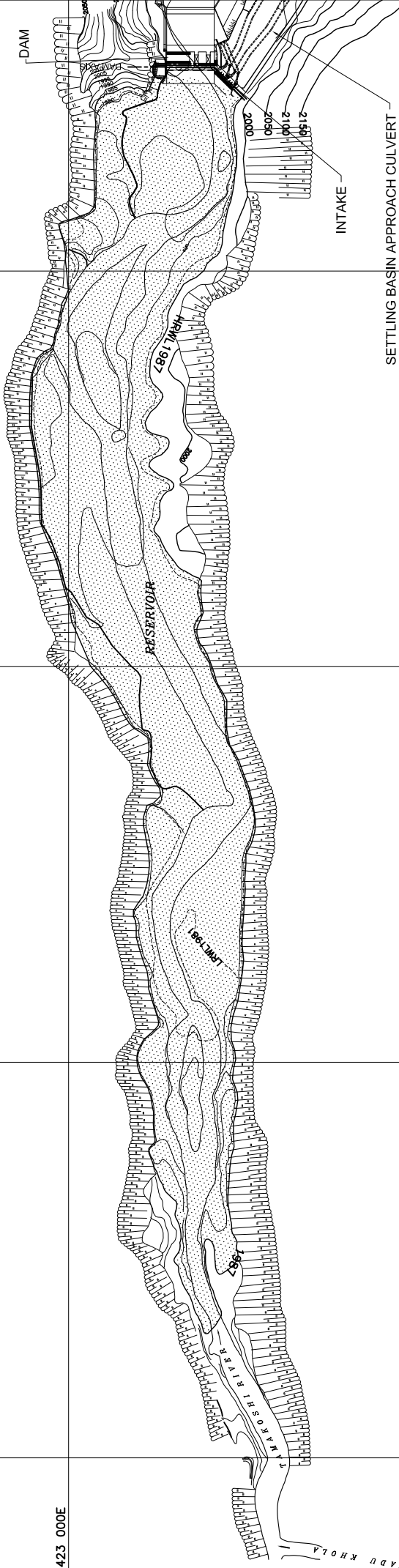
3091 500N

423 000E

422 500E

PREPARED BY: _____

PLOT SCALE 1:1



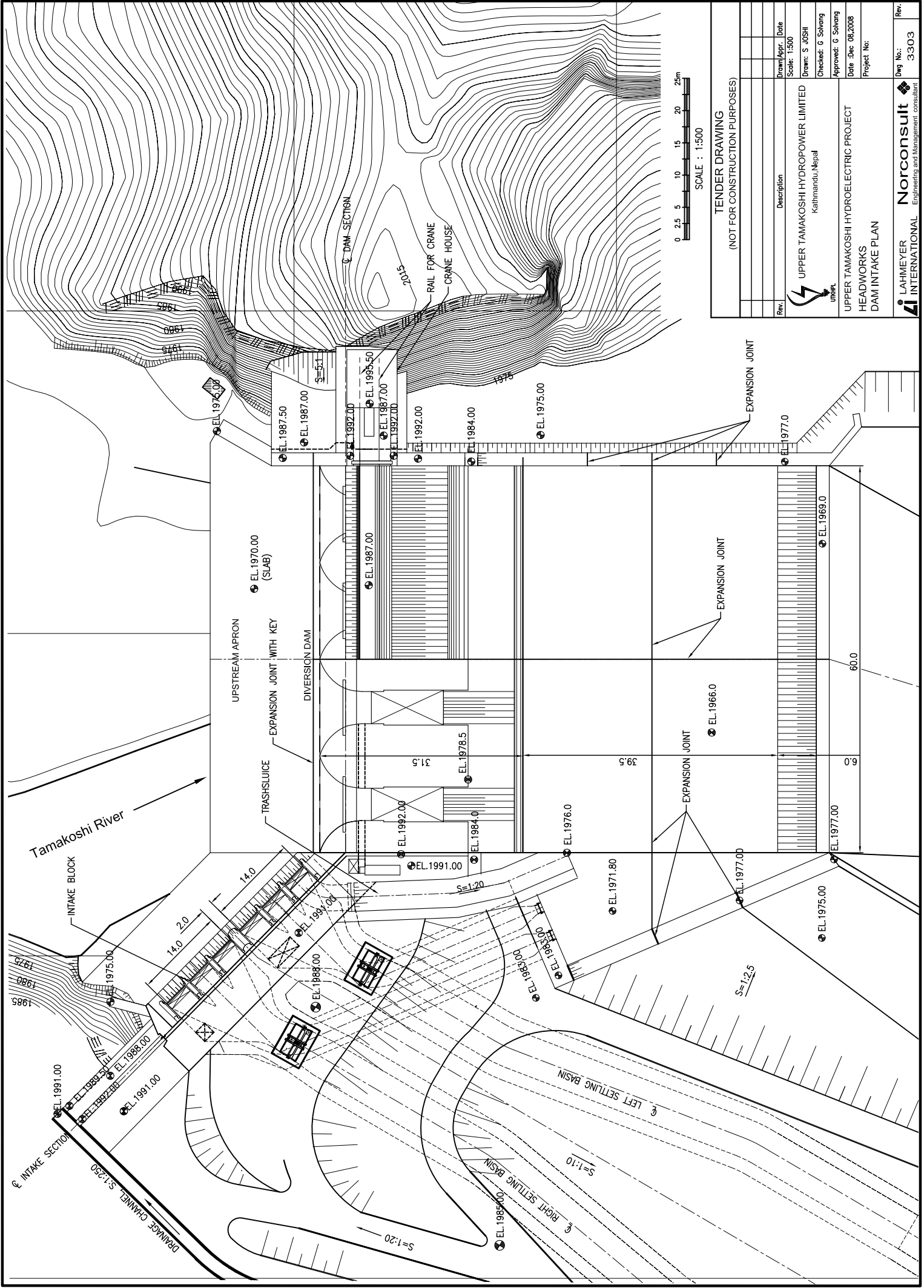
TENDER DRAWING
(NOT FOR CONSTRUCTION PURPOSES)

Rev.	Description	Drawn/Appr.	Date

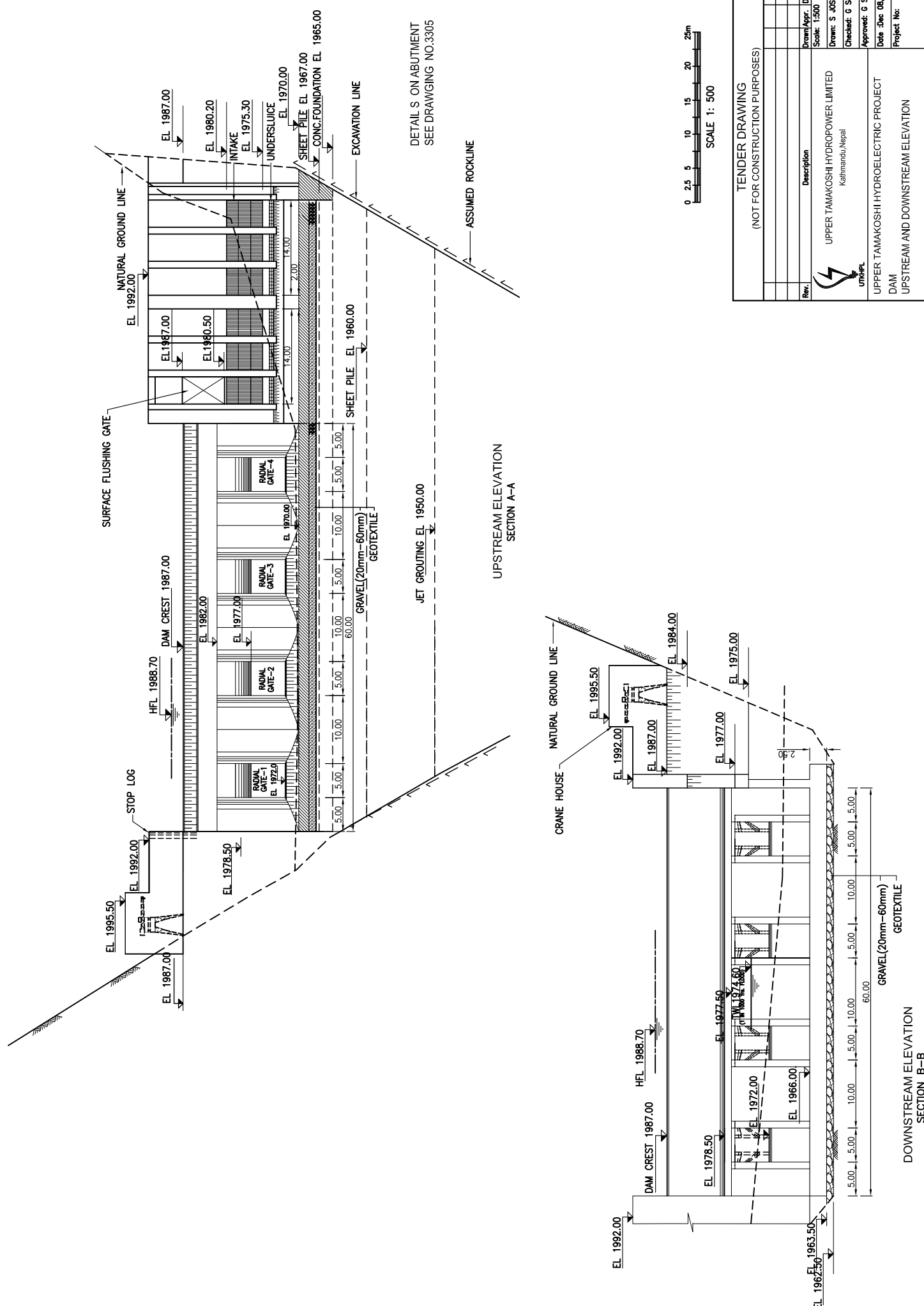
UPPER TAMAKOSHI HYDROPOWER LIMITED
Kathmandu, Nepal



UPPER TAMAKOSHI HYDROELECTRIC PROJECT HEADWORKS RESERVOIR AREA

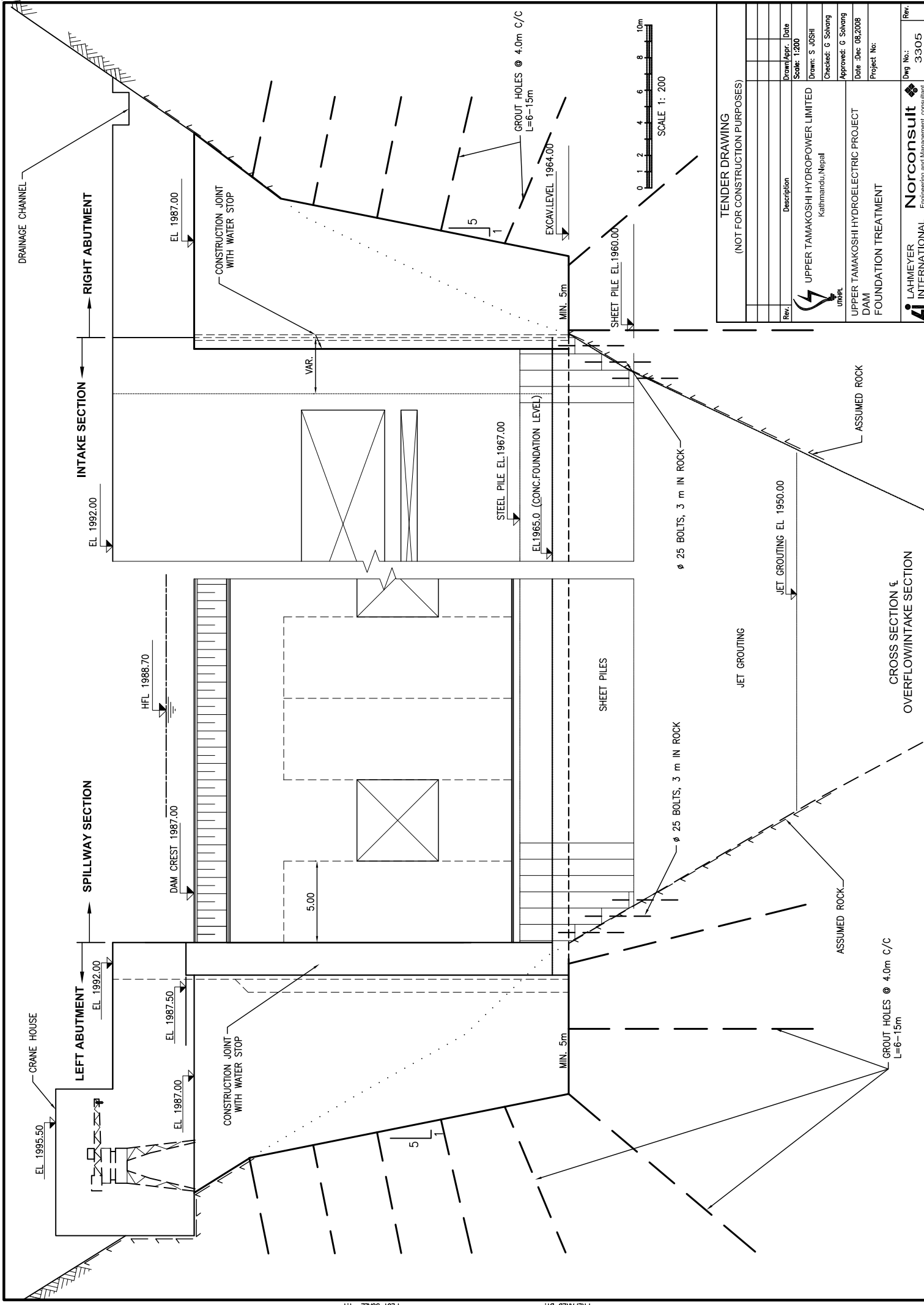
Checked: G Sohang	Drawn: S JOSHI
Approved: G Sohang	Scale: 1:5000
Date: Dec 08, 2008	Project No: _____
Project No: _____	



TENDER DRAWING (NOT FOR CONSTRUCTION PURPOSES)			
Rev.	Description	Drawn/Apr.	Date
UPPER TAMAKOSHI HYDROPOWER LIMITED Kathmandu, Nepal			
UPPER TAMAKOSHI HYDROELECTRIC PROJECT HEADWORKS DAM INTAKE PLAN		Checked: G. Solovng Approved: G. Solovng Date: Dec 08, 2008 Project No.:	Norconsult <small>Engineering and Management Consultant</small> LAHMEYER INTERNATIONAL Dwg No.: 3-303 Rev.



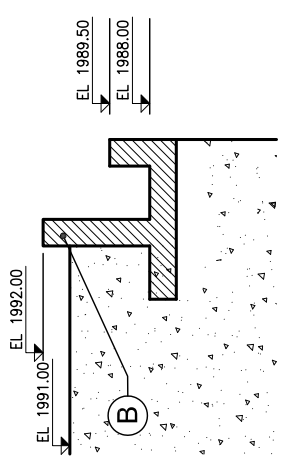
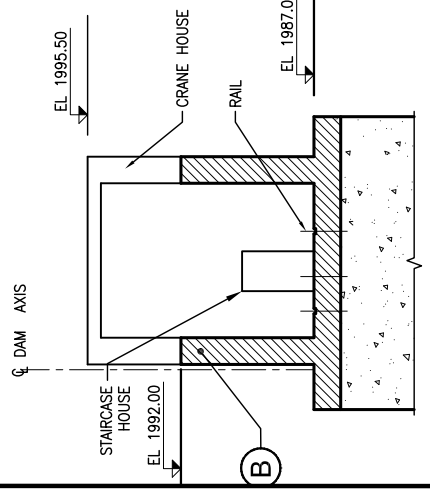
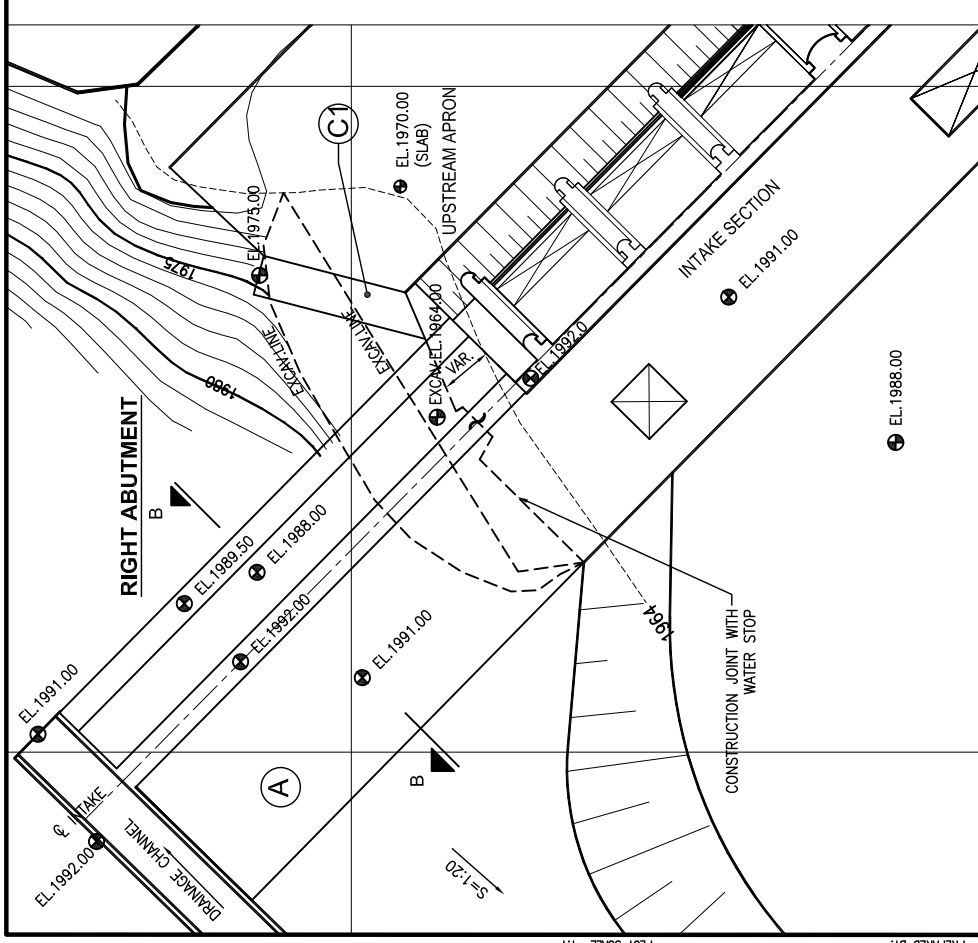
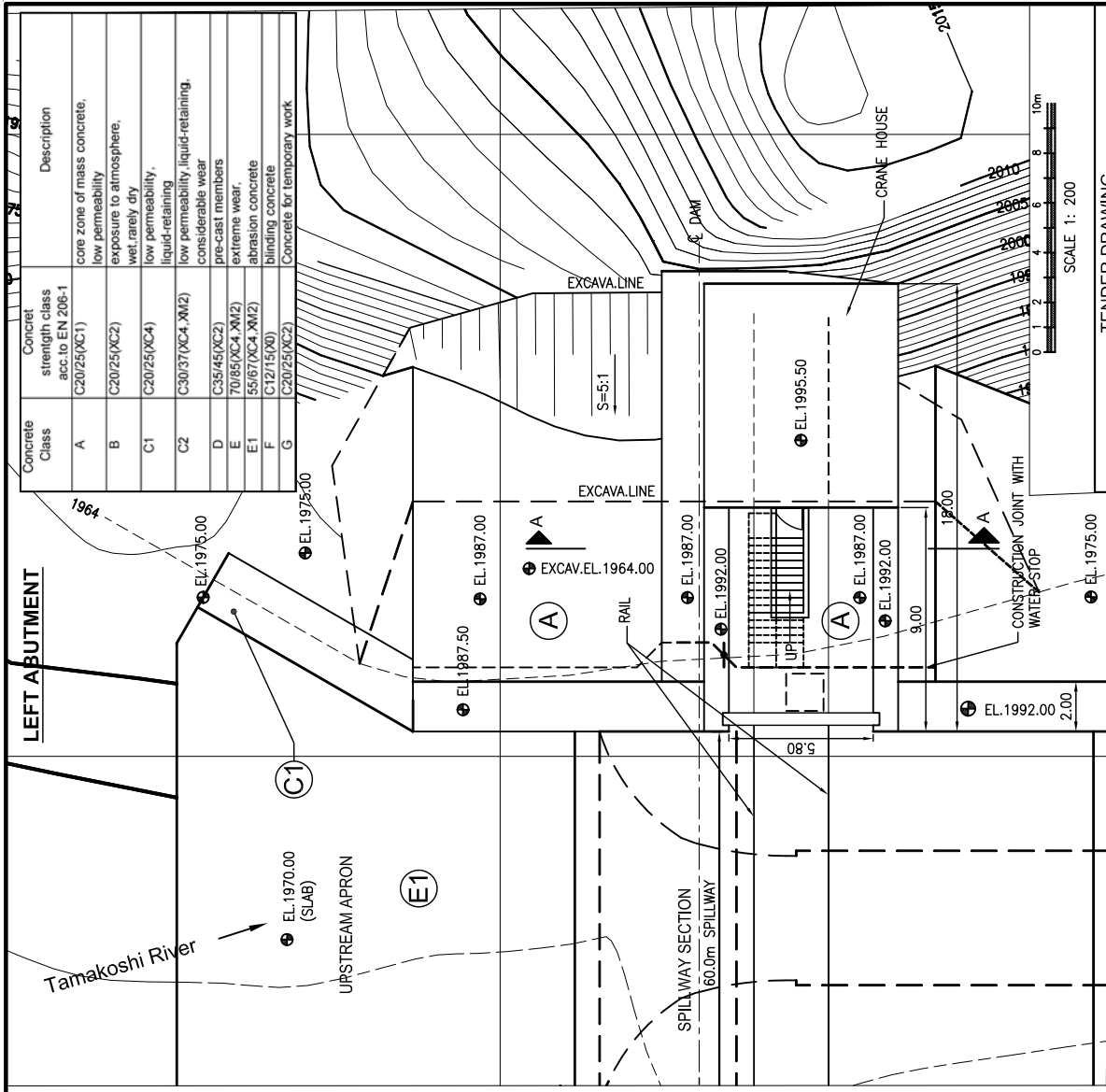
TENDER DRAWING (NOT FOR CONSTRUCTION PURPOSES)	
Rev.	Description
Drawn/ Appr.	Date
Scale:	1:500
Drawn:	S. JOSHI
Checked:	G. Solvong
Approved:	G. Solvong
Date:	Dec 08, 2008
Project No:	
 UPPER TANIAKOSHI HYDROPOWER LIMITED Kathmandu, Nepal	
UPPER TANIAKOSHI HYDROELECTRIC PROJECT DAM UPSTREAM AND DOWNSTREAM ELEVATION	
 LAHMEYER INTERNATIONAL Engineering and Management Consultant	Norconsult Engineering and Management Consultant
Dwg No.:	3304
Rev.:	



Rev.		Description	Drawn/ Appr.	Date
Scale: 1:200			Drawn: S JOSHI	
Checked: G Solovang		UPPER TAMAKOSHI HYDROPOWER LIMITED Kathmandu, Nepal		
Approved: G Solovang		UPPER TAMAKOSHI HYDROELECTRIC PROJECT		
Date: Dec 08, 2008		FOUNDATION TREATMENT		
Project No:		UNEP		

TENDER DRAWING
(NOT FOR CONSTRUCTION PURPOSES)

LAHMEYER INTERNATIONAL
Norconsult
Engineering and Management consultant
Dwg No.: 3305
Rev.



Concrete Class	Concrete strength class acc. to EN 206-1	Description
A	C20/25(XC1)	core zone of mass concrete, low permeability
B	C20/25(XC2)	exposure to atmosphere, wet rarely dry
C1	C20/25(XC4)	low permeability, liquid-retaining
C2	C30/37(XC4, XM2)	low permeability liquid-retaining, considerable wear
D	C35/45(XC2)	pre-cast members
E	70/85(XC4, XM2)	extreme wear
E1	55/67(XC4, XM2)	abrasion concrete
F	C12/15(X0)	blinding concrete
G	C20/25(XC2)	Concrete for temporary work

TENDER DRAWING
(NOT FOR CONSTRUCTION PURPOSES)

Rev.	Description	Drawn by	Date
		S. JOSHI	1:200

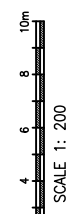
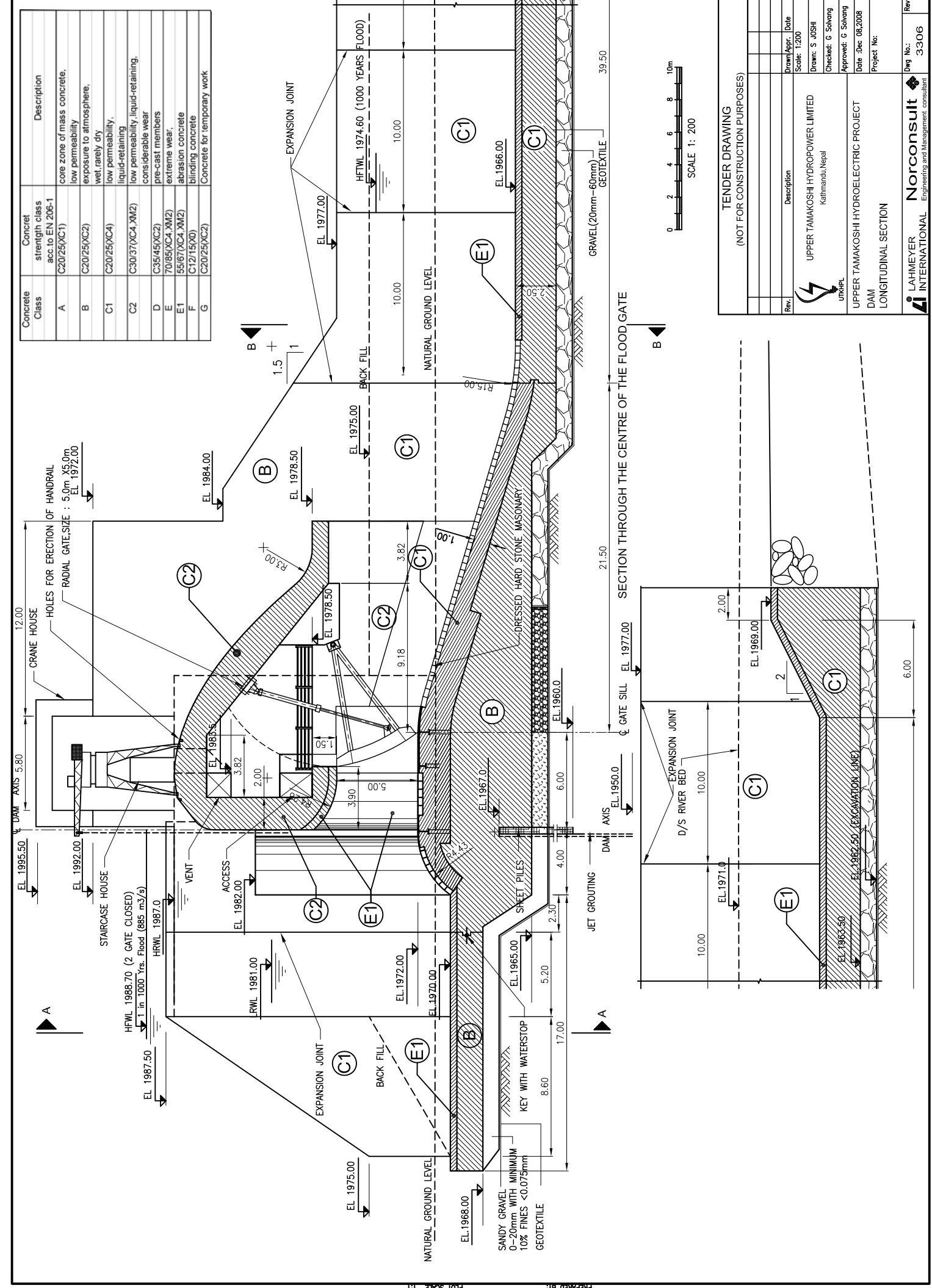
UPPER TAMAKOSHI HYDROPOWER LIMITED
Kathmandu, Nepal

Checked: G. Solvong
Approved: G. Solvong
Date: Dec 08, 2008
Project No:

Norconsult
Engineering and Management consultant

LAHMEYER INTERNATIONAL
Dng No.: 3308
Rev.

Concrete Class	Concrete strength class acc.to EN 206-1	Description
A	C20/25(XC1)	core zone of mass concrete, low permeability
B	C20/25(XC2)	exposure to atmosphere, wet, rarely dry
C1	C20/25(XC4)	low permeability, liquid-retaining
C2	C30/37(XC4, XM2)	low permeability, liquid-retaining, considerable wear
D	C35/45(XC2)	pre-cast members
E	70/85(XC4, XM2)	extreme wear
E1	55/67(XC4, XM2)	abrasion concrete
F	C12/15(X0)	blinding concrete
G	C20/25(XC2)	Concrete for temporary work



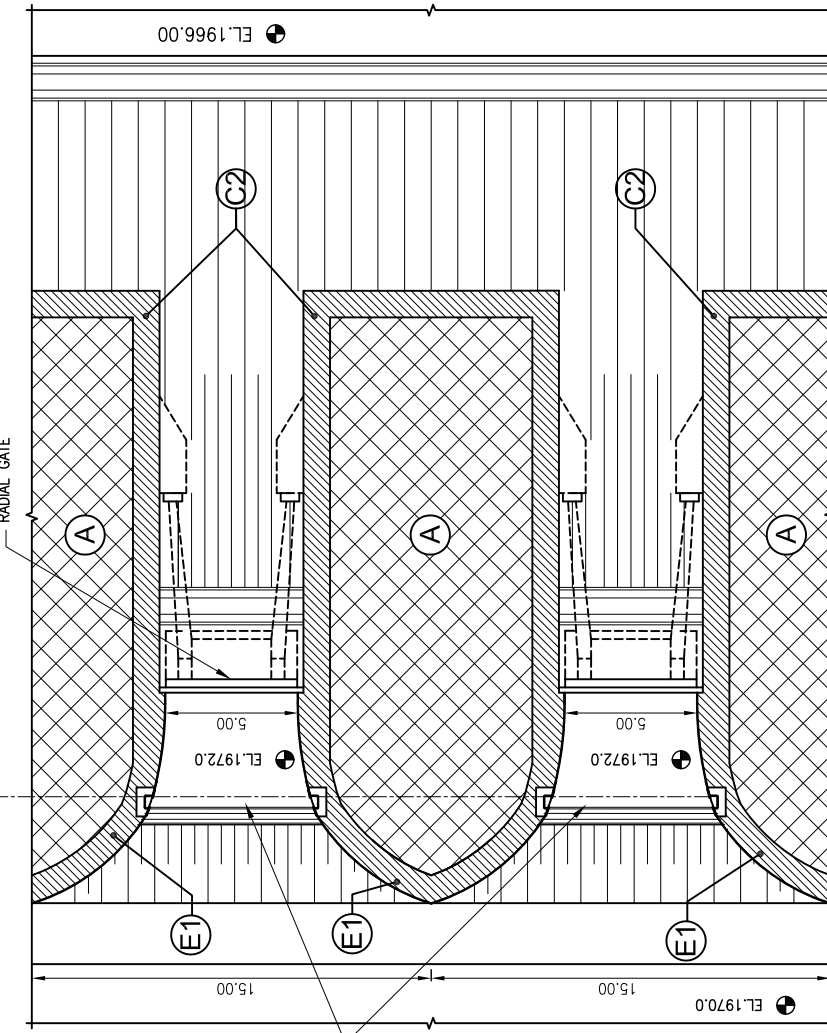
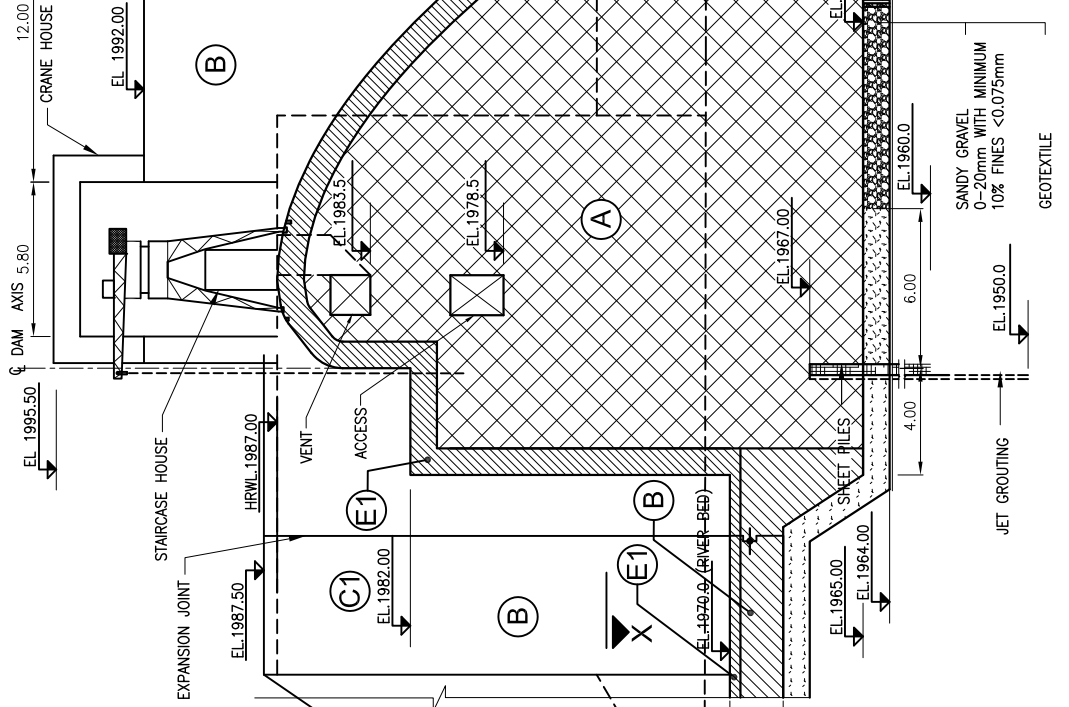
Rev.	Description	Drawn/Appr.	Date

TENDER DRAWING
 (NOT FOR CONSTRUCTION PURPOSES)

UPMHL UPPER TAMAKOSHI HYDROPOWER LIMITED Kathmandu, Nepal	Drawn: S JOSHI Checked: G Salvng Approved: G Salvng Date :Dec 08,2008 Project No:
---	---

Norconsult Engineering and Management consultant.	Dwg No.: 3-306 Rev.
--	------------------------

Concrete Class	Concrete strength class acc. to EN 206-1	Description
A	C20/25(XC1)	core zone of mass concrete, low permeability
B	C20/25(XC2)	exposure to atmosphere, wet, rarely dry
C1	C20/25(XC4)	low permeability, liquid-retaining
C2	C30/37(XC4, XM2)	low permeability liquid-retaining, considerable wear
D	C35/45(XC2)	pre-cast members
E	70/85(XC4, XM2)	extreme wear, abrasion concrete
E1	55/67(XC4, XM2)	blinding concrete
F	C12/15(X0)	Concrete for temporary work
G	C20/25(XC2)	



TENDER DRAWING
(NOT FOR CONSTRUCTION PURPOSES)

Rev.	Description	Drawn/Appr.	Date

Scale: 1:200

Checked: G. Solving
Drawn: S. JOSHI
Project No.:

Approved: G. Solving
Date: Dec 08, 2008

UPPER TAMAKOSHI HYDROPOWER LIMITED
Kathmandu, Nepal

UPPER TAMAKOSHI HYDROELECTRIC PROJECT
DAM
PLAN AND SECTION

UNPHL

LAHMEYER INTERNATIONAL
Engineering and Management consultant

Norconsult
Engineering and Management consultant

Dwg No.: 3307
Rev.:

PREPARED BY: PLOT SCALE 1:1

Appendix B – Stability Calculation

A. Stability calculation during Normal condition, NWL+ Earthquake, Design flood

General		
Discharge	m ³ /s	5000
Return Period	years	1000
Elevation of dam crest	masl	1987
Elevation of U/S foundation of dam	masl	1968
Elevation of U/S floor of dam	masl	1970
Elevation of D/S floor of dam	masl	1966
Elevation of dam toe	masl	1963.5
Elevation of HRWL	masl	1987
Elevation of LRWL	masl	1981
Elevation of HFWL	masl	1988.7
Elevation of TWL	masl	1970
Elevation of HFTWL	masl	1974.6

Geometry of weir		
Base width	m	33.8
Height of Weir	m	23.5
Width of rectangular portion	m	6.3

Soil Parameters		
Angle of internal friction of soil	degree	37.00
Unit weight of soil, γ_s	KN/m ²	18.64
Horizontal Earth pressure coefficient, k		0.25
Max allowable bearing capacity	KN/m ²	
Other parameters		
Unit weight of concrete, γ_c	KN/m ³	24.00
Unit weight water, γ_w	KN/m ³	9.81
Uplift coefficient		0.75
Coefficient of friction, μ		0.75
% of passive pressure to use		90%
Earthquake coefficient		0.34

Sediments and other properties		
Height of sediment zone (u/s), h_s	m	3.80
Height of soil above toe d/s, h_d	m	
Consider weight of water over weir		No

Consider earthquake

Yes

Load Calculation

S.N.	Description	Direction	Pressure (KN/m)		Load Type
			Start Value	End Value	
<u>Primary load - Live loads</u>					
P1	Water pressure from U/S, normal operation	+x	0	186.4	Traingular
P2	Water pressure from D/S, normal operation	-x	0	63.8	Traingular
P3	Uplift, normal operation	-y	186.39	63.8	Trapezoidal
P4	Vertical weight of water column over rectangular portion u/s, normal operation	+y	166.77	166.8	UDL
P5	Active sediment pressure	+x	0	8.3	Traingular
P6	Weight of boulders and sediment	+y		33.6	UDL
P7	Water pressure from U/S, Design flood	+x	16.677	203.1	Traingular
P8	Water pressure from D/S, Design flood	-x	0	108.9	Traingular
P9	Uplift, Design flood	-y	203.067	108.9	Trapezoidal
P10	Water weight over the weir, Design flood	+y	16.677	183.4	Varies: converted to point
P11	Vertical weight of water column over rectangular portion u/s, Design flood	+y	183.447	183.4	UDL
P12	Water weight over the weir, normal operation	+y	0	0.0	Varies: converted to point

P13	Passive pressure D/S	-x	0	207.8	Traingular
-----	----------------------	----	---	-------	------------

Dead Loads

D1	Self weight of weir	+y		8634.0
----	---------------------	----	--	--------

Earthquake load

E1	Hydrodynamic force	+x		1022.3
E2	Vertical acceleration (+y)	+y		2935.6
E3	Vertical acceleration (-y)	-y		2935.6
E4	Horizontal accelaration	+x		2935.6
E5	Horizontal accelaration (-x)	-x		2935.6

	Description	Force (KN)		Moment Arm		Moment (KNm/m)	
		Horizontal	Vertical	X	Y	Overturning	Resisting
	<u>Primary Loads</u>						
P1	Water pressure from U/S, normal operation	1770.71			10.83	19182.6	
P2	Water pressure from D/S, normal operation	-207.24			2.17		449.0
P3	Uplift, normal operation		-3752.00	18.00		67536.0	
P4	Vertical weight of water column over rectangular portion u/s, normal operation		1050.65	30.65			32202.5
P5	Active sediment pressure	15.85			5.77	91.4	
P6	Weight of boulders and sediment		33.55	30.65			1028.3
P7	Water pressure from U/S, Design flood	2087.57			11.31	23618.7	

P8	Water pressure from D/S , Design flood	-604.35			3.70		2236.1
P9	Uplift, Design flood		-3752.00	18.00		67536.0	
P10	Water weight over the weir, Design flood						
P11	Vertical weight of water column over rectangular portion u/s, Design flood		1155.72	30.65			35422.7
P12	Water weight over the weir, normal operation						
P13	Passive pressure D/S	0.00			0.00		0.0
	<u>Forces on Stilling basin</u>						
	Weight of stilling basin		3214.08				
	Weight of water		1863.90				
	Uplift		-3895.00				
	<u>Dead load</u>						
D1	Self-Weight		8634	19.78	9.68		170780.5
	<u>Earthquake load</u>						
E1	Hydrodynamic force	1022.3			10.70	10933.7	
E2	Vertical acceleration (+y)			19.78			0.0
E3	Vertical acceleration (-y)			19.78		0.0	
E4	Horizontal acceleration (+x)	2935.6			9.68	28416.2	
E5	Horizontal acceleration (-x)	-2935.6			9.68		28416.2
	<u>Load Combination</u>						
C1	Normal operation						

	P1+P2+P3+P4+P5+P6+P13+D1	1579.31	5966.20			86810.02	204460.30
C2	Transient condition (Design flood)						
	P7+P8+P9+P10+P11+P5+P6+P13+D1	1499.07	6071.27			91246.10	209467.61
C3	Normal operation+Earthquake						
	P1+P2+P3+P4+P5+P6+P13+D1+E1+E3+E4	5537.17	5966.20			126159.91	204460.30
C4	Before filling						
	D1+P5	15.85	8634.00			91.38	170780.52

	<u>Factor of Safety</u>		Factor of safety		Bearing stress (KN/m2)		
	<u>Cases</u>	eccentricity	Slide	Overtuning	At D/S	At U/s	
C1	Normal operation	-2.82	3.41	2.36	436.64	71.12	
C2	Design flood	-2.57	3.65	2.30	428.03	88.68	
C3	Normal operation+Earthquake	3.78	1.31	1.62	9.12	498.64	
C4	Before filling	-2.87	410.59	1868.93	636.57	98.24	

B. Stability calculation during PMF and GLOF

General		
Discharge	m ³ /s	5000
Return Period	years	1000
Elevation of dam crest	masl	1987
Elevation of U/S foundation of dam	masl	1968
Elevation of U/S floor of dam	masl	1970
Elevation of D/S floor of dam	masl	1966
Elevation of dam toe	masl	1963.5
Elevation of Water at PMF	masl	1991.9
Elevation of LRWL	masl	1981
Elevation of water at GLOF	masl	1997
Elevation of TWL at PMF	masl	1976
Elevation of TWL at GLOF	masl	1978.5

Geometry of weir		
Base width	m	33.8
Height of Weir	m	23.5
Width of rectangular portion	m	6.3

Soil Parameters		
Angle of internal friction of soil	degree	37.00
Unit weight of soil, γ_s	KN/m ²	18.64
Horizontal Earth pressure coefficient, k		0.25
Max allowable bearing capacity	KN/m ²	
Other parameters		
Unit weight of concrete, γ_c	KN/m ³	24.00
Unit weight water, γ_w	KN/m ³	9.81
Uplift coefficient		0.75
Coefficient of friction, μ		0.75
% of passive pressure to use		90%
Earthquake coefficient		0.34

Sediments and other properties		
Height of sediment zone (u/s), h_s	m	3.80
Height of soil above toe d/s, h_d	m	
Consider weight of water over weir		No

Load Calculation

S.N.	Description	Direction	Pressure (KN/m)	Load Type
------	-------------	-----------	-----------------	-----------

			Start Value	End Value	
<u>Primary load - Live loads</u>					
P1	Water pressure from U/S, PMF	+x	48.069	234.5	Traingular
P2	Water pressure from D/S ,PMF	-x	0	122.6	Traingular
P3	Uplift,PMF	-y	234.459	122.6	Trapezoidal
P4	Vertical weight of water column over rectangular portion u/s, PMF	+y	214.839	214.8	UDL
P5	Active sediment pressure	+x	0	8.3	Traingular
P6	Weight of boulders and sediment	+y		33.6	UDL
P7	Water pressure from U/S, GLOF	+x	98.1	284.5	Traingular
P8	Water pressure from D/S , GLOF	-x	0	147.2	Traingular
P9	Uplift, GLOF	-y	284.49	147.2	Trapezoidal
P10	Water weight over the weir, GLOF	+y	98.1	264.9	Varies: converted to point
P11	Vertical weight of water column over rectangular portion u/s, GLOF	+y	264.87	264.9	UDL
P12	Water weight over the weir, PMF	+y	48.069	48.1	Varies: converted to point
P13	Passive pressure D/S	-x	0	399.6	Traingular

Dead Loads

D1	Self weight of weir	+y		8634.0	
----	---------------------	----	--	--------	--

	Description	Force (KN)		Moment Arm		Moment (KNm/m)	
		Horizontal I	Vertical	X	Y	Overturning	Resisting
	<u>Primary Loads</u>						
P1	Water pressure from U/S, PMF	2684.02			11.91	31969.0	
P2	Water pressure from D/S ,PMF	-766.41			4.17		3193.4
P3	Uplift,PMF		-3752.00	18.00		67536.0	
P4	Vertical weight of water column over rectangular portion u/s, PMF		1353.49	30.65			41484.3
P5	Active sediment pressure	15.85			5.77	91.4	
P6	Weight of boulders and sediment		33.55	30.65			1028.3
P7	Water pressure from U/S, GLOF	3634.61			12.46	45277.2	
P8	Water pressure from D/S , GLOF	-1103.63			5.00		5518.1
P9	Uplift, GLOF		-3752.00	18.00		67536.0	
P10	Water weight over the weir, GLOF						
P11	Vertical weight of water column over rectangular portion u/s, GLOF		1668.68	30.65			51145.1
P12	Water weight over the weir, PMF						
P13	Passive pressure D/S	0.00			0.00		0.0
	<u>Forces on Stilling basin</u>						
	Weight of stilling basin		3214.08				
	Weight of water		1863.90				

	Uplift		-3895.00				
	<u>Dead load</u>						
D1	Self-Weight		8634	19.78	9.68		170780.5

	<u>Load Combination</u>						
C1	Extreme condition, PMF						
	P1+P2+P3+P4+P5+P6+P13+D1	1933.46	6269.04			99596.37	216486.53
C2	Extreme condition (GLOF)						
	P7+P8+P9+P10+P11+P5+P6+P13+D1	2546.83	6584.23			112904.62	228472.03

	<u>Factor of Safety</u>		Factor of safety		Bearing stress (KN/m2)		
	<u>Cases</u>	eccentricity	Slide	Overturning	At D/S	At U/s	
C1	PMF	-1.75	2.90	2.17	385.66	147.87	
C2	GLOF	-0.65	2.30	2.02	326.83	233.53	

Appendix C – Settlement Calculation

Calculation of Elastic Settlement

Foundation Properties				Soil Properties			
Description	Symbol	Unit	Value	Description	Symbol	Unit	Value
Shape of foundation	Rectangular			Poisson's ratio of soil	ν		0.35
Length of foundation	L	m	100	Unit weight of soil	γ_s	KN/m ³	20
Width of foundation	B	m	30	Modulus of Elasticity of soil	E_s	KN/m ²	5.00E+04
Depth of foundation	D_f	m	6.5	Base Modulus of Elasticity of soil	E_o	KN/m ²	5.00E+04
Depth to rock from surface	H	m	100	Change of elasticity with depth	k	KN/m ² /m	1
thickness of foundation	t	m	6.5				
Structure Properties							
Description	Symbol	Unit	Value				
Height of structure	h	m	23				
Unit weight of structure	γ_c	KN/m ³	24				
Strength of concrete	f _{ck}	Mpa	25				
Modulus of Elasticity of foundation structure	E_f	KN/m ²	2.35E+07				
Net applied pressure on foundation	q ₀	KN/m ²	210				

A. Calculation method

Boussinesq equation

General

Description	Symbol	Unit	Value
Calculation of settlement at		Center	
Type of foundation		Rigid	
Factor for location of foundation	α		4

Calculation

m'			3.333333
n'			6.666667
Df/B			0.217
B/L			0.300
A0			0.540
A1			1.443
A2			0.066
F1			0.6310
F2			0.0012
Shape factor (Steinbrenner, 1934)	Is		0.6316
Depth factor (Fox, 1948)	If		0.92
Settlement of foundation	Se	cm	11.95

B. Calculation method

Improved elastic equation

Equivalent diameter	Be	m	61.80
H/Be	H/Be		1.6
$\beta = E_0/(k \cdot B_e)$			809.0
Flexibility factor	K _F		4.371
Influence factor for the variation of Es with depth	I _G		0.75

Foundation rigidity correction factor	I_F	0.806
Foundation embedment correction factor	I_E	0.975

Elastic settlement below the center of foundation	S_e	cm	13.43
---	-------	----	--------------

C. Calculation of settlement by Janbu's Method

Water level	1973 masl	Density of soil	20	kn/m ³
		Density of water	10	kn/m ³
		surcharge	210	kn/m ²

Elevation	initial effective stress	final effective stress	m	M	strain	length of section	settlement (cm)
1971	0	0	500	0			
1963.5	55	265		81394	0.35%		
1950	190	339.0		92064	0.19%	13.5	3.64
1930	390	520.8		114100	0.12%	20	3.08
1910	590	720.8		134234	0.10%	20	2.25
1890	790	920.8		151720	0.09%	20	1.92
1870	990	1120.8		167388	0.08%	20	1.70
Total Settlement (cm)							12.59

Appendix D – Calculation of bearing capacity

Calculation of ultimate and allowable bearing capacity

	Symbol	Unit			
Length of foundation	L	m	100	unit weight of soil	γ 20.3
Breadth	B	m	33.8	unit weight of water	γ_s 6
Depth	D	m	6.5	Unit weight of concrete	10
Depth of foundation materials	H	m	100		24
Angle of friction of soil	ϕ		35		
cohesion of soil	c		5		
eccentricity of load	e	m	1.93		
Depth of overburden (stilling basin)			1		
water above the stilling basin			4		
Total overburden	q		64		
Inclination of resultant force with vertical	α		23.04		
N_ϕ			0.109		
effective width	B'		29.94		
Bearing Capacity factors					
N_q			33.30		
N_c			46.12		
N_γ			37.15		
Shape factors					
S_c			1.01		
S_q			1.00		
S_γ			1.00		
Depth correction factors					
d_c			1.01		
d_q			1.01		
d_γ			1.01		
inclination factors					
i_c			0.55		
i_q			0.55		
i_γ			0.12		

Ultimate bearing capacity	qf	$\frac{\text{KN}}{\text{m}^2}$	2002.09
Factor of Safety	FS		3.00
Allowable bearing capacity	qallow	$\frac{\text{KN}}{\text{m}^2}$	667.36